

UNCLASSIFIED

AD 297 361

*Reproduced
by the*

**ARMED SERVICES TECHNICAL INFORMATION AGENCY
ARLINGTON HALL STATION
ARLINGTON 12, VIRGINIA**



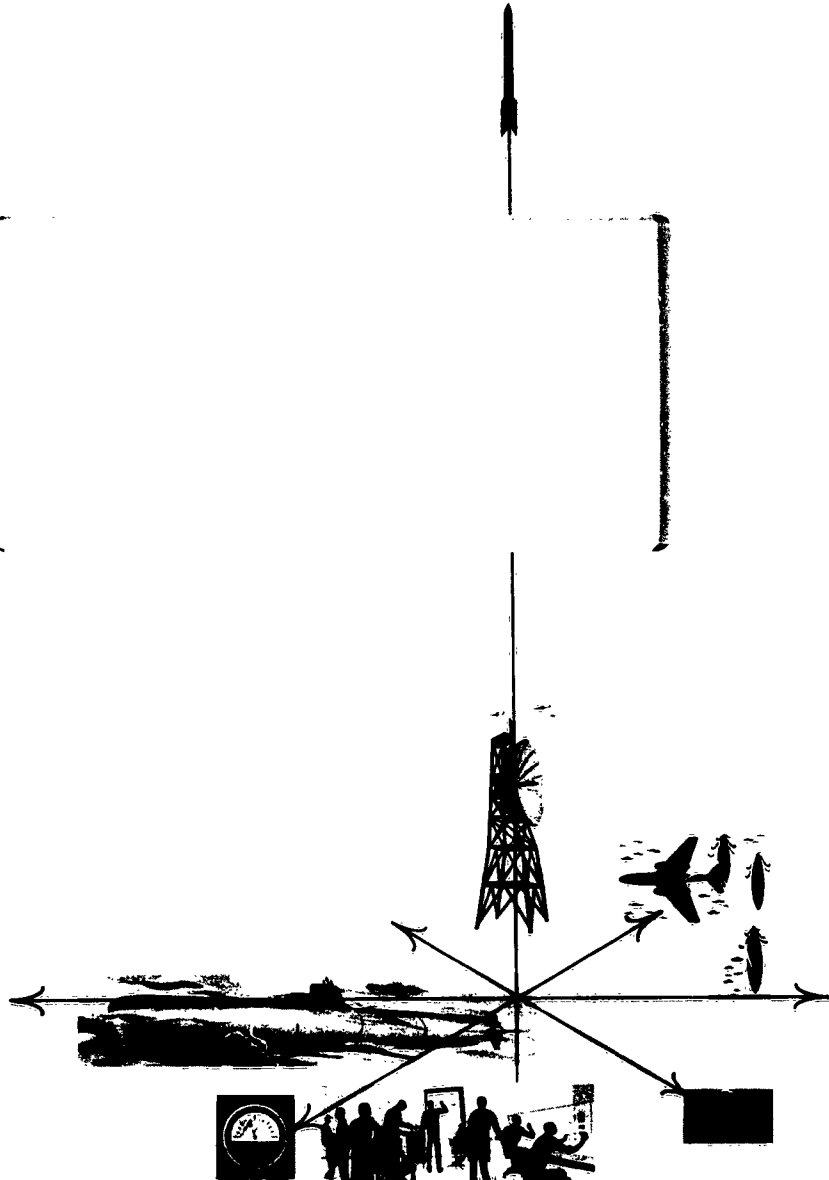
UNCLASSIFIED

NOTICE: When government or other drawings, specifications or other data are used for any purpose other than in connection with a definitely related government procurement operation, the U. S. Government thereby incurs no responsibility, nor any obligation whatsoever; and the fact that the Government may have formulated, furnished, or in any way supplied the said drawings, specifications, or other data is not to be regarded by implication or otherwise as in any manner licensing the holder or any other person or corporation, or conveying any rights or permission to manufacture, use or sell any patented invention that may in any way be related thereto.

63-2-5

CATALOGED BY ASTIA
AD NO. 297361

297 361



THE **Magnavox** COMPANY
GOVERNMENT AND INDUSTRIAL DIVISION

~~NO OTS~~

ASTIA
RECEIVED
MAR 5 1962

Serial No. TP62-690

**QUARTZ CRYSTAL OSCILLATOR CIRCUITS
FINAL REPORT**

**Contract No. DA36-039 SC-88892
Department of the Army Project No. 3G-26-05-001
1 July 1961 to 30 June 1962
U. S. ARMY SIGNAL RESEARCH AND
DEVELOPMENT LABORATORY
FORT MONMOUTH, NEW JERSEY**

ASTIA AVAILABILITY NOTICE

**Qualified requestors may obtain copies
of this report from ASTIA. ~~ASTIA~~
~~release to OTS not authorized.~~**

QUARTZ CRYSTAL OSCILLATOR CIRCUITS

FINAL REPORT

Contract No. DA36-039 SC-88892

PR&C 61-ELP/D-4209


Dated 14 December 1962

Department of the Army Project No. 3G-26-05-001


1 July 1961 to 30 June 1962

The object of this study was to facilitate and systematize the design of quartz crystal oscillators in the frequency range of 1 KC to 200 MC, through recommended circuits and design procedures. This work should lead to decreased design time and costs and increased equipment reliability.

Approved by:


H. R. Meadows
Section Chief
Staff and Systems Engineering

Prepared by:


D. Firth
Project Engineer

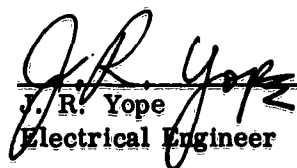

J. R. Yope
Electrical Engineer

TABLE OF CONTENTS

<u>Paragraph</u>	<u>Title</u>	<u>Page</u>
1.0	PURPOSE	1
2.0	ABSTRACT	1
3.0	PUBLICATIONS, LECTURES, REPORTS, AND CONFERENCES	2
3.1	Publications	2
3.2	Lectures	2
3.3	Reports	2
3.4	Conferences	2
4.0	FACTUAL DATA	4
4.1	Introduction	4
4.1.1	Philosophy of Approach	4
4.1.2	Report Layout	5
4.2	Quartz Crystal Characteristics	6
4.2.1	General	6
4.2.1.1	Frequency Stabilizing Properties of the Quartz Crystal	12
4.2.1.2	Oscillator Frequency Tolerance	15
4.2.1.3	Crystal Power Dissipation	17
4.2.2	Analysis of an Oscillator	19
4.2.3	Active Device Characteristics	25
4.2.4	Impedance Transforming Networks	26

TABLE OF CONTENTS (Cont)

<u>Paragraph</u>	<u>Title</u>	<u>Page</u>
4. 3	Performance Specification of an Oscillator	27
4. 4	Design Procedure	27
4. 5	Oscillator Design at High Frequencies	28
4. 5. 1	General	28
4. 5. 2	Crystal Characteristics	30
4. 5. 3	Active Device Characteristics	34
4. 5. 3. 1	Feedback Effects at High Frequencies	35
4. 5. 3. 2	Active Device Configurations Used During This Program	40
4. 5. 3. 3	Aids to Active Device Selection	41
4. 5. 3. 3. 1	Vacuum Tubes	41
4. 5. 3. 3. 2	Transistors	43
4. 5. 3. 4	Determination of Active Device Characteristics.	46
4. 5. 4	Design Procedure	50
4. 5. 4. 1	Step 1, Crystal Operating Condition	50
4. 5. 4. 2	Step 2, Selection of Crystal Type	50
4. 5. 4. 3	Step 3, Oscillator Configuration	51
4. 5. 4. 4	Step 4, Desired Active Device Characteristics	52
4. 5. 4. 5	Step 5, Selection of Active Device	54
4. 5. 4. 6	Step 6, Determination of Active Device Characteristics	55
4. 5. 4. 7	Step 7, Calculation of Oscillator Component Values.	55

TABLE OF CONTENTS (Cont)

<u>Paragraph</u>	<u>Title</u>	<u>Page</u>
4.5.4.8	Step 8, Design of Impedance Transforming Network	57
4.5.4.9	Step 9, Experimental Adjustments	57
4.6	Oscillator Design at Low Frequencies	60
4.6.1	General	60
4.6.2	Crystal Characteristics	60
4.6.3	Active Device Characteristics	63
4.6.3.1	Tubes	63
4.6.3.1.1	Typical Tube Amplifier Operating Characteristics .	66
4.6.3.2	Transistors	66
4.6.3.2.1	Power Gain, Input and Output Resistance	68
4.6.3.2.2	Common Base to Common Emitter 'h' Parameter Conversions	68
4.6.3.2.3	Typical Transistor Amplifier Operating Characteristics	69
4.6.3.2.4	Simplifications of G_p , R_{in} , and R_o Formulae . . .	70
4.6.4	Possible Oscillator Configurations	70
4.6.4.1	Oscillator Configurations Below 100 KC	70
4.6.4.1.1	Single-Stage Untuned Oscillators	71
4.6.4.1.2	Grounded Grid or Grounded Base Connections. . . .	72
4.6.4.1.3	Grounded Cathode or Grounded Emitter Connections	73

TABLE OF CONTENTS (Cont)

<u>Paragraph</u>	<u>Title</u>	<u>Page</u>
4. 6. 4. 1. 4	Triode Oscillator	74
4. 6. 4. 1. 5	Transistor Oscillator	76
4. 6. 4. 1. 6	Single-Stage Oscillator Using the Crystal to Give Phase Inversion	78
4. 6. 4. 1. 7	Two-Stage Untuned Oscillators	79
4. 6. 4. 2	Oscillator Configurations Above 100 KC	80
4. 6. 5	Impedance Transforming Networks	80
4. 6. 6	Design Procedure	81
4. 6. 6. 1	Step 1, Crystal Operation	81
4. 6. 6. 2	Step 2, Selection of Crystal Type	81
4. 6. 6. 3	Step 3, Oscillator Configuration	82
4. 6. 6. 4	Step 4, Desired Active Device Characteristics	82
4. 6. 6. 5	Step 5, Selection of Active Device	83
4. 6. 6. 6	Step 6, Determination of Active Device Characteristics	83
4. 6. 6. 7	Step 7, Calculation of Oscillator Component Values	83
4. 6. 6. 8	Step 8, Design of Impedance Transforming Network	84
4. 6. 6. 9	Step 9, Experimental Adjustments	84
4. 7	Impedance Transforming Networks	84
4. 7. 1	π Network	84
4. 7. 1. 1	π Network Analysis	84
4. 7. 1. 2	π Network Design	86
4. 7. 2	Capacitive Divider Network	90

TABLE OF CONTENTS (Cont)

<u>Paragraph</u>	<u>Title</u>	<u>Page</u>
4.7.2.1	Analysis of Capacitive Divider Network	90
4.7.3	Untuned Inductive Transformer	93
4.7.3.1	Inductive Transformer Analysis	93
4.7.3.1.1	Untuned Transformer, Heavy Secondary Load	94
4.7.3.1.2	Untuned Transformer Design, Heavy Secondary Load	97
4.7.3.1.3	Untuned Transformer, Light Secondary Load	99
4.7.3.1.4	Transformer Design, Light Secondary Load	102
4.7.4	Wien Bridge Network	103
4.7.4.1	Wien Bridge Network Analysis	103
5.0	CONCLUSIONS AND RECOMMENDATIONS	106
5.1	Conclusions	106
5.2	Recommendations	106
5.2.1	High-Frequency Oscillators	106
5.2.2	Low-Frequency Oscillators	107
6.0	IDENTIFICATION OF PERSONNEL	108
7.0	BIBLIOGRAPHY	109

OSCILLATOR DESIGN AND EVALUATION DATA

<u>Appendix</u>	<u>Title</u>	<u>Page</u>
A	150-MC Oscillator Using 2N917 Transistor	A-1
B	193-MC Oscillator Using 2N917 Transistor	B-1
C	120-MC Oscillator Using 2N2217 Transistor.	C-1
D	120-MC Oscillator Using 2N834 Transistor	D-1
E	75-MC Oscillator Using 2N2219 Transistor	E-1
F	100-MC Tube Oscillator Using 5718A Sub-Miniature Triode	F-1
G	150-MC Tube Oscillator Using 8058 Nuvistor	G-1
H	200-MC Tube Oscillator Using 5718A	H-1
I	200-MC Tube Oscillator Using 8058	I-1
J	1-KC Two-Stage Tube Oscillator Using 12AX7(Wien Bridge)	J-1
K	3-KC Two-Stage Tube Oscillator Using 12AX7(Wien Bridge)	K-1
L	1-KC Single-Stage Tube (12AT7) Oscillator Using the Quartz Crystal to Give Phase Inversion	L-1
M	1-KC Two-Stage Oscillator Using 2N336 Transistor (Tuned Output)	M-1
N	3-KC Two-Stage Oscillator Using 2N336 Transistor (Tuned Output)	N-1
O	3-KC Tuned Output Oscillator Using 2N336 Transistor . . .	O-1
P	20-KC Tuned Output Oscillator Using 2N336 Transistor. . .	P-1

LIST OF ILLUSTRATIONS

<u>Figure</u>	<u>Title</u>	<u>Page</u>
1	Equivalent Electrical Circuits of a Crystal	7
2	Impedance $ Z $, Resistance R_e , Reactance X_e , and Series Arm Reactance X_1 of a Crystal as a Function of Frequency . . .	9
3	Impedance Diagram of a Crystal	13
4	Series L C Circuit Phase Curve	13
5	Equivalent Parallel Crystal Circuit	14
6	Overall Frequency Tolerance	16
7	Effective Crystal Circuit in Series Resonant Oscillator	18
8	Crystal Dissipation Curve	19
9	Basic Oscillator	20
10	Basic Oscillator - Loop Broken	20
11	Grounded Grid Oscillator	23
12	Impedance Transforming Networks	26
13	Variation of Resistance and Reactance With Frequency of 1/2 watt Resistors	29
14	High Frequency Oscillators, Input and Output Circuits.	31
15	Active Device Configurations	36
16	Active Device Equivalent Circuit	37
17	Characteristics of a Unilateralized High-Frequency Transistor	44
18	Phase Angle Curve of a CR Lead Network	53

LIST OF ILLUSTRATIONS (Cont)

<u>Figure</u>	<u>Title</u>	<u>Page</u>
19	Diode Limiter Circuit	60
20	Transistor "Black Box"	67
21	Low Frequency Grounded Grid Oscillator	72
22	Grounded Cathode Tuned Oscillator	74
23	Grounded Emitter Tuned Oscillator	76
24	Crystal Position in Two Stage Oscillator	79
25	π Network Transformation	85
26	π Network Vector Relationships	86
27	Example of π Network Design	89
28	Capacitive Divider Coupling Network	90
29	Phase Shift Characteristics	92
30	Inductive Transformer	93
31	Primary Vector Diagram	95
32	Secondary Vector Diagram	95
33	Transformer Vector Diagram	96
34	Driven Transformer	97
35	Secondary Vector Diagram, Lightly Loaded	99
36	Driven Transformer, Lightly Loaded	100
37	Wien Bridge Network Circuit	103
38	Wien Bridge Network Vector Diagram	104

LIST OF TABLES

<u>Table</u>	<u>Title</u>	<u>Page</u>
1	Typical Crystal Parameter Values	8
2	Definitions of Symbols in Figure 2	9
3	Table of Impedance Transformations	11
4	Military Standard Crystals, High Frequency.	33
5	"Y" Parameter Variations with Frequency	45
6	Oscillator Frequency Tolerance(%)	51
7	Military Standard Crystals, Low Frequency	61
8	Twin Triode Characteristics	74

1.0 PURPOSE

The purpose of this program was to develop design procedures for quartz crystal oscillator circuits that are readily usable by the average electronic design engineer. In addition, the program included the development of performance data sheets for both vacuum tube and transistor oscillators covering the frequency range from 1 KC to 200 MC. The program was not concerned with extremely stable oscillators requiring oven control, but with non-temperature controlled medium stability circuits.

2.0 ABSTRACT

This Final Engineering Report presents extensive data supporting the design and operation of quartz crystal oscillators. Design procedures are developed for both high and low frequency oscillator circuits in the 1-KC to 200-MC range. Vacuum tubes and transistors were studied in both the low and the high frequency ranges (1 KC to 800 KC and 30 MC to 200 MC).

The report begins with a general discussion of the properties of quartz crystals, the characteristics of tubes and transistors, and impedance transforming networks. The general analysis of an oscillator is presented, a general design specification is developed, and a basic design procedure is established.

Separate sections are devoted to design procedures for high-frequency and low-frequency crystal oscillators. The report concludes with a design data section containing the results of oscillator evaluations during the program period.

3.0 PUBLICATIONS, LECTURES, REPORTS, AND CONFERENCES

3.1 Publications

None

3.2 Lectures

None

3.3 Reports

The first Quarterly Report, Magnavox Serial No. TP62-411, on the subject contract was distributed in accordance with USAELRDL instructions on 19 January 1962.

The second Quarterly Report, Magnavox Serial No. TP62-472, on the subject contract was distributed in accordance with USAELRDL instructions on 23 March 1962.

The third Quarterly Report, Magnavox Serial No. 62-554, on the subject contract was distributed in accordance with USAELRDL instructions on 20 July 1962.

3.4 Conferences

3.4.1 The first project conference on the subject contract was held at the USAELRDL Hexagon Building, Fort Monmouth, New Jersey, on 19 July 1961. In attendance were Messrs. O. P. Layden and S. Schodowski for USAELRDL and Messrs. H. G. Stewart, H. R. Meadows, and A. O. Plait for The Magnavox Company. Minutes of the meeting were prepared, submitted to USAELRDL, and are on file for reference.

3.4.2 The second project conference was held at The Magnavox Company, Fort Wayne, Indiana, on 6 October 1961. In attendance were Mr. S. Schodowski for USAELRDL and Messrs. A. O. Plait, D. Firth, and H. R. Meadows for The Magnavox Company. Minutes of the meeting were prepared, submitted to USAELRDL, and are on file for reference.

3.4.3 The third project conference was held at the USAELRDL Hexagon Building, Fort Monmouth, New Jersey, on 12 December 1961. In attendance were Messrs. O. P. Layden and S. Schodowski for USAELRDL and Messrs. O. F. Reynolds, E. D. Aldred, and H. R. Meadows for The Magnavox Company. Minutes of the meeting were prepared, submitted to USAELRDL, and are on file for reference.

3.4.4 The fourth project conference was held at The Magnavox Company, Fort Wayne, Indiana, on 23 January 1962. In attendance were Mr. O. P. Layden for USAELRDL and Messrs. H. R. Meadows, D. Firth, and A. O. Plait for The Magnavox Company. Minutes of the meeting were prepared, submitted to USAELRDL, and are on file for reference.

3.4.5 The fifth project conference was held at The Magnavox Company, Fort Wayne, Indiana, on 27 March 1962. In attendance were Mr. S. Schodowski for USAELRDL and Messrs. H. R. Meadows and D. Firth for The Magnavox Company. Minutes of the meeting were prepared, submitted to USAELRDL, and are on file for reference.

3.4.6 The sixth project conference was held at the USAELRDL Hexagon Building, Fort Monmouth, New Jersey, on 11 June 1962. In attendance were Messrs. S. Schodowski and O. P. Layden for USAELRDL and Messrs. H. R. Meadows, D. Firth, and J. R. Yope for The Magnavox Company. Minutes of the meeting were prepared, submitted to USAELRDL, and are on file for reference.

4.0 FACTUAL DATA

4.1 Introduction

This is the final report on a one-year study program under the sponsorship of USAELRDL, charged with the development of design procedures for crystal oscillators employing either tubes or transistors, in certain frequency bands where design procedures had not previously been established. The specific frequency bands of investigation were:

- (a) Crystal-controlled vacuum tube oscillator design from 1 KC to 800 KC.
- (b) Crystal-controlled transistor oscillator design from 1 KC to 16 KC.
- (c) Crystal-controlled vacuum tube oscillator design from 150 MC to 200 MC.
- (d) Crystal-controlled transistor oscillator design from 30 MC to 200 MC.

Oscillator design at frequencies intermediate to those of (a), (b), (c), and (d) above is covered in the final reports of two other study programs sponsored by the USAELRDL (Reference 1 and 2, Paragraph 7.0).

The contract period was from 1 July 1961 to 30 June 1962, and approximately 28 man-months of effort were involved.

4.1.1 Philosophy of Approach

To some extent, the design of quartz crystal oscillators has always been surrounded by an aura of mystery; capable engineers who would not normally resort to "cut and try" methods do so when faced with crystal oscillator design.

This appears to be due in part to the historical literature which tends to emphasize the more obscure details of the subject at the expense of the essentials. Technical articles of this type tend to overawe the designer faced with the mundane task of designing an oscillator of more moderate performance. Not that such discussions are without value, but reports of this type often wrongly assume that the reader is fully conversant with the details of the design of less sophisticated oscillators.

The objective of this report is to present to the user the essential knowledge that is required to appreciate the design problem, to supplement this with information concerning the components of the oscillator circuit, and to associate these into a design procedure that leads to satisfactory designs.

Because of the normally non-linear operation of an oscillator, a true mathematical model would consist of a series of non-linear equations describing the action of the circuit. These equations would define the circuit action completely, and from them it would be possible to predict all the operating characteristics of an oscillator. However, the difficulties of this approach are formidable. Even simple non-linear equations are difficult to manipulate, and when it is considered that the non-linear characteristics of a transistor, tube, or quartz crystal vary with power level, frequency and temperature, the difficulties of this approach are apparent.

As is usual under these circumstances, the design approach falls back on the use of linear describing equations, which are at least valid for establishing the necessary conditions for oscillation to commence, and supplements this approach with experimentally gathered information to allow a reasonable degree of circuit performance prediction. This simplifies the oscillator equations considerably while increasing the importance of the experimental data. Because of this, the major part of this program was devoted to the study of the practical aspects of oscillator design, with detailed evaluations of various oscillators covering the frequency bands under discussion.

4.1.2 Report Layout

This report consists of the following four sections:

- (a) An introductory section containing general information concerning the properties of:
 - (1) Quartz crystals
 - (2) Tube and transistor characteristics
 - (3) Impedance transforming networks

Other topics covered in this section are:

- (4) A general analysis of an oscillator
- (5) The general design specification of the performance of an oscillator

- (6) A rudimentary design procedure establishing the design decisions that are required to produce a design meeting the specification
- (b) A section devoted to high-frequency crystal oscillator design, discussing quartz crystal and active device characteristics in specific terms applicable to design at high frequencies. This information is then regrouped to form a step-by-step design procedure.
- (c) A section devoted to low-frequency crystal oscillators having a similar form to section (b).

Appended to sections (b) and (c) is a sub-section containing analyses of several impedance transforming networks together with design information.

- (d) A design data section containing the results of the evaluations of the experimental oscillators constructed during the contract period.

4.2 Quartz Crystal Characteristics

4.2.1 General

A quartz crystal resonator is an electromechanical transducer having piezoelectric properties. The application of an electrical potential to the quartz crystal produces a mechanical stress within the crystal structure similar to that obtained by the application of mechanical force. Conversely, the application of mechanical force to the crystal creates a potential difference across the crystal structure. Therefore, by suitably connecting two or more electrodes to a quartz crystal, it can be made to vibrate by applying an alternating voltage to these electrodes. If the output of the alternating voltage source is held constant and the frequency continuously varied, certain frequencies will be found at which the amplitude of the mechanical vibration becomes a maximum. These are the frequencies at which the quartz crystal goes into mechanical resonance.

Because of the electromechanical coupling in the crystal, the mechanical motion of the crystal appears at the input terminals as an electrical tuned circuit at frequencies in the immediate vicinity of the mechanical resonant frequencies. The important electrical properties of the quartz crystal are:

- (a) The high effective Q of the quartz crystal; that is, the high ratio of energy stored in the crystal relative to the energy dissipated in storing that energy.

- (b) The wide range of frequencies over which quartz crystals can be made to resonate.
- (c) The excellent stability of the electrical parameters of the quartz crystal when subjected to temperature changes.

These three properties account for their wide use in stable oscillator designs.

The equivalent electrical circuit of a quartz crystal resonator is shown in Figure 1. L_1 and C_1 are primarily dependent on the mass and compliance of the quartz, and R_1 is mostly determined by the means of supporting the crystal and attaching the electrodes.

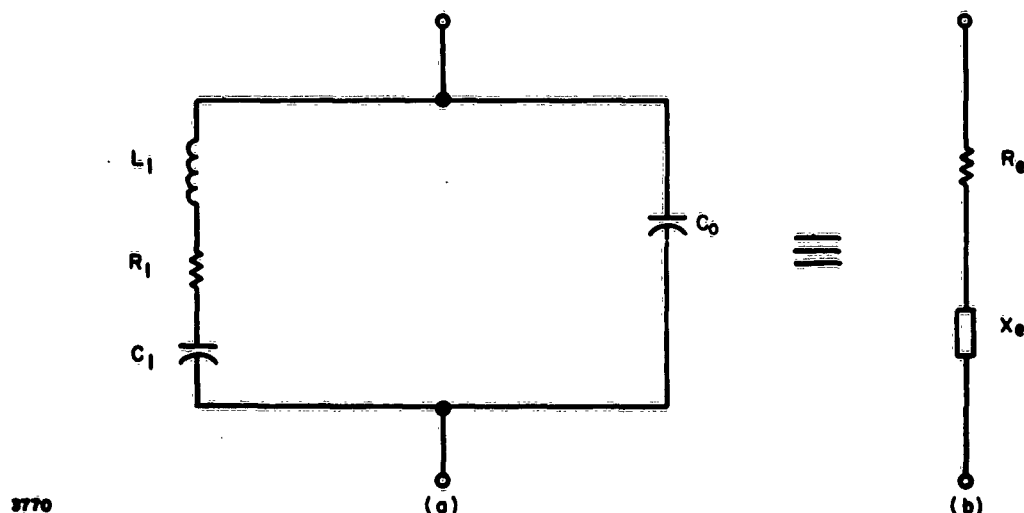


Figure 1. Equivalent Electrical Circuits of a Crystal

These are the motional impedance elements of the crystal, so called because they are the effective electrical equivalents of the vibratory motion of the crystal. C_0 is an actual electrical capacitance due to the electrode attachments to the quartz and to the stray capacitance in the assembly. Typical values of the parameters for 200 KC, 2 MC, and 30 MC crystals are shown in Table 1.

This circuit is not a valid representation of the electrical characteristics of a crystal at all frequencies. Every mechanical structure has several modes of resonance. A simple bar, for example, has flexural, torsional, shear, and extensional modes of oscillation in each of the three axes.

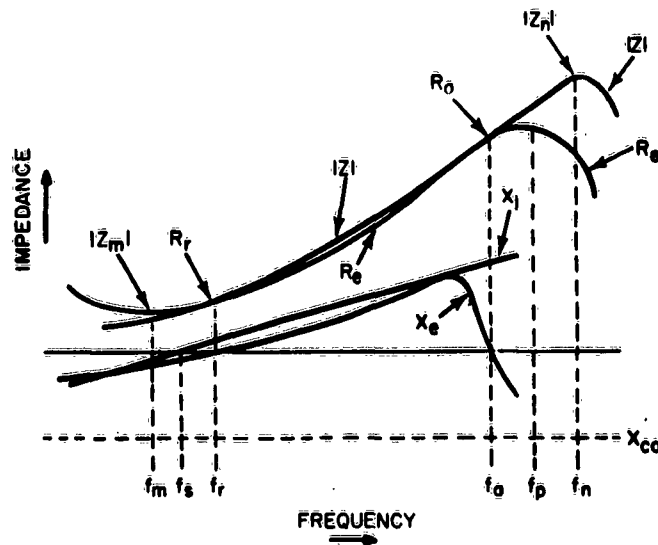
TABLE 1. TYPICAL CRYSTAL PARAMETER VALUES

Parameters	200 KC	2 MC	30 MC
R_1	2 K	100 ohms	20 ohms
L_1	27 H	520 MH	11 MH
C_1	0.024 PF	0.012 PF	0.0026 PF
C_0	9 PF	4 PF	6 PF
Q	18×10^3	54×10^3	10^5

Furthermore, mechanical resonance can be excited at the overtones of each of these basic modes. The manufacturer shapes, proportions, and clamps the crystal so as to make one of these mechanical resonances predominant while suppressing all others that could possibly occur at frequencies immediately adjacent to this desired one. If, as is normally the case, sufficient suppression of the undesired resonances is achieved, the circuits of Figure 1 are valid electrical equivalents of the electro-mechanical characteristics of the crystal in the frequency band immediately around the predominant mechanical resonance frequency.

With this restriction, the behavior of the quartz crystal can be discussed in terms of the electrical equivalent circuit of Figure 1 (a) where L_1 , C_1 , R_1 , and C_0 are essentially independent of frequency. In the frequency band of interest, this circuit can be considered as a series combination of a resistance R_e and a reactance X_e as shown in Figure 1 (b). The values of R_e and X_e are frequency dependent and vary in the general manner indicated in Figure 2 as functions of frequency. The various symbols are defined in Table 2, and the impedance levels should be regarded as plotted to a logarithmic scale. Figure 2 and Table 2 are reproduced from the "I. R. E. Standards on Piezoelectric Crystals - The Piezoelectric Vibrator: Definitions and Methods of Measurement, 1957." *

*Contained in the March 1957 Proceedings of the I. R. E.



3771

Figure 2. Impedance $|Z|$, Resistance R_e , Reactance X_e , and Series Arm Reactance X_1 of a Crystal as a Function of Frequency

TABLE 2. DEFINITIONS OF SYMBOLS IN FIGURE 2

Symbol	Definition
r	Capacitance ratio = $\frac{C_0}{C_1}$
f_m	Frequency of minimum impedance
f_s	Motional arm resonance frequency = $\frac{1}{2\pi \sqrt{L_1 C_1}}$
f_r	Resonance frequency ($X_e = 0$)
f_a	Antiresonance frequency ($X_e = 0$)
f_p	Parallel resonance frequency = $\frac{1}{2\pi} \left[\frac{1}{L_1 C_1} \left(1 + \frac{1}{r}\right) \right]^{1/2}$
f_n	Frequency of maximum impedance
R_r	Resonance resistance ($X_e = 0$)
R_a	Antiresonance resistance ($X_e = 0$)
Z_m	Impedance at f_m (minimum crystal impedance)
Z_n	Impedance at f_n (maximum crystal impedance)

Interpreting the points of interest on the curves of Figure 2 from left to right, f_s is the frequency at which the motional arm is series resonant. At this frequency the crystal appears at its terminals as a combination of R_1 in parallel with C_0 . At high frequencies, where it is common practice to tune C_0 with an inductive shunt, f_s is the desirable crystal operating point. At a slightly higher frequency, the motional arm reactance X_1 is inductive and of such a value that its equivalent inductance when transformed to a parallel element (see Table 3 (b)) resonates with C_0 . The formulae illustrating this effect are:

$$X_p = X_1 \left(1 + \frac{1}{Q_r^2} \right) = X_{C_0} \quad (1)$$

$$\text{and} \quad R_p = R_r = R_1 (1 + Q_r^2) \quad (2)$$

$$\text{where} \quad Q_r = \frac{X_1}{R_1} \text{ at frequency } f_r$$

Equation (1) shows that $X_p \gg X_1$, provided that $Q_r \ll 1$; that is, $X_1 \ll R_1$. Equation (2) shows that R_r differs from R_1 by the factor $(1 + Q_r^2)$, and since this is practically equal to 1 under the assumed conditions, R_r is almost equal to R_1 .

As the frequency is further increased, the value of $|Z|$ also increases rapidly until at frequency f_a , X_e again falls to zero and R_e has the value R_a . At this frequency the equivalent motional arm inductance X_1 again resonates with C_0 and Equations (1) and (2) can be restated as:

$$X_p = X_1 \left(1 + \frac{1}{Q_a^2} \right) = X_{C_0} \quad (3)$$

$$R_p = R_a = R_1 (1 + Q_a^2) \quad (4)$$

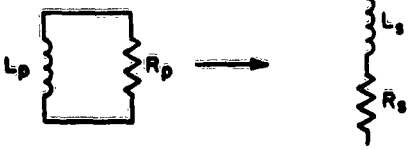
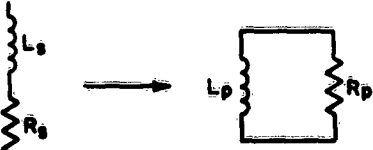
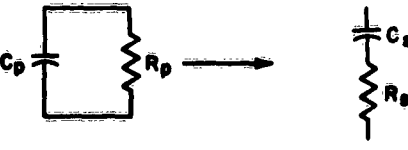
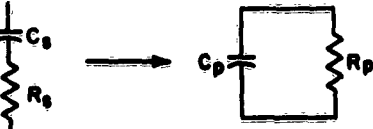
$$\text{where } Q_a = \frac{X_1}{R_1} \text{ at frequency } f_a$$

At f_a , however, $Q_a \gg 1$ (see behavior of X_1 characteristic) and, therefore,

$$X_p \approx X_1 \quad (5)$$

$$\text{and} \quad R_p = R_a \approx R_1 Q_a^2 \quad (6)$$

TABLE 3. TABLE OF IMPEDANCE TRANSFORMATIONS

(a) 	$R_s = R_p \left[\frac{1}{1 + \frac{R_p^2}{\omega^2 L_p^2}} \right] = R_p \left[\frac{1}{1 + Q^2} \right]$ $L_s = L_p \left[\frac{1}{1 + \frac{\omega^2 L_p^2}{R_p^2}} \right] = L_p \left[\frac{1}{1 + \frac{1}{Q^2}} \right]$
(b) 	$R_p = R_s \left[1 + \frac{\omega^2 L_s^2}{R_s^2} \right] = R_s [1 + Q^2]$ $L_p = L_s \left[1 + \frac{R_s^2}{\omega^2 L_s^2} \right] = L_s \left[1 + \frac{1}{Q^2} \right]$
(c) 	$R_s = R_p \left[\frac{1}{1 + \omega^2 C_p^2 R_p^2} \right] = R_p \left[\frac{1}{1 + Q^2} \right]$ $C_s = C_p \left[1 + \frac{1}{\omega^2 C_p^2 R_p^2} \right] = C_p \left[1 + \frac{1}{Q^2} \right]$
(d) 	$R_p = R_s \left[1 + \frac{1}{\omega^2 C_s^2 R_s^2} \right] = R_s [1 + Q^2]$ $C_p = C_s \left[\frac{1}{1 + \omega^2 C_s^2 R_s^2} \right] = C_s \left[\frac{1}{1 + \frac{1}{Q^2}} \right]$

Other frequencies of lesser interest are f_m and f_n , the frequencies at which the crystal exhibits its minimum and maximum impedances, respectively, and f_p , the frequency at which the motional arm reactance would be in series resonance with C_0 if this were possible. It should be noted that f_p does not coincide with the antiresonant frequency f_a because of the finite Q of the motional arm.

The impedance curves of Figure 2 can also be presented as an impedance plane loci as shown in Figure 3. This presentation is valid, provided that

$$\frac{1}{2\pi (f_n - f_m) C_0} \gg R_1.$$

An indication of the bandwidth in which these effects occur may be obtained by noting that for most crystals, the capacitance ratio r lies between 200 and 500. Substituting a typical value of $r = 300$ into the equation for f_p , the ratio of f_p to f_s gives:

$$\frac{f_p}{f_s} = \left(1 + \frac{1}{r}\right)^{1/2} \approx 1 + \frac{1}{2r} = 1.0017 \quad (7)$$

For example, if $f_s = 1$ MC, then the bandwidth within which the crystal resonance effects occur will be typically less than 2 KC.

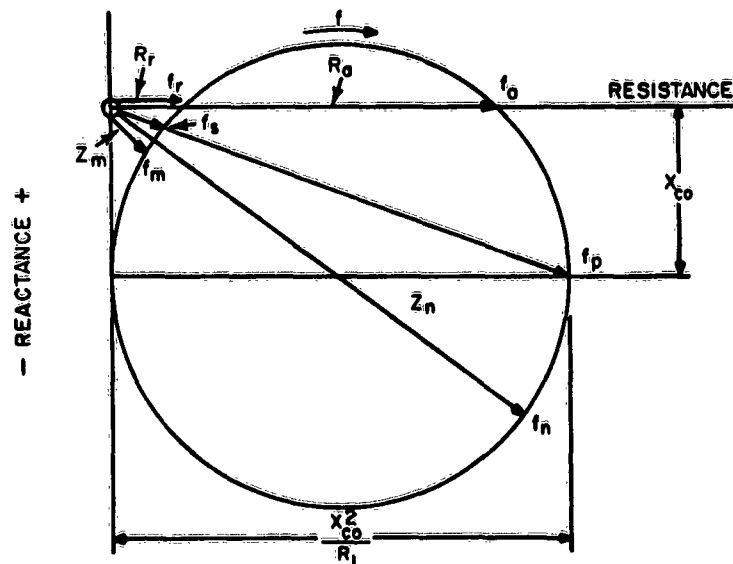
The spacing between f_s and f_r can be shown to be very small (Reference 3, Paragraph 7.0); frequency differences of 1 or 2 parts per million are typical. The frequency difference between f_s and f_m is equal to that between f_s and f_r .

4.2.1.1 Frequency Stabilizing Properties of the Quartz Crystal

The frequency stability of an oscillator is dependent on the stability of the phase shifts existing within the feedback loop and the rate of change of phase shift with frequency, $\frac{d\phi}{df}$, of the frequency controlling element. The total loop phase shift in the oscillator has to remain zero at all times if oscillation is to be maintained, and any phase changes occurring external to the frequency controlling element have to be cancelled by an equal but opposite phase change in this element. A large $\frac{d\phi}{df}$ is therefore the important characteristic of the frequency controlling element, and the quartz crystal can exhibit this characteristic for two conditions of operation; that is, when the crystal operates at resonance or at parallel resonance.

(a) Operation at Resonance

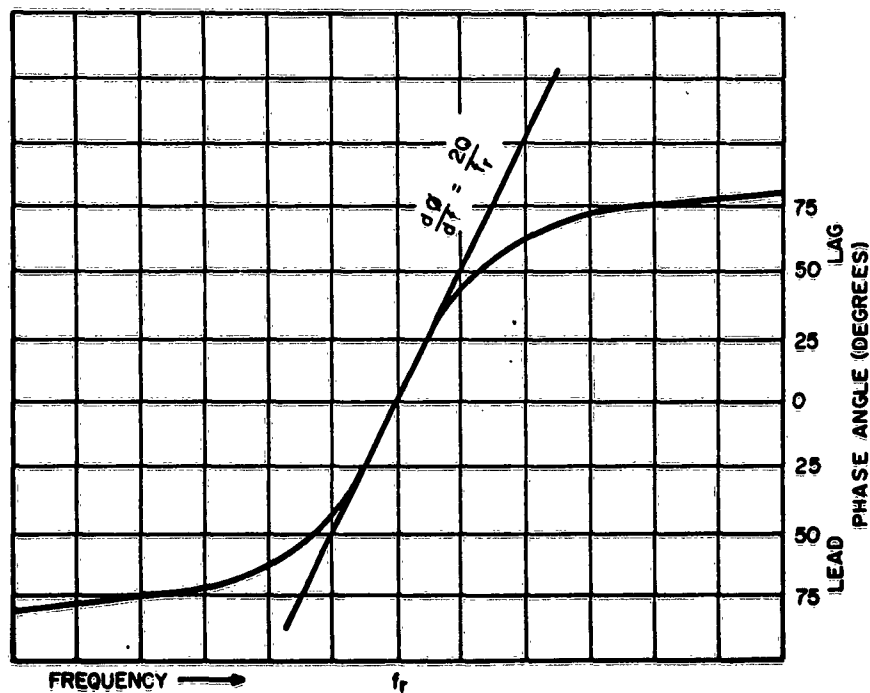
When the crystal is operated at resonance, the frequency stabilizing effect occurs in the vicinity of f_r and is dependent on the ability of the crystal to shift the



3772

Figure 3. Impedance Diagram of a Crystal

phase of the crystal current relative to that of the drive voltage. Figure 3 shows the relatively large phase change that occurs between f_s and f_r , two frequencies separated by only a few parts per million and which is indicative of a large $\frac{d\phi}{df}$. The behavior



3773

Figure 4. Series LC Circuit Phase Curve

of the phase shift with frequency is of the form shown in Figure 4, the phase angle part of the universal resonance curve of a tuned LC circuit (Reference 4, Paragraph 7.0). It can be shown that, in the immediate vicinity of f_r :

$$\frac{d\phi}{df} = \frac{2Q}{f_r} \quad (8)$$

This indicates the importance of the crystal Q on its frequency stabilizing properties. However, in order to make use of this property, it is necessary to sample the crystal current and this can be done only by the inclusion of an impedance in series with the crystal. In this process, power has to be supplied to this impedance (see Paragraph 4.2.2); that is, this impedance has a resistive component effectively in series with the crystal. This network therefore has greater losses than the crystal alone and, consequently, has a lower Q than that of the crystal. Because of the dependence of oscillator frequency stability on crystal Q , it is in the interest of frequency stability to make this effective series resistance small relative to R_r . Similarly, the driving source will also introduce a resistance in series with the crystal, resulting in a further degradation of the crystal Q .

A similar reduction in the frequency stabilizing property of the crystal will also occur if the frequency of oscillation is not in the immediate vicinity of f_r , since as Figure 4 shows, the slope of the phase curve $\frac{d\phi}{df}$ decreases at frequencies removed from f_r .

(b) Operation at Parallel Resonance

In parallel resonance operation, the crystal in conjunction with an external parallel capacitor C_L forms a parallel resonant circuit as shown in Figure 5, where:

$$X_1 = X_{L_1} - X_{C_1} \quad (9)$$

$$\text{and} \quad C_T = C_0 + C_L \quad (10)$$

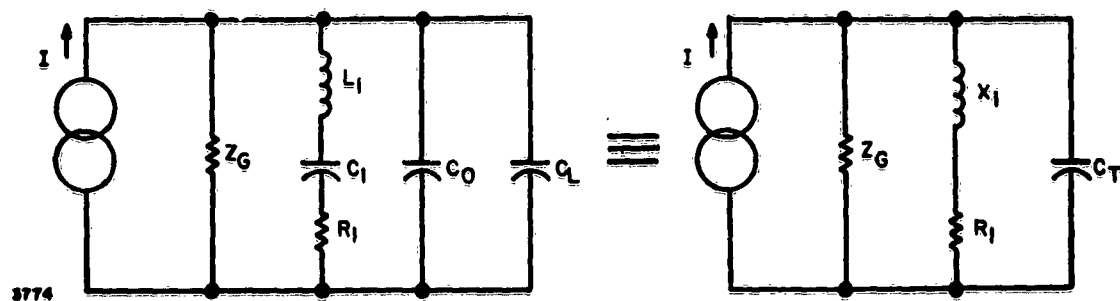


Figure 5. Equivalent Parallel Crystal Circuit

The antiresonant frequency f'_a is intermediate between f_s and f_a and can be regarded as a special case of f_a . If this circuit is fed from a constant current source, the behavior of the phase angle of the crystal voltage relative to the phase of the supply current is similar to that shown in Figure 4, if the sign of the phase shift is reversed. Equation (8) is again applicable in determining the rate of change of phase angle, and the reduction of this rate by the external circuit can best be illustrated by transforming R_1 into its parallel equivalent resistor R'_a . Equation (4) shows that:

$$R'_a = R_1 (1 + Q'^2_a) \quad (11)$$

where

$$Q'_a = \frac{X_1}{R_1} \text{ at frequency } f'_a$$

Direct comparison can now be made between R_G , the effective resistance of the driving source acting in parallel with the crystal, and R'_a . A value of $R_G = R'_a$ will reduce the Q and, hence, $\frac{d\phi}{df}$ by 2. A similar Q degradation occurs due to the effective parallel resistance of the circuit used to sample the voltage across the crystal.

Both methods of crystal operation indicate the importance of the crystal Q on oscillator stability and the need to minimize the degrading effect of the driving and phase shift sampling circuits. In practice, because of the effects discussed in Paragraph 4.2.2, a compromise is necessary, and loading that reduces the Q by a factor of 2 or 3 is considered permissible.

4.2.1.2 Oscillator Frequency Tolerance

All military standard crystal units have a specified frequency tolerance to which they must conform. This specification guarantees that any crystal manufactured to the standards of the particular crystal type number will be in resonance, or parallel resonance with a specified loading capacitor, at the nominal frequency stamped on the crystal holder to within the given tolerance, and over the specified operating temperature range. This tolerance makes allowances for:

- (a) The effect of temperature on the crystal resonance (or parallel resonance) frequency and the variations in the magnitude of this effect from unit to unit.
- (b) The accuracy with which the crystal unit resonance (or parallel resonance) frequency can be adjusted in manufacture.

As an illustration, Figure 6 defines the frequency tolerance of a wide temperature range crystal. The tolerance is assumed to be ± 0.005 percent, and the characteristics are typical of an AT-cut crystal showing the changes of f_r or f_a as a function of temperature. f_n is the nominal crystal frequency as marked on the crystal holder. As shown in curves (a) and (b), the actual deviation due to temperature may be no more than ± 0.002 percent, but an additional ± 0.003 -percent manufacturing allowance is contained in the overall frequency tolerance. In a large batch of crystals of the same nominal frequency, crystals will be found exhibiting the extremes of curves (a) and (b) as well as the intermediate characteristics shown in (c).

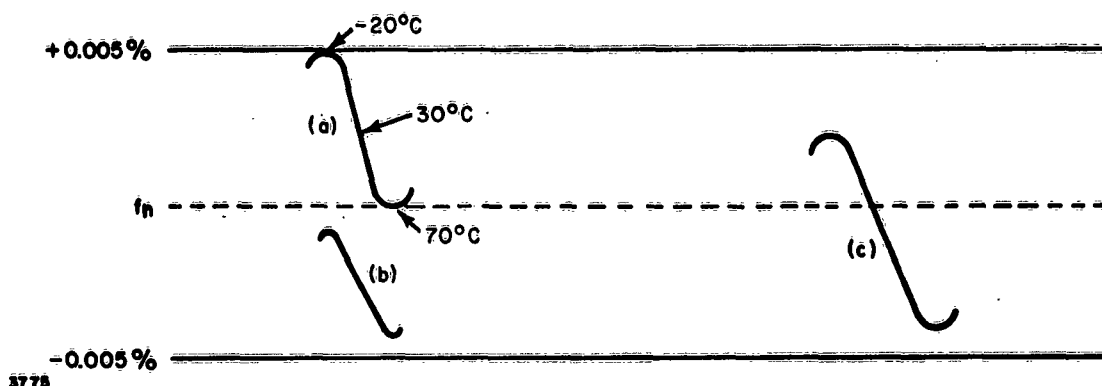


Figure 6. Overall Frequency Tolerance

The overall oscillator frequency tolerance is partially determined by the crystal frequency tolerance. Any phase shift or changes of phase occurring within the remainder of the oscillator circuit will require equal and opposite compensating phase changes in the crystal. Since the crystal phase angle cannot change without a proportionate change in oscillator frequency, an additional frequency tolerance in excess of that of the crystal is incurred. This effect can be considered as having the following two components:

- (a) A constant miscorrelation of oscillator and crystal frequencies due to a constant phase error existing in the remainder of the oscillator circuit. This phase error can be due to numerous causes which cannot be discussed meaningfully without digressing into a general discussion of oscillator characteristics. It is sufficient to state that such constant phase errors can occur and may result in considerable mis-correlation between the oscillator and crystal frequencies.
- (b) A variant oscillator frequency error due to changes in the phase angle of the remainder of the oscillator circuit due to the effects of temperature, voltage, aging, etc.

The correction of a constant phase error is a simple matter requiring only that a complementary phase shift be introduced to give frequency correlation. The existence of a fixed phase error can be determined by using a Crystal Impedance Meter, one of the functions of which is to determine the f_r or f_a of a crystal. Comparison of the frequency measured, using this apparatus under the prescribed testing conditions, with that of the oscillator shows the amount of miscorrelation due to fixed phase error in the oscillator. Adjustments can then be made to the oscillator circuit until agreement between the two frequencies is reached.

The above process requires little effort, and large values of miscorrelation are inexcusable when the effect on oscillator overall frequency tolerance is considered. However, it is reported that miscorrelation is responsible for the great majority of crystal misapplications in military equipments, and it is clear that increased emphasis is required on this point in oscillator design.

The variable phase error component is more difficult to correct because of the temperature dependence of virtually all the circuit components. Because of this it is advisable to use high-quality components in all parts of the circuit where signal flow occurs. If this is insufficient, temperature compensating components will be required.

The experiences of this program show that if only the precaution of using high-quality components is used, the overall oscillator frequency tolerance can be expected to be 1.2 to 2 times that of the crystal alone. For example, a number of oscillators using a crystal with an overall frequency tolerance of ± 0.005 percent will each have an overall frequency tolerance of between ± 0.006 and ± 0.01 percent, depending on the phase stability of the remainder of the oscillator circuit.

4.2.1.3 Crystal Power Dissipation

The crystal power dissipation level can have a marked influence on the performance of a crystal. The major effect is the increased frequency drift with time as the power dissipation is increased. All military standard crystals have specified maximum power dissipation which should not be exceeded under any circumstances.

The crystal specification only defines $R_r \text{ max}$, the maximum value of R_r and the range of values encountered in practice can be wide, particularly for crystals designed to operate below 20 MC. Most crystals will have R_r values of 0.25 to 0.5 $R_r \text{ max}$ but the total range is likely to be of the order of $\frac{1}{9} R_r \text{ max}$ to $R_r \text{ max}$.

The effects of the possible variation of R_r on crystal dissipation are analyzed with the aid of Figure 7 which shows the crystal connected as a series element between a supply source of resistance R_G and a load R_{in} . This is typical of the crystal operating conditions in a series resonant oscillator. The crystal dissipation P_c will be:

$$P_c = \frac{V^2 R_r}{(R_G + R_{in} + R_r)^2} \quad (12)$$



3776

Figure 7. Effective Crystal Circuit in Series Resonant Oscillator

Referring to Paragraph 4.2.1.1 regarding the crystal Q degradation due to the terminating resistance levels, a value of $(R_G + R_{in}) = \frac{1}{3} R_r \text{ max}$ will result in a Q degradation of 4 for a crystal having $R_r = \frac{1}{9} R_r \text{ max}$.

Assuming this to be a suitable terminating level:

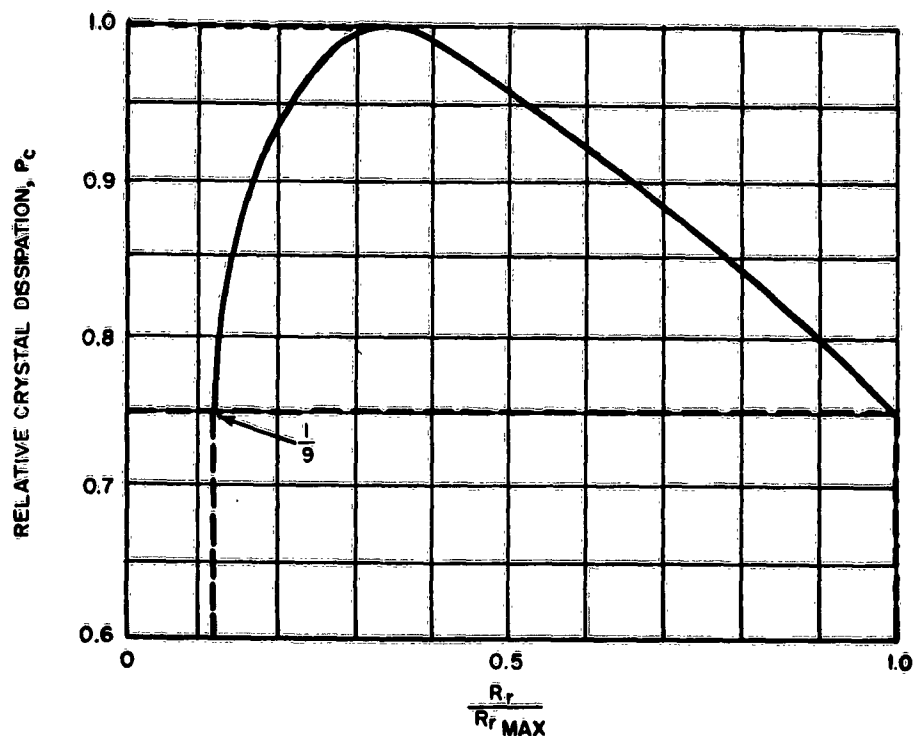
$$P_c = \frac{\frac{V^2}{R_r \text{ max}}}{\frac{R_r}{R_r \text{ max}} \left(1 + \frac{R_r \text{ max}}{3 R_r}\right)^2} \quad (13)$$

$R_r \text{ max}$ is a constant for a given crystal type, and if V is held constant, the crystal power dissipation equation reduces to:

$$P_c = \frac{k}{\frac{R_r}{R_r \text{ max}} \left(1 + \frac{R_r \text{ max}}{3 R_r}\right)^2} \quad (14)$$

Normalizing and plotting Equation (14) for a range of $\frac{R_r}{R_r \text{ max}}$ values gives the graph of Figure 8 (parameter $R_G + R_{in} = \frac{1}{3} R_r \text{ max}$).

This curve shows that, under the given terminating conditions, a crystal having $R_r = \frac{1}{3} \cdot R_r \text{ max}$ will have the highest dissipation for a fixed value of input voltage V . In practice, V will not be constant due to the imperfect limiting action of the active device and will be larger for lower values of R_r . The maximum dissipation will, therefore, probably occur for a crystal of $0.2 R_r \text{ max}$.



3777

Figure 8. Crystal Dissipation Curve

The dashed lines indicate the limits of crystal dissipation that will occur for crystal resonant resistances lying between $\frac{1}{9} R_{r \text{ max}}$ and $R_{r \text{ max}}$ for the given terminating condition. In this example the change in dissipation is not large. This is due to the particular value of terminating resistance chosen; smaller values would result in larger deviations.

Equation (12) is, of course, the well known power transfer equation if R_G and R_{in} are lumped together. It follows that maximum crystal power dissipation will always occur for the condition where the crystal resistance equals the combined sum of the source and load resistance.

4.2.2 Analysis of an Oscillator

The previous discussion establishes the necessary elements of an oscillator; namely, a tuned circuit element and an active device. It also points out the interaction that occurs between these components and the necessity of minimizing this interaction. This, in turn, implies the manipulation of impedance levels within the oscillator circuit to satisfy this condition and, hence, the use of impedance transforming networks.

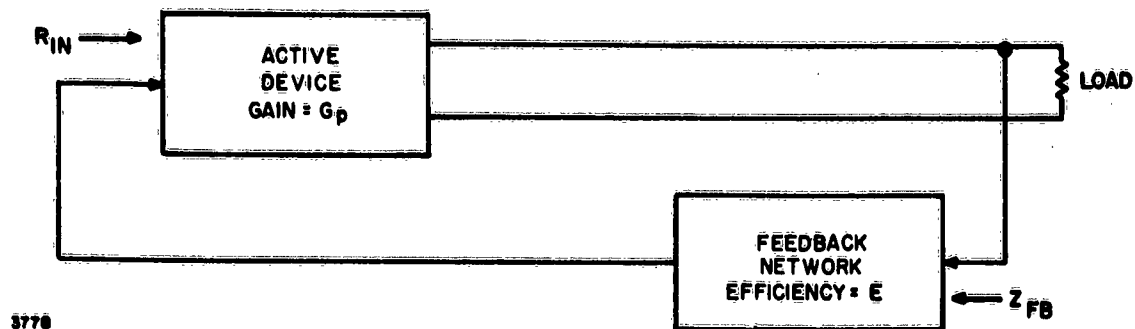


Figure 9. Basic Oscillator

Figure 9 shows the basic oscillator. The block marked "ACTIVE DEVICE" represents the tube or transistor with its associated biasing networks, and the block labelled "FEEDBACK NETWORK" contains the crystal together with any required impedance matching transformers. The feedback network receives power from the output of the active device and supplies power to the control electrode of the active device.

Linear network theory shows that oscillation can only occur when these two conditions are satisfied:

Condition (a)- The loop power gain must be equal to or greater than unity.

Condition (b)- The loop phase angle must equal zero.

These conditions can be interpreted for convenience of analysis as shown in Figure 10, which shows the oscillator circuit of Figure 9 with the connection between the active device output and the feedback network broken and with an additional load impedance Z_{FB} (equal to that of the feedback network when loaded with the active device input impedance) connected to the active device output.

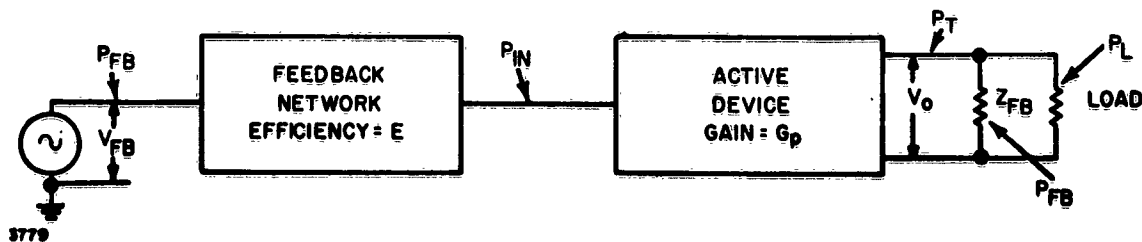


Figure 10. Basic Oscillator - Loop Broken

If the applied signal voltage V_{FB} produces an output voltage V_o equal to V_{FB} , then Condition (a) is satisfied, since the power into the feedback network equals the power into Z_{FB} , which, by definition, equals the feedback network input impedance. In addition, the phase V_o relative to V_{FB} must equal zero degrees or, the equivalent, any integral multiple of 360 degrees.

In a practical design, if the loop gain was unity, the oscillator performance would be poor, since the loop gain is a function of the active device gain which is, in turn, dependent on power supply, external load, and ambient temperature variations. Small changes in any of these factors would probably reduce the loop gain below unity, with a resultant cessation of oscillation. A more practical requirement is that the loop gain should be greater than unity to insure that the gain never falls to unity under the most adverse operating conditions likely to be encountered. Condition (a) must, therefore, be modified to read as follows:

Condition (c) - The loop power gain must be greater than unity.

Referring to Figure 10, the active device power gain may be defined as:

$$G_p = \frac{\text{Power into the total load resistance } R_T}{\text{Power into the active device input}} = \frac{P_T}{P_{in}} \quad (15)$$

and the feedback network efficiency as:

$$E = \frac{\text{Power into the active device input}}{\text{Power into the feedback network}} = \frac{P_{in}}{P_{FB}} \quad (16)$$

Then the net power gain between the feedback network input and the active device output is:

$$G'_p = E \cdot G_p = \frac{P_T}{P_{FB}} \quad (17)$$

$$\text{but} \quad P_T = P_L + P_{FB} \quad (18)$$

$$\text{and therefore } P_{FB} \cdot E \cdot G_p = P_L + P_{FB} \quad (19)$$

$$\text{or} \quad P_{FB} (G'_p - 1) = P_L \quad (20)$$

Now assuming that all reactive elements in the load and feedback network input impedance are tuned out, P_L and P_{FB} are the power dissipation in R_L and R_{FB} , respectively, and the relationship between them can be obtained by noting that:

$$P_L = \frac{V_o^2}{R_L} \quad (21)$$

and $P_{FB} = \frac{V_o^2}{R_{FB}} \quad (22)$

Substituting in Equation (20) gives:

$$\frac{R_{FB}}{R_L} = G'_p - 1 \quad (23)$$

Further manipulation gives:

$$R_T = R_L \cdot \frac{G'_p - 1}{G'_p} \quad (24)$$

and $R_T = \frac{R_{FB}}{G'_p} \quad (25)$

In these equations, any losses in the output tuning network are considered to be part of P_L .

Gathering the equations together:

$$G'_p = E \cdot G_p \quad (26)$$

$$\frac{P_L}{P_{FB}} = G'_p - 1 \quad (27)$$

$$\frac{R_{FB}}{R_L} = G'_p - 1 \quad (28)$$

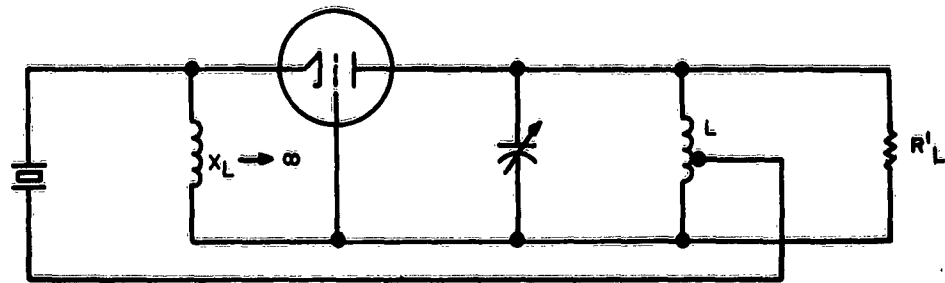
$$\frac{R_T}{R_L} = \frac{G'_p - 1}{G'_p} \quad (29)$$

$$\approx 1 \text{ if } G'_p \geq 10$$

$$\frac{R_{FB}}{R_T} = G'_p \quad (30)$$

These equations show that G'_p governs the necessary impedance levels associated with the oscillator. It also determines the maximum power output of the oscillator, since the maximum permissible feedback power $P_{FB \text{ max}}$ is limited by the permissible crystal dissipation; the crystal being one of the dissipative elements in the feedback network.

A simple example will illustrate the use of these formulae. Referring to Figure 11 and making the following assumptions:



3780

Figure 11. Grounded Grid Oscillator

- (a) The power gain G_p of the triode is 50 when loaded with $R_T = 10 \text{ K}$.
- (b) The input resistance R_{in} of the triode under these conditions is 200 ohms.
- (c) The effective resistance of the crystal at resonance R_T is 100 ohms.
- (d) The maximum allowable crystal dissipation is 2 MW.
- (e) The effective parallel loss resistance of the coil L is 40 K.

To finalize the design, the values of R_L and R_{FB} have to be determined:

$$E = \frac{R_{in}}{R_{in} + R_T} = 0.67 \quad (31)$$

then $G'_p = 34 \quad (32)$

and $R_L = \frac{G'_p \cdot R_T}{G'_p - 1} \approx R_T = 10 \text{ K} \quad (33)$

The coil losses are included in this value and $R'_L = 13 \text{ K}$ (34)

$$R_{FB} = G'_p \cdot R_T = 340 \text{ K} \quad (35)$$

The impedance reflected into the plate side of the impedance transformer L must be 340 K when the secondary side is loaded with $R_e + R_{in}$. The impedance transformer ratio T_r will therefore be:

$$T_r = \frac{340 \times 10^3}{300} = 1100 \quad (36)$$

For simplicity in this example, it is assumed that the coil L has unity coupling between turns, giving a turns ratio of:

$$N = \sqrt{1100} = 33 \quad (37)$$

As previously stated, in any practical design the required feedback power will be at least twice the amount indicated in these equations, to allow for circuit variations. This can be taken into account by introducing a modified value of G'_p ; i.e., by using $G''_p = \frac{G'_p}{2}$ or $\frac{G'_p}{3}$ in Equations (33) and (35). The resulting R_{FB} will be

decreased, giving increased feedback power.

The permissible power output to the load R'_L before crystal overdrive occurs can be determined by noting that 33 percent of the feedback power is dissipated in the crystal. The maximum permissible feedback power is therefore 6 MW.

$$\begin{aligned} P_{out} &= P_{FB} \cdot G'_p \\ &= 6 \times 10^{-3} \times 34 = 204 \text{ MW} \end{aligned} \quad (38)$$

Using a more realistic value of G'_p ($G'_p = 11$, for example) will give a power output in the region of 60 to 70 MW. It is then a simple matter to determine the values of all components to complete the design.

This example demonstrates the simplicity of oscillator design once the parameters of the various circuit elements are known. In some cases, these parameters are directly available through manufacturer's data sheets and present no problem other than that of interpretation. In other instances, little directly usable information is available, and the determination of the characteristics of the circuit elements becomes a major design problem.

The next three sections give general background information concerning the characteristics of the oscillator circuit elements.

4.2.3 Active Device Characteristics

In Paragraph 4.2.2 the importance of the power gain of the active device in the oscillator equations is noted. The characteristics of the active device that influence an oscillator design are:

- (a) The power gain of the device as a function of output loading
- (b) The input impedance of the device as a function of output loading
- (c) The phase angle between input and output as a function of output and input loading
- (d) Power output versus supply voltage, current, and load
- (e) Variations in the above due to changes in temperature
- (f) Gain stability as a function of gain magnitude

From DC to 10 MC the manufacturer's data sheets usually supply sufficient parameter information to enable characteristics (a) to (e) to be determined by calculation with a reasonable degree of accuracy, while (f) is of minor importance at these frequencies. Above 10 MC the parasitic reactive elements and the physical dimensions of the active device begin to have an increasing effect on operation. The available data is ordinarily not sufficiently detailed to account for these effects, and the prediction of active device performance characteristics becomes less accurate as the operating frequency increases. Even if this was not the case, the stray reactance introduced by the physical circuit layout would have a similar effect, lowering the accuracy with which the characteristics of the active device (together with its associated network) can be predicted.

For these reasons, the technique of determining the active device characteristics at high frequencies, advocated in Paragraph 4.5.3.4, is an experimental method in which the active device characteristics are measured in a circuit similar in layout to that envisioned for the oscillator circuit. Unfortunately, the amount of data that can be obtained in this way is rather limited unless specialized instrumentation is available. Characteristics (a), (b), and (f) can be determined with fair accuracy using a relatively simple measuring procedure, while (c), (e), and, to some extent, (d) must depend on oscillator design experience.

In Paragraphs 4.5.3. and 4.6.3, design information is presented on the selection of tubes and transistors, together with methods of calculation or measurement of their characteristics.

4.2.4 Impedance Transforming Networks

Because of the large differences in impedance levels likely to exist between the crystal and the active device, at least one impedance transforming network is usually necessary in an oscillator. Possible applications of impedance transforming networks in oscillators are:

- (a) To transform the impedance level of the feedback network to that required at the active device output
- (b) To transform the input impedance of the active device to a suitable terminating level for the feedback network
- (c) To transform the oscillator load to a level suitable for connection to the active device.

In applications (a) and (b) an additional requirement has to be met. Not only must the network transform impedance levels, it must also introduce a desired amount of phase shift between input and output. This will normally be 0 degrees or 180 degrees, depending on the oscillator configuration, but it may be desirable to introduce small additional phase shifts to compensate for those introduced in other parts of the circuit. This requirement can be met by applying suitable formulae to the impedance transformer design.

Commonly used impedance transforming networks are shown in Figure 12. These networks are normally used with a tuning reactance as shown in dashed lines in (a) to (e), although these components play no part in the impedance transforming action. These networks, or the tuning coil in the case of (d), contain resistive elements in the form of coil losses that result in power loss. This power loss reduces the efficiency of power transfer through the network and must be accounted for in the oscillator design. Analyses of the networks of Figure 12 are made in Paragraph 4.7.

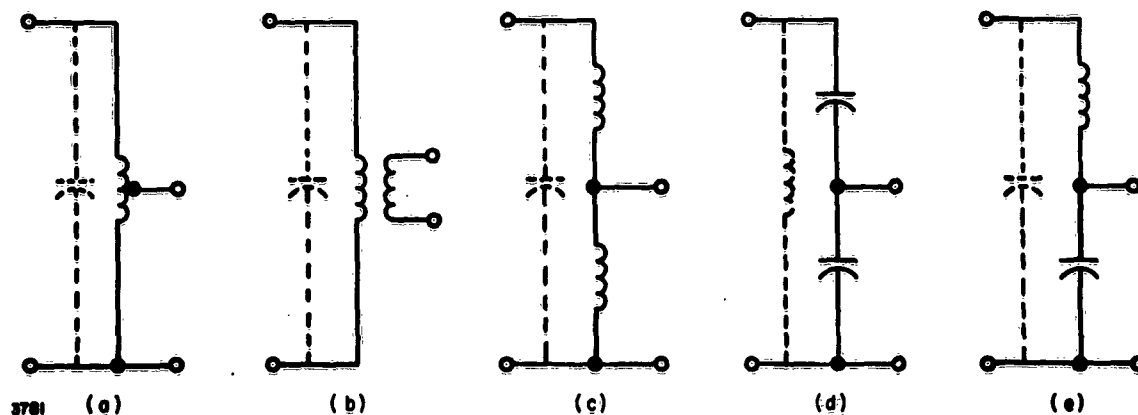


Figure 12. Impedance Transforming Networks

4.3 Performance Specification of an Oscillator

Prior to the design of an oscillator, a specification is written fixing the oscillator performance requirements. These requirements are normally specified in the following form:

- (a) The frequency of oscillation, the frequency tolerance, and the frequency stability required of the oscillator when subjected to a certain range of environmental stress, to specified variations in oscillator loading, and to permissible power source variations. The minimum time period between readjustment of oscillator frequency to compensate for frequency drifts due to aging, and the maximum harmonic output may also be specified.
- (b) The power output and its variation, when subjected to a certain range of environmental stress, specified variations in oscillator loading, and permissible power source variations.
- (c) The load impedance into which the oscillator will work. In some instances the load will be a mixer circuit or other non-linear input impedance circuit and, in this case, the load impedance is likely to be only vaguely defined.
- (d) The permissible input power, the input voltage level, and the expected range of variation.
- (e) The oscillator package size.

In addition, the type of active device; that is, tube or transistor, and the maximum cost may be specified.

4.4 Design Procedure

Based on this specification, a process of selection is necessary to arrive at a final design. This involves the selection of:

- (a) The crystal operating condition. At frequencies up to 20 MC to 25 MC, there is a choice between operation at resonance or parallel resonance; at higher frequencies, only crystals operating at resonance are available.
- (b) A particular type of crystal from those available at the desired frequency of operation.

- (c) The oscillator configuration. This will be governed by (b).
- (d) The desired active device characteristics based on (b) and (c).
- (e) A particular type of tube or transistor based on (d).
- (f) The type or types of impedance transforming network that will be used based on (b), (c), and (e).

There is a wide freedom of choice during this selection process, particularly in steps (c) through (f); and in order to optimize the design, this freedom of choice has to be limited by consideration of the known operating characteristics of tubes, transistors, impedance transforming networks, and experimental oscillator performance evaluation data at the desired operating frequency. From these considerations criteria can then be developed that will increase the possibility of optimizing the design of oscillators.

4.5 Oscillator Design at High Frequencies

4.5.1 General

At frequencies above 20 MC the characteristics of the various components of an oscillator begin to be frequency-dependent due to the presence of parasitic reactance in its various forms. Circuit layout is also more critical for the same reasons and may be the determining factor in the level of performance that can be attained. Further, measurements become more difficult to make with any assurance of a reasonable accuracy. These effects are relatively mild at the lower frequencies under discussion and become worse as the frequency increases.

The prerequisite for design is to know the characteristics of the test equipment that will be used and to appreciate this influence on the circuit under test. It is not always sufficient to rely on manufacturers' specifications, since aging and other factors may degrade performance considerably. As an example, one vacuum-tube voltmeter used during early design evaluations had a parallel input resistance of a few hundred ohms in addition to the specified capacitance of 3 PF at 200 MC. Another vacuum-tube voltmeter had a parallel input resistance of 5 K at 150 MC until the detector diode was changed, after which the parallel input resistance increased to over 25 K.

Effects of this nature considerably influence the interpretation of measurements and should be constantly kept in mind. Similarly, circuit components are likely to differ considerably from their nominal values. Mica capacitors of nominal value exceeding 10 PF cannot be relied on to have an actual capacitance approaching the nominal value at the higher frequencies. This effect can be important, particularly in impedance transforming networks. Carbon resistors also vary considerably from their nominal

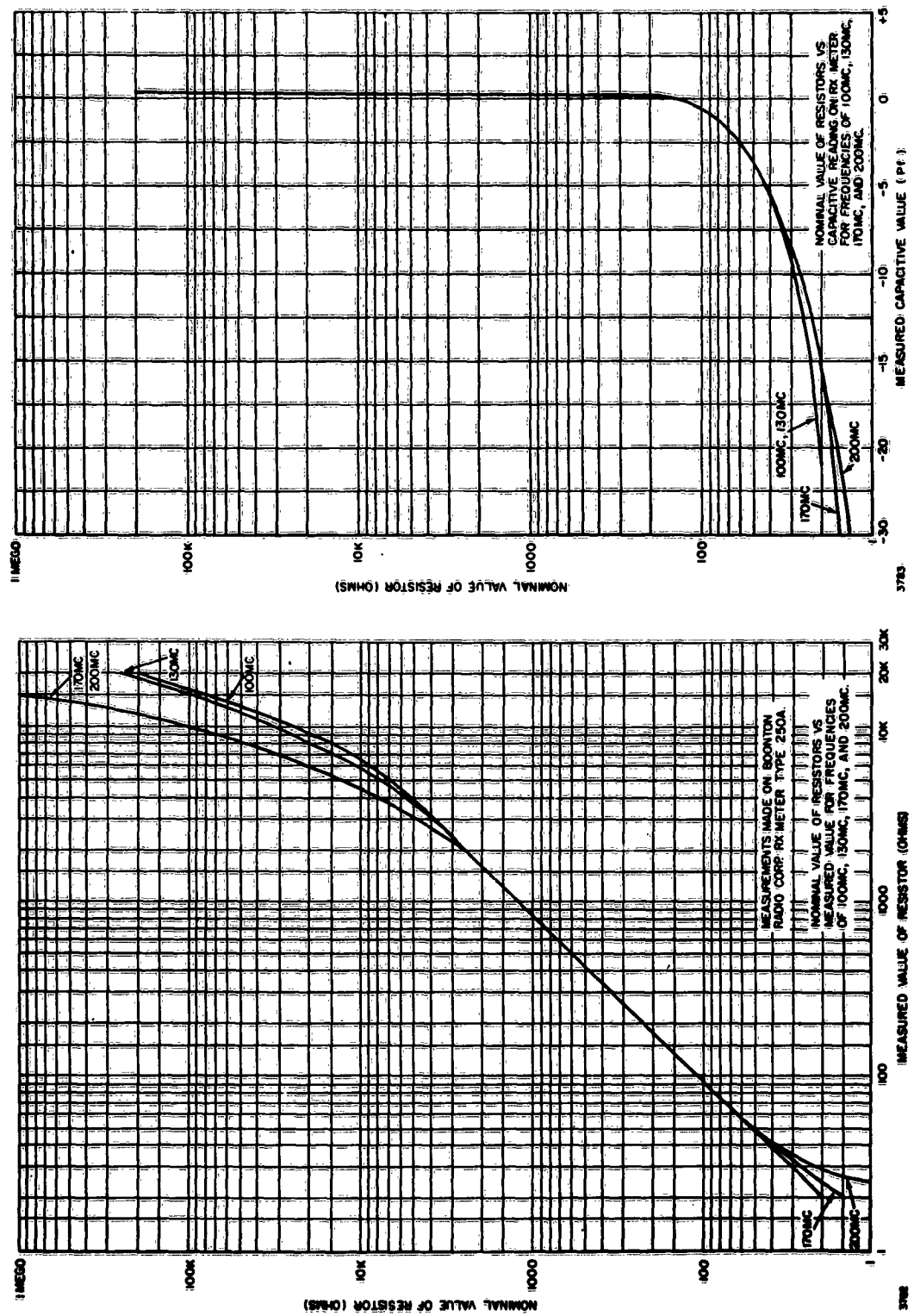


Figure 13. Variation of Resistance and Reactance With Frequency of 1/2 Watt Resistors

values as shown in Figure 13. The deviation is particularly large for resistor values greater than 2 K and less than 40 ohms. These characteristics are those of a widely used make of 1/2 watt resistor. The same make of 1/4 watt resistor exhibits essentially similar frequency characteristics. In many cases this effect will be of little consequence; for example, in decoupling networks, etc. In other instances, such as using a resistor to load the oscillator, it will be essential to know the actual value of resistance with reasonable accuracy.

Circuit wiring will also influence the performance of these elements. It is of little use to employ a component with a desired characteristic if the component will be wired into the circuit with long lead lengths. One inch of 20-gauge wire has a self-inductance of approximately 0.02 UH, corresponding to a reactance of 25 ohms at 200 MC. When working at low impedance levels, this inductance can have appreciable effect on circuit performance. Long lead lengths also increase mutual inductive coupling (the effects of which are more difficult to interpret) and stray capacitive coupling (which will have a maximum effect at high impedance points of the circuit).

Because of the possible wide deviations from nominal of the components that will be used in an oscillator, it is advisable to measure the component values at the particular operating frequency to insure that design conditions are being fulfilled. In fact, the experiences of this program suggest that impedance measuring equipment is essential to the design effort at the high frequencies. Throughout that part of the program dealing with high-frequency oscillators, an RX meter was in constant use and proved invaluable in aiding the design effort.

The circuit layout problems posed during initial experimental design evaluation are somewhat different from those in a final design. It will be necessary to take measurements and change components in the circuit to evaluate the performance, while this will not be necessary in the final design. A more open construction is therefore necessary initially, to allow access for voltage measuring probes and to facilitate the changing of components. Figure 14 shows photographs of the layouts used for all the high frequency oscillator test circuits evaluated during this program. In these layouts the output and input circuits were separated by the screening plate shown extending across the chassis. The necessity of employing this screen is not known. It was included during the early evaluations as an additional safeguard and, since the layout met the measurement needs, it remained throughout the program.

4.5.2 Crystal Characteristics

Table 4 shows the military standard crystals applicable to oscillator design above 20 MC. More detailed information on most of these crystals is contained in Reference 5, Paragraph 7.0. There are no military standards for crystals operating at frequencies above 125 MC, but crystals meeting the general requirements of types

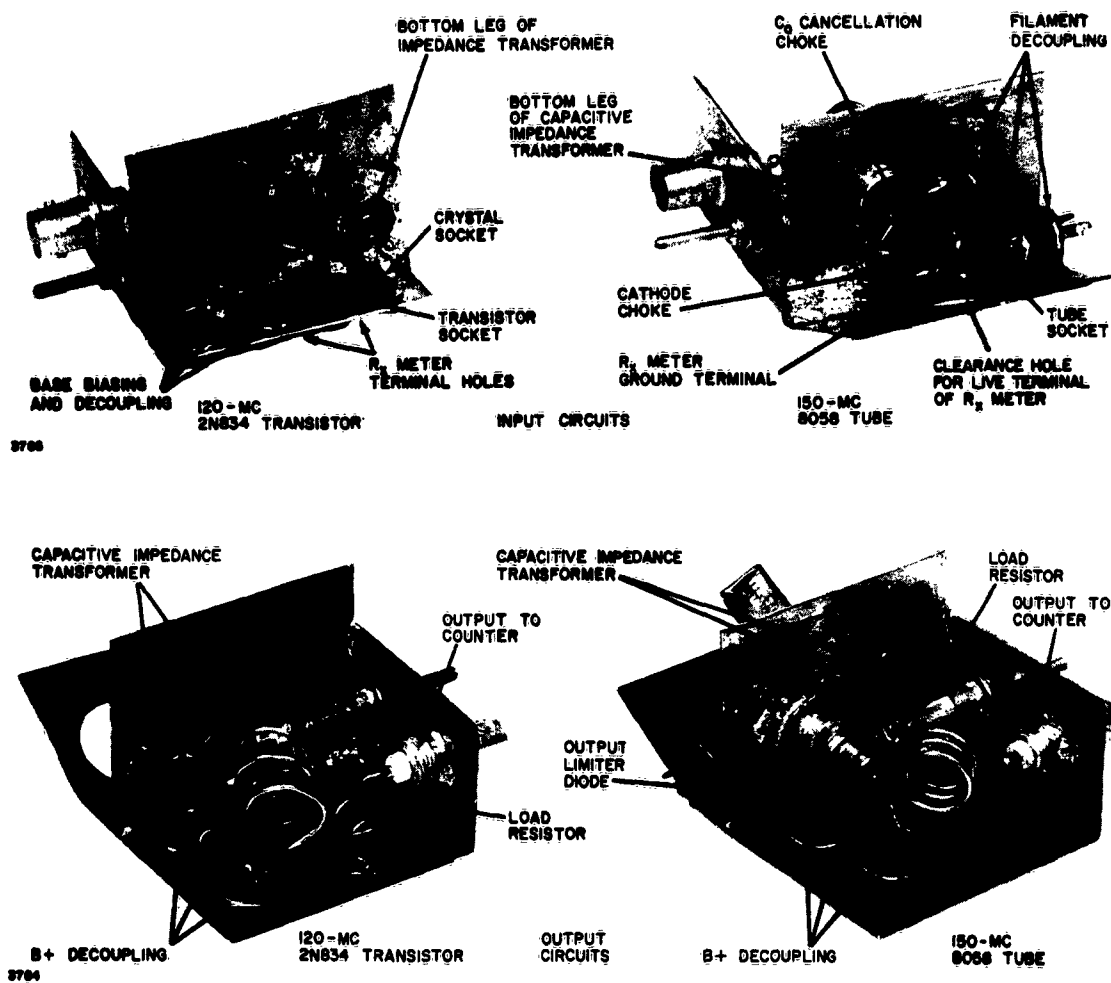


Figure 14. High Frequency Oscillators, Input and Output Circuits

CR-54A/U or CR-56A/U can be obtained for operation at up to at least 200 MC. The major difference is that R_1 may be as high as 100 ohms instead of the 60-ohm maximum value of R_F specified for the CR-54A/U or CR-56A/U units.

All the tabulated crystals are designed to operate at resonance. The circuit of Figure 1 can still be regarded as a useful equivalent circuit, although parasitic reactance in the crystal holder has a bearing on the performance at the higher frequencies.

At frequencies above 125 MC, a slightly different approach is required. The C_0 of these crystals is typically 7 PF, giving a reactance X_{C_0} of 180 ohms to 114 ohms in the 125 MC to 200 MC band. In order that resonance will occur, it is necessary that $\frac{X_{C_0}}{R_1}$ should be greater than 2 and preferably greater than 4. For values of $\frac{X_{C_0}}{R_1} < 2$, the crystal always appears capacitive; and for $\frac{X_{C_0}}{R_1}$ values between 2 and 3, the phase

shifting ability of the crystal is severely degraded. Since these conditions are not satisfied for R_1 values of 60 ohms to 100 ohms (the range in which these crystals can be expected to fall), it is necessary to increase the effective reactance of X_{C_0} . This is normally done by connecting a low Q inductance in parallel with the crystal, the value of the inductor being such as to cancel out X_{C_0} at the frequency of resonance. The coil is arranged to be of low Q in order to make the cancellation uncritical, but the effective parallel resistance of the coil should be 10 to 20 times the value of R_1 to avoid degrading the crystal resonance characteristic.

In order to determine the value of the cancellation inductor, it is necessary to know the value of C_0 at the operating frequency. C_0 measurements at frequencies well below the operating frequency have little meaning, since the effect of the crystal holder parasitic reactive elements is to increase the effective value of C_0 . C_0 must therefore be measured at a frequency near to the operating frequency, but sufficiently lower so that the series arm element does not appreciably affect the measurement. A measuring frequency 5 percent to 10 percent below the operating frequency is normally satisfactory.

In many instances, cancellation coils are used in oscillators operating below 125 MC. The reason for this is that X_{C_0} forms a low impedance feedback path independent of the crystal. The remainder of the oscillator is usually capable of introducing large phase shifts with only a small reduction in power gain.

TABLE 4. MILITARY STANDARD CRYSTALS, HIGH FREQUENCY

WIDE TEMPERATURE RANGE CRYSTALS						
Nominal Frequency (Megacycles)	Operating Temperature (Centigrade)	Frequency Tolerance (Percent)	Drive Level	Holder	Type	Maximum Equivalent Resistance (Ohms)
(*) 10 to 61	-55° to +105°	±0.005	20MW	HC-6/U	CR-51 A/U	40
10 to 61	-55° to +105°	±0.005	2 and 4 MW	HC-6/U	CR-52 A/U	40
(*) 15 to 50	-55° to +105°	±0.005	2 MW	HC-10/U	CR-24/U	50 and 75
17 to 61	-55° to +105°	±0.005	2 MW	HC-18/U	CR-55/U	40
17 to 61	-55° to +105°	±0.0025	2 MW	HC-18/U	CR-67/U	
17 to 61	-55° to +105°	±0.005		HC-18/U	CR-72/U	
17 to 61	-55° to +105°	±0.0025		HC-18/U	CR-76/U	
17 to 62	-55° to +105°	±0.002		HC-25/U	CR-77/U	
35 to 50	-55° to +105°	±0.003		HC-29/U	CR-73/U	
(*) 50 to 87	-55° to +105°	±0.005	20MW	HC-6/U	CR-53 A/U	60
50 to 125	-55° to +105°	±0.005	2 MW	HC-6/U	CR-54 A/U	50 and 60
50 to 125	-55° to +105°	±0.005	2 MW	HC-18/U	CR-56 A/U	50 and 60
TEMPERATURE CONTROLLED CRYSTALS						
10 to 61	75° ±5°	±0.0025	2 and 1 MW	HC-6/U	CR-65/U	40
10 to 75	75° ±5°	±0.002	2 and 1 MW	HC-6/U	CR-32 A/U	40 and 50
17 to 61	85° ±5°	±0.002	2 and 1 MW	HC-18/U	CR-61/U	40
45 to 75	85° ±5°	±0.0015		HC-26/U	CR-74/U	
50 to 87	75° ±5°	±0.00125		HC-6/U	CR-75/U	
50 to 125	85° ±5°	±0.002	1 MW	HC-18/U	CR-59 A/U	50 and 60

(*) GOVERNMENT PERMISSION REQUIRED PRIOR TO USE

Therefore, oscillation via C_0 is possible if the amplifier gain is sufficient. The cancellation coil reduces the possibility of this occurring.

The standard military crystal test sets for the frequency range discussed here are the Crystal Impedance Meters TS-683/TSM and the AN/TSM-15, covering the frequency ranges of 10 MC to 140 MC and 75 MC to 200 MC, respectively. The TS-683/TSM is supplied with a selection of fixed substitution resistors for use between 50 MC and 140 MC in determining crystal resonance resistance, and a variable substitution resistor for use below 50 MC. The AN/TSM-15 is supplied with six variable substitution resistors which, between them, cover the resistance range of 10 ohms to 110 ohms, with a negligible reactive component over the range of 75 MC to 200 MC.

4.5.3 Active Device Characteristics

It is desirable to know the values of the active device characteristics that influence performance. These are:

- (a) Power gain as a function of output load
- (b) Input impedance as a function of load
- (c) Phase angle of output voltage relative to input voltage as a function of input and output terminations
- (d) Power output as a function of supply power and load impedance
- (e) Variations of the above as a function of temperature
- (f) Gain stability as a function of load

These characteristics become increasingly difficult to determine as the operating frequency is increased. At frequencies above 10 or 20 MC, calculations based on the simple formulae adequate for low-frequency operation begin to lose accuracy because of the effects of parasitic reactance. Improvement of these formulae to account for the new effects results in unwieldy expressions. Also, since the additional parameters (cathode lead inductance, transit time, mutual couplings, etc.) are not normally known with any certainty unless measurements are performed, this approach is likely to defeat its object; that is, to design by calculation rather than by experiment. The physical layout of the active device and its associated components may also introduce comparable parasitic reactance, making the prediction of performance difficult.

The alternative approach is to experimentally measure as many of the active device characteristics as possible at the desired operating frequency and under

circuit conditions approaching those in which the active device will be used. In practice, this consists of measuring the power gain versus load, and input impedance versus load. From these measurements an indication of gain stability as a function of load can also be obtained. This leaves items (c), (d), and (e) yet to be determined. Item (d) can be calculated with reasonable accuracy by methods discussed later. Item (e) can only be determined experimentally with any degree of accuracy. Because it is easier to measure the overall effects of temperature on an oscillator, as indicated by the output frequency and power changes, than to measure the active device characteristic variations, the design recommendations given later rely on information gathered in this way as a substitute for (e). The measurement of Item (c) requires specialized equipment at high frequencies and, since this will not normally be available to the designer, past experience must again be relied on.

Before this process of measurement is implemented, the designer must choose a particular active device type; and, to avoid the waste of time incurred if the choice is inappropriate, a basis for this selection must be developed. Furthermore, it is desirable that this basis be formed on the information contained in the manufacturer's data sheets.

One effect that cannot be easily gauged from the data sheets concerns the inherent feedback within the active device. This effect is particularly important at the higher frequencies because the feedback path is either wholly or partially through the stray capacitance of the active device and its associated circuits. This feedback is not necessarily positive feedback at the desired oscillator frequency, where the input and output circuits of the active device are essentially resistive due to the conjugate matching employed. The danger is that at adjacent frequencies these tuning networks are likely to produce large phase shifts which, in conjunction with that in the inherent feedback path, will result in positive feedback and possible oscillation. It should also be noted that, at the desired oscillator frequency, this undesired feedback path is in parallel with the desired feedback path containing the crystal. The necessary condition for oscillation to occur is that the combined feedback signal from the two paths should result in 0 degrees phase shift. The desired feedback path will have to compensate for any phase shift present in the undesired feedback path and may result in the crystal operating off resonance.

The following discussion is intended to show the effect of the inherent feedback paths more clearly and the methods available for counteracting it. The discussion is in no way rigorous; for more detailed discussions, see References 6, 7, and 8 of Paragraph 7.0.

4.5.3.1 Feedback Effects at High Frequencies

The behavior of any active device can be characterized by a set of four parameters which may be specified in various forms. The form used here, and the one

most applicable at high frequencies, is the admittance or 'y' parameter form. For the three methods of connecting a tube or transistor as shown in Figure 15, the equations characterizing the active device are:

$$I_1 = Y_i V_1 + Y_r V_2 \quad (39)$$

$$I_2 = Y_f V_1 + Y_o V_2 \quad (40)$$

where the positive direction of I_1 , I_2 , V_1 , and V_2 is taken as indicated in Figure 15, and where:

$$Y_i = G_i + jB_i = \frac{I_1}{V_1} \quad \text{when } 2, 2' \text{ are short circuited} \quad (41)$$

$$Y_r = G_r + jB_r = \frac{I_1}{V_2} \quad \text{when } 1, 1' \text{ are short circuited} \quad (42)$$

$$Y_f = G_f + jB_f = \frac{I_2}{V_1} \quad \text{when } 2, 2' \text{ are short circuited} \quad (43)$$

$$Y_o = G_o + jB_o = \frac{I_2}{V_2} \quad \text{when } 1, 1' \text{ are short circuited} \quad (44)$$

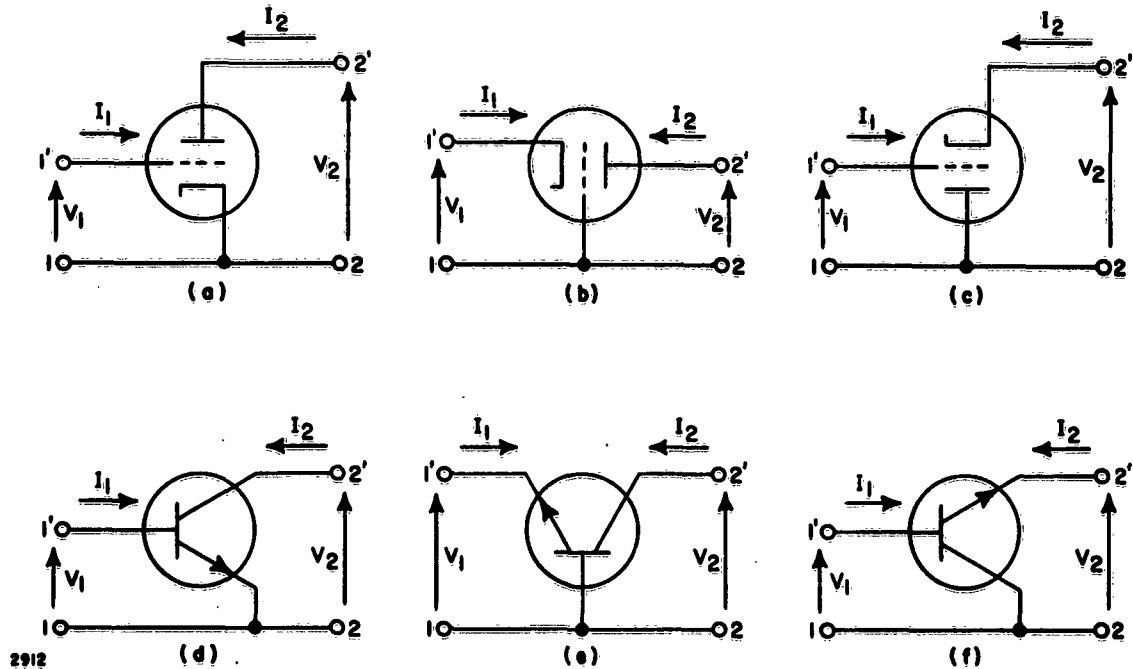


Figure 15. Active Device Configurations

The four parameters will, in general, be different for each of the connections shown in Figure 15 (a) to (c) and (d) to (f), and can be distinguished from each other by an additional suffix indicating the grounded element. From Equations (39) and (40) the equivalent circuit of Figure 16 can be developed, which also shows a load of admittance Y_L and a driving source of admittance Y_G , where:

$$Y_L = G_L + jB_L \quad (45)$$

$$Y_G = G_G + jB_G \quad (46)$$

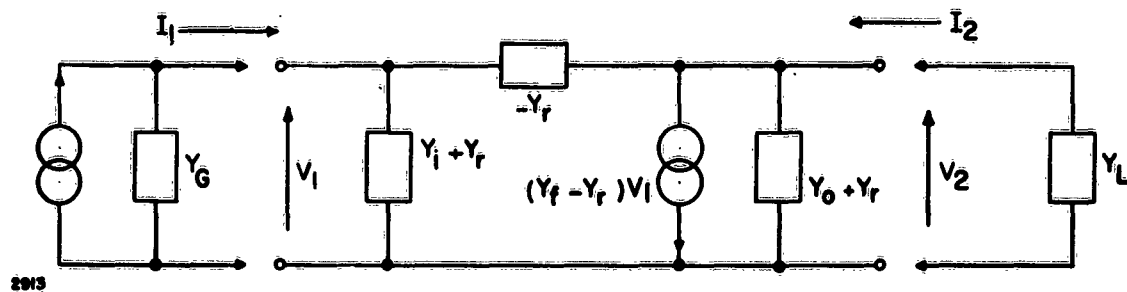


Figure 16. Active Device Equivalent Circuit

Referring to Figure 16, the nodal equations are:

$$I_1 = (Y_i + Y_G) V_1 + Y_r V_2 \quad (47)$$

$$0 = Y_r V_1 + (Y_o + Y_L) V_2 \quad (48)$$

The power output is given by:

$$P_o = V_2^2 G_L \quad (49)$$

$$= \frac{I_1^2 Y_f^2 G_L}{|(Y_i + Y_G)(Y_o + Y_L) - Y_r^2|} \quad (50)$$

The maximum available power P_{av} from a source of admittance

$Y_G = G_G + jB_G$ is:

$$P_{av} = \frac{I_1^2}{4G_G} \quad (51)$$

and is supplied to the active device when the input is conjugately matched to the source. The transducer power gain G_t is defined as:

$$G_t = \frac{P_o}{P_{av}} \quad (52)$$

$$= \frac{4 |Y_f|^2 G_L \cdot G_G}{|(Y_i + Y_G)(Y_o + Y_L) - Y_f \times Y_r|^2} \quad (53)$$

The denominator of Equation (53) is the vectorial difference of

$(Y_i + Y_G)(Y_o + Y_L)$ and $(Y_f \times Y_r)$; and if these terms approach a comparable magnitude and phase angle, G_t will approach infinity. It can be shown (References 6 and 7, Paragraph 7.0) that the circuit is likely to oscillate if:

$$|Y_f \cdot Y_r| + R_e(Y_f \cdot Y_r) \geq 2(G_i + G_G)(G_o + G_L) \quad (54)$$

where $R_e(Y_f \cdot Y_r)$ is the real part of $Y_f \cdot Y_r$. Conversely, the amplifier is unconditionally stable if the stability factor K is greater than unity. This is defined as:

$$K = \frac{2(G_i + G_G)(G_o + G_L)}{|Y_f \cdot Y_r| + R_e(Y_f \cdot Y_r)} \quad (55)$$

The amount by which K exceeds unity is a direct indication of the circuit stability. K values as high as 10 have been suggested as desirable in transistor amplifier circuits undergoing severe environmental stress. This takes into account the relatively large parameter spread encountered in transistors of the same type, and suggests that a K value of 3 or 4 would be adequate for a vacuum tube amplifier, where the parameters are less temperature dependent and where the parameter spread between units of the same type is smaller.

The cause of this tendency of the amplifier toward instability is the term $-Y_r$, the admittance coupling the output and input of the active device. In a vacuum tube this consists primarily of the parasitic capacitance between plate and cathode or plate and grid for grounded grid or grounded cathode amplifiers, respectively. In a transistor, $-Y_r$ is a combination of resistance and capacitance in the semiconductor material and the header capacitance. In neither case does $-Y_r$ contribute to the useful forward gain of the amplifier, and its minimization is desirable in an active device.

There are two alternative methods of stabilizing the amplifier power gain: by unilateralization (or neutralization) or by mismatch.

(a) Stabilization by Unilateralization or Neutralization

Referring to Figure 16, if an admittance Y_f is introduced in parallel with $-Y_r$, the two cancel, resulting in zero coupling between output and input. The transducer gain becomes:

$$G_{t \text{ unil}} = \frac{4 |Y_f|^2 G_L G_G}{|(Y_i + Y_G)(Y_o + Y_L)|^2} \quad (56)$$

and the amplifier is unconditionally stable. The amplifier is then said to be unilateralized. If the added admittance fully or partially cancels only the susceptive part of $-Y_r$, the amplifier is said to be neutralized.

If conjugate matching of input and output is employed, maximum gain is obtained and is given by:

$$G_{t \text{ max}} = \frac{|Y_f|^2}{4G_i G_o} \quad (57)$$

(b) Stabilization by Mismatch

Referring to Equation (55), the stability factor is increased if the numerator is increased and the denominator is held constant. This means that G_G and G_L have to be increased, since G_i and G_o are active device parameters. The optimum conditions of mismatch (that is, that producing the highest gain for a given stability) is obtained when:

$$\frac{G_G}{G_i} = \frac{G_L}{G_o} = m \quad (58)$$

where m is termed the mismatch factor. Provided that:

$$G_i G_o (m + 1)^2 \gg Y_f \cdot Y_r \quad (59)$$

and the susceptive components of Y_i and Y_o are tuned out, the expression for power gain is:

$$G_{pmm} = \frac{4m}{(m + 1)^4} \cdot \frac{|Y_f|^2}{G_i G_o} \quad (60)$$

(c) Comparison of Power Gain Using the Two Stabilizing Methods

Stabilizing the amplifier gain by mismatch results in a smaller power gain relative to that obtainable by unilateralization for a given stability. This is obvious when it is considered that mismatching results in inefficient power transfer, whereas matching can be employed with a unilateralized amplifier. A direct comparison can be obtained by taking the ratio of Equation (60) to Equation (57):

$$\frac{G_{pmm}}{G_{p\text{ unil}}} = \frac{16m}{(m + 1)^4} \quad (61)$$

If $m = 1$ (that is, no mismatch), the stability factor is given by:

$$K = \frac{8G_i \cdot G_o}{|Y_f Y_r| + R_e(Y_f \cdot Y_r)} \quad (62)$$

Employing mismatch and letting $m = 2$:

$$K = \frac{18G_i G_o}{|Y_f \cdot Y_r| + R_e(Y_f \cdot Y_r)} \quad (63)$$

This results in an improvement of 2.25 in K , while the loss in power gain, relative to that obtainable using unilateralization, will be 4 DB. A similar comparison employing $m = 3$ shows an improvement in stability of 4 times greater than that for $m = 1$, with a power gain loss of 7 DB compared to a unilateralized amplifier. These losses are not too great when the unilateralized power gain capability is relatively high; that is, 20 DB or greater. Otherwise the gain will be seriously affected.

4.5.3.2 Active Device Configurations Used During This Program

Only two types of active device configuration have been investigated in detail during this program: the grounded grid triode and the grounded base transistor configurations. A grounded emitter transistor amplifier and a grounded cathode tetrode amplifier were evaluated at a frequency of 200 MC. Both circuits showed good gain capabilities at this frequency. The tetrode had a stable gain of 300 and the transistor a stable gain of 50. However, attempts to incorporate these amplifiers in oscillator circuits were unsuccessful due to the large undesired phase angle deviations occurring in the active device. Attempts were made to correct for these effects, but without success, and the experiments had to be abandoned because of time limitations.

It is doubtful if much was to be gained from using these configurations in any case. The tetrode design was undertaken because of the possibility of obtaining higher gain and, hence, larger power output than that obtainable using a grounded grid triode.

This would certainly have been the case except for the undesired phase shift problems that arose. However, this would only be gained at the expense of increased circuit complexity due to the presence of the screen grid and the necessity of using two impedance transforming networks, one of them having phase inverting properties. The same result could be obtained using the two halves of a double triode with approximately the same number of components; one triode being used in the oscillator circuit, and the other used as a buffer amplifier. This approach might possibly result in increased isolation of the oscillator from the load, but at the expense of increased power drain.

The grounded emitter transistor oscillator design was undertaken purely as a parallel effort to the tetrode design. Little advantage could be foreseen for this configuration in view of the excellent gains obtained previously with the grounded base circuit and because of the inherently higher gain variations of the grounded emitter configuration, particularly with temperature.

Configurations other than the grounded base and grounded grid are occasionally mentioned in the following sections. However, this is done purely for completeness, and it is emphasized that the two above-mentioned configurations are the ones covered in this part of the report under high-frequency oscillators.

4.5.3.3 Aids to Active Device Selection

4.5.3.3.1 Vacuum Tubes

The low-frequency parameters of a vacuum tube can be used to indicate the gain capabilities at high frequencies, provided that the effects of parasitic reactance are small. The relevant low-frequency equations are:

(a) Grounded Grid Triodes

$$\text{Power gain, } G_p = (U + 1) \cdot \frac{R_T}{R_p + R_T} \quad (64)$$

where R_T is the total load resistance. The maximum power gain is, therefore:

$$G_{p \text{ max}} = (U + 1) \quad (65)$$

when $R_T \gg R_p$.

$$\text{Cathode input resistance, } R_{in} = \frac{R_p + R_T}{U + 1} \quad (66)$$

(b) Grounded Grid Pentodes or Tetrodes

$$\text{Power gain, } G_p = g_m \cdot R_T \quad (67)$$

and the cathode input resistance:

$$R_{in} = \frac{1}{g_m} \quad (68)$$

if $R_p \gg R_T$.

(c) Grounded Cathode Pentodes or Tetrodes

$$\text{Power Gain, } G_p = g_m^2 \cdot R_T \cdot R_{in} \quad (69)$$

$$\text{where } R_{in} = \frac{1}{\omega^2 g_m} \left(\omega_{gk}^2 + \frac{1}{TK_e} \right) \quad (70)$$

where ω_{gk} = angular frequency of resonance of the grid-cathode stray capacitance with the cathode leakage inductance

ω = angular frequency of operation

T = time delay due to transit time of electrons between grid and cathode

K_e = constant dependent on tube geometry

In general, ω_{gk} and TK_e will not be known; however, the tube manufacturer sometimes specifies R_{in} at a particular frequency f_g , and a usable value of input resistance at the desired operating frequency f_d can be obtained by multiplying the given value of R_{in} by $\frac{f_g^2}{f_d^2}$.

The power gain obtainable in either of these connections is proportional to the total load resistance R_T , the maximum value of which is limited in the following two ways.

- (a) The effective parallel resistance of the tuning inductor R_D . Assuming a value of 10-PF capacitance composed of strays and tuning capacitance in the plate circuit, the capacitive reactance at 100 MC is 160 ohms. The Q of the inductance will be between 50 and 200, depending on space requirements, etc., resulting in an R_D of from 8 K to 32 K. For the same total tuning capacitance, these values will be 4K and 16 K at 200 MC. The actual load R_L will be in parallel with R_D and, in order to obtain a reasonable ratio of power into the load versus power con-

sumed in the inductor, the ratio of $\frac{R_D}{R_L}$ should be large. Even when compromising to the utmost and making $R_L = R_D$, this results in R_T values of 4 K to 16 K at 100 MC and 2 K to 8 K at 200 MC, placing a definite limit on the usable values of R_T . This latter condition is not desirable, since for a given power input the power output of interest is the power into R_L , not the power into R_T .

These considerations result in an additional characteristics requirement for a triode. The tube should not only have a high U , but also a low R_p in order to give reasonable gain with a low value of R_T . Since U and R_p are interrelated by the formula:

$$U = g_m \cdot R_p \quad (71)$$

the tube must also have a high mutual conductance.

- (b) As indicated in Paragraph 4.5.3.1, the stability of the tube circuit is dependent on the value of R_T and may be the limiting factor governing the maximum permissible value of R_T .

In the case of the grounded grid triode, the maximum available stable gain is likely to be of the order of $\frac{U}{2}$ to $\frac{U}{3}$ because of the effects noted in (a) and (b), while

Equation (66) will give a reasonably accurate indication of the input resistance, provided that the circuit is not tending to instability. At lower frequencies both these effects will have less influence on performance.

When considering pentodes or tetrodes for grounded grid operation, R_T will be mostly limited by the dynamic resistance of the tuning inductance, since the inherent feedback is reduced with this type of tube structure. The maximum available power gain will, therefore, be $g_m \cdot R_T$, where R_T lies in the range of 2 K to 10 K.

4.5.3.3.2 Transistors

The typical power gain characteristics of a matched, unilateralized high-frequency transistor are shown in Figure 17. Power gain curves for common emitter and common base amplifiers are plotted from DC to a frequency f_{max} defined as the frequency at which the power gain falls to unity (0 DB). f_{max} is the maximum frequency at which the transistor is capable of oscillating when all the output power is fed back to the input. Since such an oscillator is supplying no output power, the

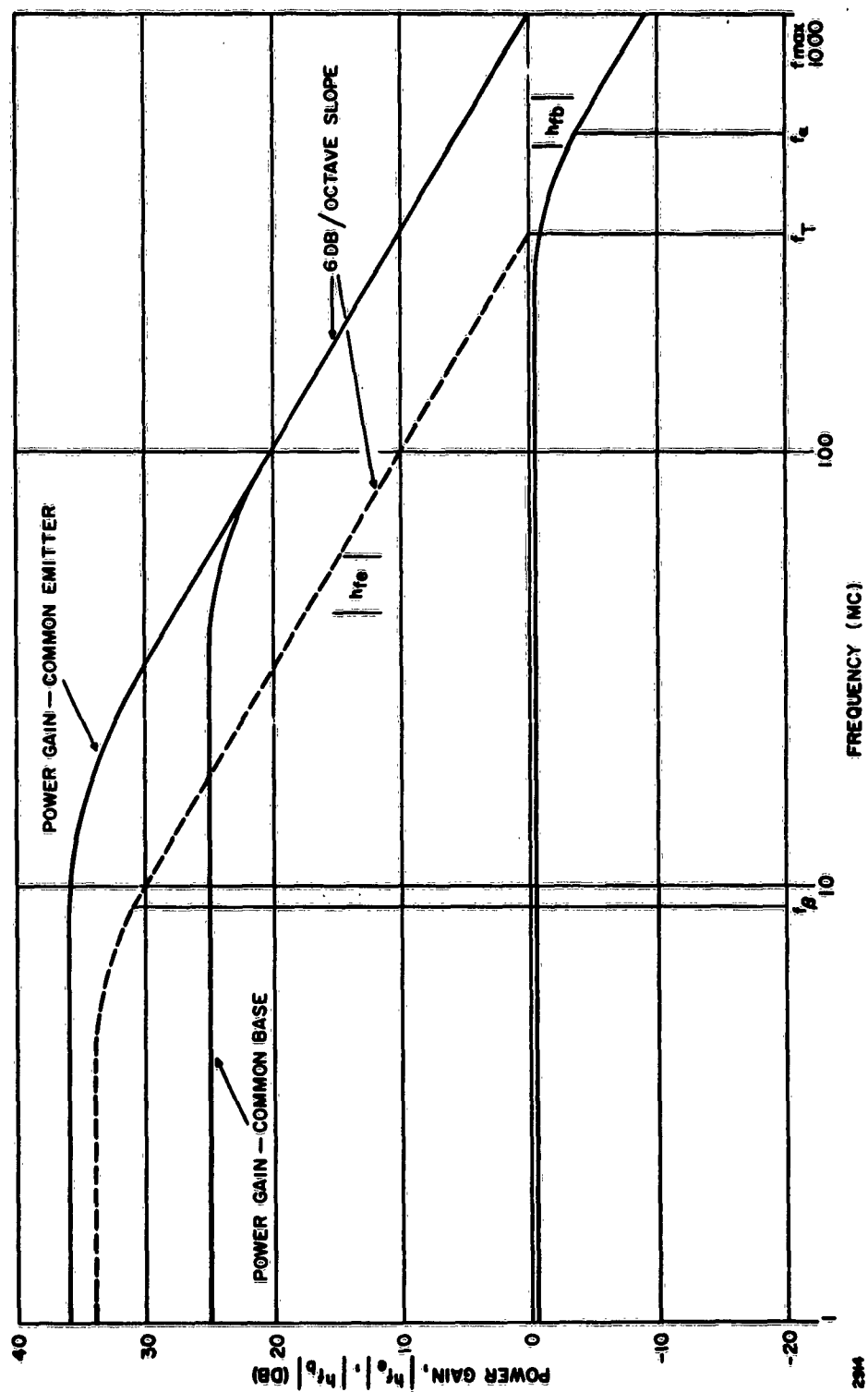


Figure 17. Characteristics of a Unilateralized High-Frequency Transistor

transistor cannot be defined as operating in any particular mode, and it therefore follows that f_{\max} defines the frequency at which the power gain falls to 1, independent of the configuration in which the transistor is connected. At frequencies below f_{\max} , the power gain increases at a rate of 6 DB per octave until the low-frequency power gain is approached.

Other high-frequency characteristics shown in Figure 17 are $|h_{fe}|$ and $|h_{fb}|$, the common emitter and common base short circuit current gain magnitudes, respectively. $|h_{fe}|$ also exhibits a 6-DB per octave slope at high frequencies, the "cutoff" frequency being f_{β} , the frequency at which h_{fe} is 3 DB down on h_{FE} , the low-frequency current gain. Another term related to $|h_{fe}|$ is f_T , the frequency at which $|h_{fe}|$ falls to 1. $|h_{fb}|$ has the same general characteristic, the cutoff frequency f_{α} being that frequency at which $|h_{fb}|$ falls 3 DB below h_{FB} , the low-frequency common base current gain. f_T and f_{α} are vaguely interrelated, f_{α} being typically 1 to 2.5 times f_T .

Manufacturer's data sheets give values for some of these quantities and, with this information and a knowledge of the generalized power gain curve, the gain capabilities of a transistor at any frequency can be predicted with reasonable accuracy.

The determination of the input and output impedance or admittance levels of the transistor are not as simple. The parameters determining these quantities are those stated in Paragraph 4.5.3.1, and Table 5 shows the typical variations of these parameters over the frequency range from 10 MC to 200 MC.

TABLE 5. Y PARAMETER VARIATIONS WITH FREQUENCY

Parameter	Variation
G_{oe} (G_{ob})	Varies over a range of 10:1
B_{oe} (B_{ob})	Varies over a range of 2:1
G_{ie}	Varies over a range of 10:1
B_{ie}	Varies over a range of 3:1
G_{fe}	Varies over a range of 6:1
B_{fe}	Varies over a range of 6:1
G_{re}	Varies over a range of 5:1
B_{re}	Varies over a range of 5:1
The second suffix (e) or (b) refers to grounded emitter or grounded base configuration, respectively.	

Occasionally, a manufacturer presents this parameter data in graphical form, showing the typical variation with frequency and transistor power levels of the individual parameters. These are rare instances, however; in the majority of cases no high-frequency parameter information other than the magnitude of the high-frequency common emitter current gain h_{fe} is given.

G_i , B_i , G_o , and B_o can be measured using a two-terminal impedance bridge, but the forward and reverse admittance measurements require a three-terminal bridge, an instrument not normally available to the designer. The simplest solution is to measure the input impedance of the transistor in the amplifier in which it will be used in the oscillator circuit, for various values of load resistance. This measurement is as easy to make as that of G_i and B_i , and the desired data (input impedance as a function of load) is obtained directly. This subject is discussed further in Paragraph 4.5.3.4.

The bias conditions of the transistor influence its characteristics appreciably. The data sheet values of f_{max} , f_T , f_B , $|h_{fe}|$, etc., are normally given for specified values of collector current and voltage. Data sheets of high-speed switching transistors frequently give curves of f_T versus collector current and voltage. This information is usually sufficient to enable a desired biasing condition to be chosen.

The loading due to the output tuned circuit effective parallel resistance R_D will normally have negligible effect in transistor oscillators because of the low values of output load resistance necessary to maintain stability.

4.5.3.4 Determination of Active Device Characteristics

If the design frequency is sufficiently low (20 MC or 30 MC), the power gain and input impedance as a function of load can be determined with reasonable accuracy by calculation, using the low-frequency parameters.

The performance can then be checked experimentally using the load resistance determined in a single-tuned amplifier circuit driven from a signal generator. Input and output voltages are measured with the output circuit tuned to resonance and a value obtained for the input resistance of the active device using the substitution method. In this method, the input voltage to the active device is measured, then the signal generator is disconnected from the active device and connected to a resistor, and the voltage across the resistor is measured. Adjustment of the value of the resistor, until the voltage across it equals that previously measured across the active device, will determine the active device input resistance to the desired accuracy.

From the above measurements the power gain can be obtained. This is based on the assumption that the active device input impedance is essentially resistive at these frequencies; this is justifiable for transistors with an f_T of 300 to 400 when

operated in the common base configuration, and particularly so for grounded grid triodes or pentodes.

A more accurate approach, and the only adequate one at higher frequencies, uses the same basic approach with the exception that an impedance measuring bridge is substituted for the signal generator as a driving source. Input and output voltages are again measured with the output tuned to resonance, while the input impedance is measured directly by the impedance bridge.

The impedance bridge used during this program was a Boonton RX meter which has a frequency range of 500 KC to 250 MC. As supplied by the manufacturer, the RX meter is not entirely suitable for the measurement of active device input impedance because of the high signal level existing at the bridge terminals. The maximum input voltage that can be applied to the emitter-base junction of a transistor before non-linearity occurs is typically 10 MV RMS. Since the output of the bridge is at least 10 times this level, it follows that the bridge output voltage requires reduction to obtain meaningful results. The simple modifications required are fully described in the RX meter instruction manual, and require less than one hour to complete. Other impedance meters can be used for these measurements, but the user is advised to insure that the output level is suitable for this application.

After modification, the RX meter has certain peculiarities of operation which may be misleading. These are:

- (a) When operated at low bridge voltage levels, the bridge operating frequency is strongly dependent on the bridge oscillator voltage level. Slight adjustment of the bridge output voltage results in sufficient change of bridge frequency that it will be necessary to readjust the detector oscillator tuning to maintain a detector signal. (The detector oscillator frequency is 100 KC removed from the operating frequency to give a 100-KC intermediate frequency.)
- (b) The feedthrough of the detector oscillator signal to the RX meter terminals has an amplitude of several millivolts, which is of the same order as the desired bridge signal for transistor measurements. If the bandwidth of the transistor amplifier is sufficiently wide, this signal is amplified and appears at the output; this may mislead the operator into thinking that the circuit under measurement is oscillating. At test frequencies in the region of 170 MC and above, this feedthrough signal level begins to be excessive (values exceeding 20 MV have been measured). The values of gain and input impedance measured under these conditions are suspect because of possible non-linear operation, but appear to be adequate for the intended purpose.

An alternative approach is available using the RX meter (see reference 9, Paragraph 7.0). This consists of stopping the internal detector oscillator and substituting a mixer signal of lower amplitude from an external source, at a frequency several megacycles removed from the bridge frequency. The resulting heterodyne frequency is detected using a sensitive receiver. It is also possible that some improvement could be obtained using the existing circuit by reducing the amplitude of the mixer oscillator signal. The detector circuit sensitivity is more than adequate with the described modifications, and some degradation could be allowed if a reduction in feedthrough resulted.

The determination of the active device characteristics is made in the following manner.

Step 1

Assuming that the active device configuration and biasing conditions have been determined from the previous discussion, the active device is incorporated into a single-tuned circuit amplifier. The tuning inductance used in the output circuit should resonate with from 12 PF to 15 PF for designs at 200 MC and prorated for lower frequencies. The final oscillator package size should be kept in mind during the construction of this coil, since it can be used in the final design, and the coil loss in the oscillator circuit will then be similar to that of the measurement circuit. The amplifier input circuit is left untuned, with possibly an inductor in the input biasing circuit to minimize losses in parallel with the active device.

The circuit layout should follow good engineering practice as to lead lengths, decoupling methods, etc., and should allow access for input and output voltage measuring probes and for the RX meter connections. With the objective of building the prototype oscillator on this chassis, provision should also be made for installing the additional circuitry using minimum lead lengths. Figure 14 shows tube and transistor oscillators constructed on a chassis that proved adequate for this purpose. During this measurement phase the impedance transforming network, crystal, output limiter diode, and C_o cancellation coil are not included in the circuit. This chassis is designed to be installed on the ground terminal post of the RX meter with the "live" terminal protruding through a clearance hole in the chassis into a position immediately adjacent to the active device input connection.

Step 2

Adjust the RX meter to the frequency of interest, and measure the input impedance of the voltmeters that will be used for measuring input and output AC voltage. This voltmeter loading should be applied as a correction when calculating power gain from the measured results. When a transistor circuit is being tested, the voltmeter

used for input voltage measurement should have the sensitivity necessary to measure 10 MV with reasonable accuracy. In addition, measure the actual resistance of a number of resistors for use in loading the amplifier output. An indication of the desired range of actual resistance values required at any frequency can be obtained from the experimental evaluation sheets contained in this report.

Step 3

Position the amplifier on the RX meter, and connect the "live" terminal of the RX meter to the amplifier input via a capacitor of low impedance. Measurement is again recommended. Connect a load resistor of 200 ohms or 1 K across the amplifier output for a transistor or tube circuit, respectively. Set the output signal level of the bridge to be compatible with the linear signal handling ability of the active device.

Step 4

Apply power to the active device, and tune the amplifier to resonance. Null the bridge and note the input and output voltage and the parallel input impedance components indicated by the bridge. When the amplifier employs a transistor in the grounded base configuration, the parallel inductive component is usually too small to tune directly with the internal tuning capacitor, and the addition of external capacitance is necessary to obtain a null.

Because of the small range of capacitance measuring capabilities of the RX meter, it is necessary to calibrate this external capacitor by the substitution method. A coil is wound to tune with the bridge capacitor at the upper end of its range (100 PF), the capacitor to be calibrated is then placed in parallel with this coil across the bridge terminal, and the RX meter is again nulled. The difference in the RX meter capacitor setting when measuring the coil alone and when measuring the coil and external capacitor in parallel is equal to the external capacitor value. Values of capacitance up to 120 PF can be calibrated in this way.

Step 5

Repeat Step 4 for ascending values of load resistance across the amplifier output. Almost invariably, as the process of increasing the load resistor value and measuring gain and input impedance proceeds, the resistive component of the active device input impedance will be found to increase in value. Eventually, if the load resistor value is increased sufficiently, it will be found impossible to null the bridge or, alternatively, the null will occur at a high resistive component value. This can be interpreted as complete instability of the test circuit, the positive feedback present in the amplifier being sufficient to supply virtually all the required input power.

Step 6

Plot graphs of power gain and input resistance as a function of total resistance R_T . R_T consists of the load resistance, the voltage measuring probe resistance, and the effective parallel resistance of the tuning inductor.

4.5.4 Design Procedure

From the background data assembled in the preceding sections and the design evaluation data sheets, it is now possible to select the most important information and relate it to the decisions required in the design procedure that was developed in the general discussion, Paragraph 4.4.

4.5.4.1 Step 1, Crystal Operating Condition

In the frequency range under discussion, only resonance or series resonance crystals are applicable.

4.5.4.2 Step 2, Selection of Crystal Type

This selection has to be from those available and is based on the following two requirements:

- (a) Overall oscillator frequency tolerance
- (b) Frequency of oscillation

Only wide operating temperature range crystals are considered here, but an indication of the performance level attainable with temperature controlled crystals can be obtained from the discussion.

With reference to requirement (a) above, oscillator evaluations at these frequencies show that when a vacuum tube is employed, the effect of the oscillator components other than the crystal on the frequency stability with temperature can be made less than ± 0.0005 percent. Adding another ± 0.0005 percent for variations between tubes and other discrepancies suggests an overall oscillator frequency tolerance ± 0.001 percent wider than that of the crystal alone. Referring to Table 4, and using the values quoted in the preceding sentence, this suggests that in the range of 10 MC to 17 MC the best attainable overall frequency tolerance will be ± 0.006 percent. From 17 MC to 62 MC, the minimum will be ± 0.003 percent using a CR-77/U crystal. Above 62 MC, only ± 0.005 percent crystals are available, and the overall oscillator tolerance will be ± 0.006 percent.

For transistor oscillators, the increase in frequency tolerance with temperature above that of the crystal alone was no greater than ± 0.002 percent. Adding another ± 0.001 percent for variations of transistor parameters, etc., suggests that an overall oscillator frequency tolerance ± 0.003 percent wider than that of the crystal alone is possible.

It should be noted that no attempts were made to correct the added frequency tolerance with temperature introduced by the active device. In the case of the tube oscillator, there appears to be little to gain by doing this, in view of the limited effect. However, in the transistor oscillator, it should be possible to at least halve the tolerance quoted.

Table 6 shows the minimum overall oscillator frequency tolerances likely to be obtained at various frequencies.

TABLE 6. OSCILLATOR FREQUENCY TOLERANCE (%)

Frequency (MC)	Tube Oscillator	Transistor Oscillator
10-17	± 0.006	± 0.008
17-62	± 0.003	± 0.005
62-200	± 0.006	± 0.008

If, in a particular design, closer frequency tolerances than these are required, temperature control of the crystal will be required. In extreme cases, temperature control of the entire circuit will be necessary.

Referring to requirement (b), Table 4 lists the available military standard crystals. The contents of this table can be extended by noting that crystals conforming to the CR-54A/U or CR-56A/U Specification (with the exception that $R_1 \leq 100$ ohms) can be supplied in the frequency range of 125 MC to 200 MC.

4.5.4.3 Step 3, Oscillator Configuration

The grounded grid triode and the grounded base transistor active device configurations were the only ones used successfully in this frequency range. Attempts to design oscillators using a grounded cathode tetrode and a grounded emitter transistor were unsuccessful at 200 MC due to the large excess phase shift occurring in the amplifier circuits. No similar designs at lower frequencies were attempted. However, based on the results obtained at 200 MC, neither of these circuits appears practical

at frequencies above 100 MC; and in the case of the transistor, a more likely figure would be 30 MC.

Because of this limited experience with alternatives, the only configurations discussed here are the grounded grid triode and the grounded base transistor circuits. The relative advantages of the triode over the transistor are:

- (a) Better oscillator overall frequency stability (see discussion of Step 2 of the Design Procedure, Paragraph 4.5.4.2).
- (b) Possible lower cost when high-temperature operation is required; that is, when only silicon transistors can be contemplated. This is particularly true when the frequency of operation is higher than 120 MC.

The advantages of the transistor over the triode are:

- (a) Considerably higher power output at all frequencies
- (b) Reduced power dissipation
- (c) Decreased circuit complexity
- (d) Less difficult to design (particularly for $f > 100$ MC)
- (e) Smaller oscillator package size

These relative comments show that the transistor is superior to the triode in every respect, other than oscillator overall frequency tolerance and, to a lesser extent, cost. The use of a transistor is recommended in all oscillator designs for which their frequency tolerance degradation is acceptable.

4.5.4.4 Step 4, Desired Active Device Characteristics

Several of the desired active device characteristics are independent of frequency and crystal parameters. These are:

- (a) High stable gain. This is desirable independent of power output requirements, since if the power output requirement is moderate, the gain (in excess of that necessary for oscillation with the specified load) can be employed in reducing the effects of the circuit on the frequency of oscillation and the frequency stability. The gain variations with temperature and between units should be small.

- (b) Low effective parallel reactance relative to the resistance levels at both input and output. This helps in the design of impedance transforming networks, higher efficiencies being possible when external circuit reactance does not limit the design.
- (c) The phase shift between input and output under tuned conditions should not exceed ± 10 degrees. This follows from the fact that, if the phase shift is small, the variations between units will be small. Also, phase shifts of this magnitude can be corrected easily, using networks with stable phase angle characteristics; while the introduction of larger phase shift correction is obtained only at the expense of increased phase sensitivity to component value changes. An example of this is the simple CR phase-lead network which has a phase curve as shown in Figure 18. This curve shows that when operating at the frequency where $\frac{\omega}{CR} = 5$, the variation in phase angle of the CR network resulting from the use of components with a ± 10 percent tolerance will not exceed ± 2 degrees. If the working point is moved to $\frac{\omega}{CR} = 1$ in order to obtain increased phase shift, the possible variation in phase shift using ± 10 percent tolerance components will be approximately ± 6 degrees.

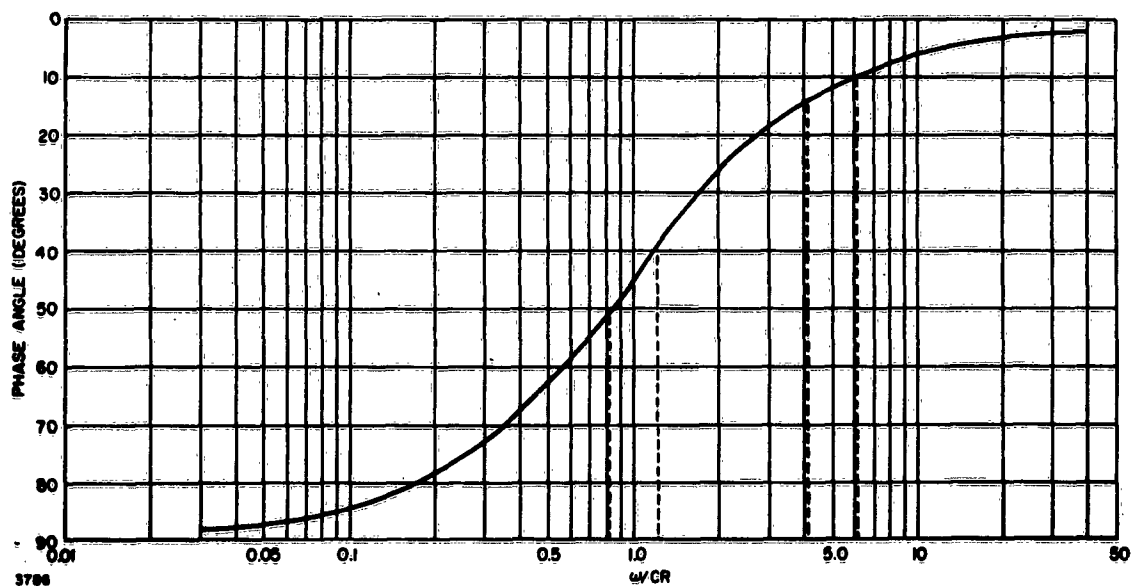


Figure 18. Phase Angle Curve of a CR Lead Network

Other desirable characteristics of the active device are:

- (a) An input resistance approximately equal to the crystal resonance resistance (or series resistance), since this will obviate the need for an impedance transforming network.
- (b) A low output resistance compared to the effective load resistance due to the impedance transformer losses. This characteristic is frequency dependent; the higher the frequency of operation, the lower the desirable output resistance.

4. 5. 4. 5 Step 5, Selection of Active Device

Bearing in mind the characteristics of the triodes and transistors available, the following recommendations are made.

(a) Triodes for Operation Below 100 MC

$$U \geq 40$$

$$R_p \leq 10 \text{ K}$$

$$C_{gk} \leq 4 \text{ PF}$$

(b) Triodes for Operation Above 100 MC

$$U \geq 40$$

$$R_p \leq 6 \text{ K}$$

$$C_{gk} \leq 2 \text{ PF}$$

The characteristics quoted for operation above 100 MC are equally applicable for operation below 100 MC; however, the requirements are less stringent at the lower frequencies.

Other physical features that point to good high frequency characteristics are:

- (c) Small electrode structure mounted close to the tube pins , resulting in minimum lead inductance
- (d) Multiple grid connections

Several commercial tubes having excellent characteristics are available in miniature tube type envelopes. However, there do not appear to be any military type equivalents, possibly because the close electrode spacing and lack of rigidity are incompatible with military environmental stress levels.

There are also several coaxial triodes available that are designed with high stress levels in mind. These have performance characteristics superior to the commercial tubes mentioned in the preceding paragraph in that the lead inductance is further reduced and the grid forms a true screen between plate and cathode. However, these tubes are quite expensive and would not normally be considered for this application.

The nuvistor triode type 8058, which was used successfully at frequencies up to 200 MC, represents a compromise both in cost and performance between the coaxial triodes and the commercial tubes, having less isolation between input and output than the former and greater rigidity than the latter.

(e) Transistors

$$f_{\max} \geq 4 \text{ times the operating frequency}$$

$$f_T \geq 2 \text{ times the operating frequency}$$

$$C_{ob} < 5 \text{ PF}$$

It is also desirable that the transistor power dissipation rating should not be excessively large when compared with the required oscillator power output. High power dissipation transistors tend to have more internal feedback because of the larger junction areas.

4.5.4.6 Step 6, Determination of Active Device Characteristics

Using the data sheet information relating the active device characteristics to the bias conditions, design a suitable biasing network for the active device. Incorporate this into a single tuned amplifier design as discussed in Paragraph 4.5.3.4; and, using the methods discussed there, determine the power gain and input resistance as a function of load resistance.

4.5.4.7 Step 7, Calculation of Oscillator Component Values

Select an operating point from the power gain and input resistance - versus - R_T curves obtained in Step 6, by specifying a value of R_T . The bases for selecting a value of R_T are:

- (a) The behavior of the R_{in} curve. Almost invariably, $\frac{dR_{in}}{dR_T}$ increases

rapidly with increasing values of R_T , indicating the tendency of the amplifier to oscillation for large R_T values. The operating point must therefore be selected for a value of R_T that adequately suppresses this effect. An empirical rule developed from the experience of the design evaluation is that the working value of R_{in} should not exceed twice the value that R_{in} approaches as R_T is decreased to a low value.

A useful check on the adequacy of the chosen working point is obtained when the oscillator is operated; as the oscillator output tuning is varied, the oscillator output voltage will fall to zero on either side of the optimum tuning point. If this tuning characteristic exhibits a hysteresis effect; that is, the oscillator output voltage does not vary smoothly when tuned through the operating range, but instead has a jerky action, it is a sure indication that the selected value of R_T is too high and should be reduced.

- (b) The ratio of load resistance R_L to the effective tuned circuit losses R_D in parallel with R_L . R_T is comprised of R_L and R_D , and the true power gain is determined by the power into R_L alone. If this is taken into account, the maximum true power gain may be obtained at a lower value of R_T than that stipulated in Item (a).

In transistor amplifiers this effect seldom requires consideration, since R_L is generally considerably smaller than R_D ; but in triode amplifiers, where the output impedance level is higher, this effect should be considered.

When these conditions, Items (a) and (b), are satisfied, the usable power gain for a tube will be in the region of $\frac{U}{3}$ to U , and for a transistor somewhere between 200 to 300. Knowing:

- | | |
|--|-----------------------------|
| (c) The active device power gain, G_p | } for a particular value of |
| (d) The active device input resistance, R_{in} | |
| (e) The crystal series or resonance resistance, R_1 or R_r | |

The following values can be calculated using Equations (26) to (30) of paragraph 4.2.2:

- (f) The feedback efficiency, E

(g) The load resistance, R_L

(h) The effective load in parallel with R_L due to the feedback network, R_{FB}

$$E = \frac{R_{in}}{R_{in} + R_1} \quad \text{or} \quad \frac{R_{in}}{R_{in} + R_r} \quad (72)$$

$$G'_p = G_p \cdot E \quad (73)$$

$$R_L = \frac{G'_p}{G'_p - 1} \cdot R_T \quad (74)$$

$$R_{FB} = G'_p \cdot R_T \quad (75)$$

As a safety factor, it is recommended that the value of G'_p , used in determining R_L and R_{FB} , should be one-half to one-third of the value obtained from Equation (73).

4.5.4.8 Step 8, Design of Impedance Transforming Network

The impedance to be transformed is $R_{in} + R_1$, and the transformed value should be R_{FB} . The required transformation ratio is therefore:

$$T_r = \frac{R_{FB}}{R_{in} + R_1} \quad \text{or} \quad \frac{R_{FB}}{R_{in} + R_r} \quad (76)$$

Knowing T_r and the impedance levels involved, a suitable impedance transforming network can be designed from the formulae in Paragraph 4.7. In designing this network, the reactive component of the active device output impedance must be taken into account.

4.5.4.9 Step 9, Experimental Adjustments

Convert the amplifier circuit into an oscillator by adding the impedance transforming network and the crystal. Tune the oscillator for maximum output voltage. Monitor the output frequency and determine the mis-correlation between the actual frequency and the crystal f_r or f_s , depending on which applies. If the actual frequency is above the crystal frequency, the crystal has to introduce a phase lead to offset a phase lag in the remainder of the oscillator circuit, or vice-versa. This mis-correlation can be corrected by introducing a small additional phase shift into the

impedance transforming network as indicated in Paragraph 4.7. However, before applying this correction it is useful to determine the loop gain in the circuit, by reducing the loop gain until oscillation is just maintained. A practical method is to increase the transformation ratio of the impedance transforming network. The operating transformation ratio should then be one-half to one-third of that obtained from this test, and will allow for variations in the active device and other component characteristics. It will also reduce the power output variations under conditions of changing load, power supply voltage, and temperature.

In the event that a Crystal Impedance (CI) meter is unavailable and consequently R_r or R_1 cannot be determined by these means, an indication of the frequency correlation can be obtained by substituting a resistor (equal to $R_r \text{ max}$) for the crystal and noting the frequency of oscillation. For good correlation, the frequency of oscillation with the resistor substituted for the crystal should be close to that obtained with the crystal in circuit. This implies that the substitution resistor should not be reactive, and it is suggested that this be confirmed by measurement at the frequency of interest. If X_{co} is being tuned out, it will, of course, be necessary to remove the tuning coil when substituting the resistor for the crystal.

If desired, this approach can be elaborated to yield the approximate value of R_r or R_1 by comparing the oscillator output voltage for the two conditions of test. If the output voltages are approximately equal, the value of R_r or R_1 is approximately equal to the substitution resistor value.

The crystal power dissipation should also be determined. This can be easily done at oscillator frequencies up to 50 MC by measuring the voltage at each of the crystal terminals and calculating the difference voltage V_d . An approximate value of crystal power dissipation P_c is:

$$P_c = \frac{V_d^2}{R_r} \quad (77)$$

The V T V M probe capacity and resistance should be negligible in comparison with the circuit levels.

At higher frequencies this requirement becomes increasingly difficult to meet, since the probe loading affects the frequency of oscillation and the oscillator drive conditions appreciably. In many cases oscillation will cease when the probe is connected to the active device input side of the crystal. Normally, the effect of probe loading is small when connected to the feedback side of the crystal, since the impedance level

there is usually low (approximately $\frac{R_T \cdot R_o}{R_T + R_o} \cdot \frac{1}{T_r}$). Measuring this voltage, and knowing R_{in} and R_r allows an approximate determination of crystal dissipation to be made.

It is important that the crystal dissipation not exceed the crystal rating. In transistor oscillators operating at bias levels of approximately 5 MA to 12 MA and 10 V to 15 V, this does not present a problem because of the high power gain and low power handling capability of the transistor. However, in tube oscillators, the low power gain and high power handling capabilities can easily cause excessive crystal dissipation.

One method commonly used to reduce crystal dissipation consists of connecting a parallel CR network in the grid-to-ground circuit to obtain a self-biasing action. As the oscillation builds up, the grid is back-biased due to grid current, thereby reducing the power gain, and hence, the power output. A second method consists of reducing the B^+ voltage, thereby limiting the possible output voltage swing. Using a combination of these methods, it is possible to vary the crystal power dissipation. This approach has several disadvantages, particularly at frequencies above 100 MC. These are:

- (a) The power gain decreases more rapidly than the output power limiting capability of the tube.
- (b) The gain and power output of the tube are critically dependent on B^+ voltage and load changes. A 10-percent change in B^+ changes power output approximately 50-percent.
- (c) The active device is no longer operating under the conditions established by the design procedure.

Because of these effects, an alternative method using a diode to limit the plate voltage swing is recommended for this purpose. Figure 19 shows the limiter circuit. The diode is reverse biased by the volt-drop across resistor R due to the plate current. This volt-drop determines the output voltage level at which limiting will occur and can be varied easily by adjusting the value of R. This method completely divorces the power limiting action from the loop power gain characteristics, and gives a considerable improvement in oscillator performance over that obtainable using the other methods. In addition to improving the output power stability with B^+ , R_L , and temperature variations, an improvement of frequency stability with temperature was obtained. Using the first two limiting schemes, the typical frequency stability was ± 0.004 percent, while the diode limiter resulted in a typical frequency stability of 0.0025 percent.

The diode requirements are:

- (a) Low capacitance when reverse-biased (less than 2 or 3 PF)
- (b) Sufficiently high peak-inverse voltage rating
- (c) High rectification efficiency at the operating frequency

5787

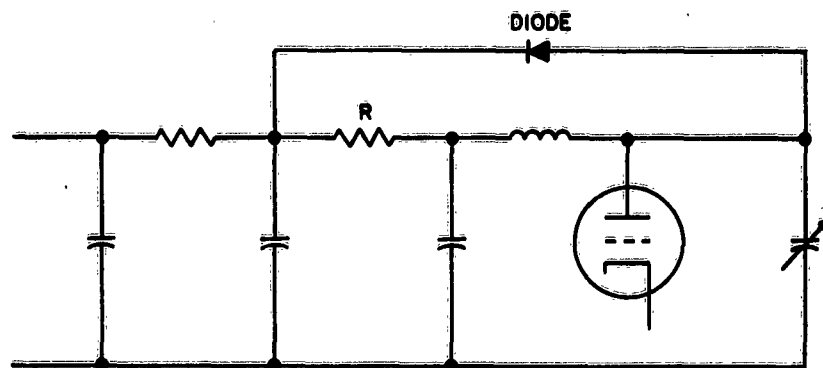


Figure 19. Diode Limiter Circuit

4. 6 Oscillator Design at Low Frequencies

4. 6. 1 General

Below 800 KC, the characteristics of the various oscillator components are well defined; component characteristics can be relied on; active device characteristics can be calculated from data sheet information with reasonable accuracy; phase shifts can be readily controlled, etc. However, as the design frequency decreases, the oscillator complexity tends to increase and, in many ways, low-frequency oscillator design becomes more difficult than design at high frequencies. A major factor in the increased complexity is the characteristics of the quartz crystals applicable to low-frequency design. Another factor is the lack of variable capacitors and inductors of reasonable physical size with sufficient tunable range.

These difficulties are not insuperable, and if oscillator size and weight are unimportant, no problem exists. If these factors are important, it is necessary to use a more complex oscillator circuit.

4. 6. 2 Crystal Characteristics

Table 7 shows the military standard crystal types applicable below 800 KC. More detailed information is contained in Reference 5, Paragraph 7. 0. There are no military specifications at this time for crystals operating between 500 KC and 800 KC or below 16 KC. However, crystals operating down to 800 CPS can be obtained.

Inspection of Table 7 shows that the major characteristics of the military standard crystals are:

- (a) A poor frequency tolerance relative to that of higher frequency crystals
- (b) Low allowable power dissipation below 80 KC
- (c) Large resonant resistance, particularly below 100 KC

TABLE 7. MILITARY STANDARD CRYSTALS, LOW FREQUENCY

WIDE TEMPERATURE RANGE CRYSTALS

Nominal Frequency (Kilocycles)	Operating Temperature (Centigrade)	Frequency Tolerance (Percent)	Drive Level	Holder	Type	Operation P-Parallel R-Resonance	Maximum Equivalent Resistance (Kilohms)
16-100	-40° to +70°	±0.012	0.1 MW	HC-13/U	CR-38 A/U	P, C _L =20PF	110 to 90
16-100	-40° to +70°	±0.012	0.1 MW	HC-13/U	CR-50 A/U	R	100 to 60
* 80-200	-40° to +70°	±0.01	2 MW	HC-21/U	CR-15 B/U	P, C _L =32PF	5 to 6
* 80-200	-40° to +70°	±0.01	2 MW	HC-21/U	CR-16 B/U	R	2 to 2.5
90-250	-40° to +70°	±0.02	2 MW	HC-13/U	CR-37 A/U	P, C _L =20PF	5 and 5.5
* 160-330	-55° to +75°	±0.004	0.1 MW	HC-15/U	CR-39/U	R	0.15 and 0.6
200-500	-40° to +85°	±0.01	2 MW	HC-6/U	CR-25 A/U	R	2.5 to 7.5
* 200-500	-40° to +85°	±0.01	2 MW	HC-6/U	CR-46 A/U	P, C _L =20PF	5.3 to 8.5
200-500	-40° to +70°	±0.01	2 MW	HC-6/U	CR-63 A/U	P, C _L =20PF	5.3 to 8.5

TEMPERATURE CONTROLLED CRYSTALS

* 80-200	75° ±5°	±0.002	2 MW	HC-21/U	CR-29 A/U	P, C _L =32PF	5 to 6
* 80-200	75° ±5°	±0.002	2 MW	HC-21/U	CR-30 A/U	R	2 to 2.5
90-250	75° ±5°	±0.003	2 MW	HC-13/U	CR-42 A/U	P, C _L =32PF	4.5 and 5
* 160-330	70° ±5°	±0.003	0.1 MW	HC-15/U	CR-40/U	R	0.15 and 0.6
200-500	75° ±5°	±0.002	2 MW	HC-6/U	CR-26 A/U	R	2.5 to 7.5
200-500	75° ±5°	±0.002	2 MW	HC-6/U	CR-47 A/U	P, C _L =20PF	5.3 to 8.5

* GOVERNMENT PERMISSION REQUIRED PRIOR TO USE

Manufacturer's data for crystals operating below 16 KC continues the trends shown in Table 7 with widening frequency tolerances, increasing resonant resistance, and decreasing power dissipation. Typical values are:

- (a) Frequency tolerance, $\pm 0.015\%$
- (b) Maximum dissipation, 10 UW
- (c) Maximum effective resonant resistance, 200 K
- (d) Crystal Q, 5000 to 50,000

Table 7 shows that an abrupt change in the resonant resistance of the crystals occurs in the vicinity of 90 KC to 100 KC. At lower frequencies, the large value of resonant resistance tends to prohibit their use in oscillators of the Pierce type. There are two reasons for this:

- (a) Low series arm Q when operated with the specified load capacitor C_L
- (b) The large value of effective crystal resistance, R'_a , incompatible with circuit levels at frequencies where reason (a) does not apply

To illustrate reason (a), a CR-38A/U crystal of 80-KC nominal frequency will have a C_0 of approximately 5 PF. Combining this with a $C_L = 20$ PF gives a $C_T = 25$ PF. Therefore, at 80 KC, $X_{CT} = 80$ K. For operation in Pierce type oscillators, X_{CT} should be greater than twice and preferably 4 times the series arm resistance R_1 . The specification sheet shows that R_T may be as high as 100 K, which does not satisfy the requirements. Many CR-38A/U crystals have a resonant resistance considerably below the maximum permissible value and could therefore be operated satisfactorily in this circuit. However, if conditions approaching those of the example occur with the highest permissible value of R_T , oscillation will not be possible with all crystals.

To illustrate reason (b), a CR-38A/U crystal of 16 KC nominal frequency will have a C_0 of approximately 7 PF. Combining this with a $C_L = 20$ PF gives a $C_T = 27$ PF. At 16 KC, $X_{CT} = 370$ K. R_1 , the series arm resistance will be somewhat smaller than R_T , which in this case is 110 K maximum. The minimum series arm Q is therefore approximately 4. Inserting these values in the formula:

$$R'_a = (1 + Q^2) R_1 \quad (78)$$

gives:

$$R'_a \approx 1.6 \text{ MEGO}$$

A crystal having $R_T = 110$ K is of low Q relative to other crystals of the same type having lower R_T values. Consequently, the crystal loading due to the remainder of the oscillator circuit should be minimized to avoid further Q degradation. Combined active device input and driving source loading of at least 5 MEGO would be desirable. These resistance levels are incompatible with either tubes or transistors, and although impedance transformers could possibly remedy this, the high impedance levels make this type of operation undesirable.

For these reasons, the low-frequency crystals designed for operation at parallel resonance in conjunction with a specified load capacitor are usually operated with the loading capacitor in series with the crystal. The crystal and loading capacitor combination behaves like a resonant circuit in the vicinity of the crystal parallel resonant frequency, and can therefore be treated in the same manner as a crystal designed for operation at resonance. Some advantage is gained in that, if the loading capacitor is made variable, minor oscillator frequency errors can be corrected.

At frequencies above 100 KC, R_p is at least one order of magnitude smaller, permitting operation in Pierce type oscillators. While the value of R_a will still be large, the series arm Q will also be greater, permitting heavier loading of the crystal by the external circuit.

The crystals designed for use below 16 KC have four electrical connections. These can be paired for operation as a conventional two-terminal crystal or, alternatively, the crystal can be used as a two-terminal pair network. When connected in this way, the crystal operates as a mechanical bandpass filter with 0 degrees or 180 degrees phase shift between input and output at mid-frequency; the phase angle depending on the circuit connections to the crystal. It will be shown that this method of operation can greatly simplify the oscillator circuit.

4. 6. 3 Active Device Characteristics

For the types of active device likely to be used in oscillator circuits at these frequencies, the characteristics are virtually independent of frequency from DC to 500 KC. Practically all transistors of milliwatt power rating have current gain cutoff frequencies higher than 2 MC, while certain audio frequency triodes are the only vacuum tubes having performance limitations below 500 KC.

Power gain and input impedance calculations can, therefore, be based on the low-frequency active device parameters normally given in the data sheets. The applicable formulae are given below.

4. 6. 3. 1 Tubes

(a) Grounded Grid Configuration

The power gain of a grounded grid amplifier is:

$$G_p = \frac{(U + 1) R_T}{R_T + R_p} \quad (79)$$

where

U = tube amplification factor

R_p = tube plate resistance

R_T = total load resistance in the plate circuit

The maximum power gain $G_p \text{ max}$ is obtained when $R_T \gg R_p$, giving:

$$G_p \text{ max} = U + 1 \quad (80)$$

The input resistance (cathode input) is:

$$R_{in} = \frac{R_p + R_T}{U + 1} \quad (81)$$

The output resistance R_o is:

$$R_o = R_p + (U + 1) R_G \quad (82)$$

where

R_G = generator source resistance

(b) Grounded Cathode Configuration

The power gain expression is:

$$G_p = \frac{U^2 \cdot R_T \cdot R_g}{(R_T + R_p)^2} \quad (83)$$

where

R_g = value of the grid leak resistor

The maximum power gain is obtained when $R_T = R_p$, giving:

$$G_p \text{ max} = \frac{U^2}{4} \cdot \frac{R_g}{R_p} \quad (84)$$

The input resistance is:

$$R_{in} = R_g \quad (85)$$

The output resistance is:

$$R_o = R_p \quad (86)$$

The formulae, as given, are directly applicable to triode amplifiers, but require modification when used for pentode or tetrode circuits because of the large values of U and R_p encountered in multigrid tubes. The modified formulae are as follows:

(c) Grounded Grid Configuration

$$G_p = g_m \cdot R_T \quad (87)$$

where g_m is the mutual conductance of the tube and is related to U and R_p by the expression:

$$U = g_m \cdot R_p \quad (88)$$

$$R_{in} = \frac{1}{g_m} \quad (89)$$

$$R_o = R_p \quad (90)$$

(d) Grounded Cathode Configuration

$$G_p = g_m^2 \cdot R_T \cdot R_g \quad (91)$$

$$R_{in} = R_g \quad (92)$$

$$R_o = R_p \quad (93)$$

The introduction of an unbypassed cathode resistor R_K changes the power gain formula for the triode to:

$$G_p = \frac{U^2 \cdot R_T \cdot R_g}{[R_T + R_p + (U + 1)R_K]^2} \quad (94)$$

and for a multigrid tube to:

$$G_p = \frac{g_m^2 \cdot R_T \cdot R_g}{(1 + g_m \cdot R_K)^2} \quad (95)$$

Additional information is contained in Reference 4, Paragraph 7.0.

4.6.3.1.1 Typical Tube Amplifier Operating Characteristics

The typical values of power gain and input and output resistance to be expected are:

(a) Grounded Grid Triode

G_p : 20 to 80
 R_{in} : 150 ohms to 2 K
 R_o : 8 K to 80 K

(b) Grounded Grid Pentode or Tetrode

G_p : 50 to 250
 R_{in} : 100 ohms to 1 K
 R_o : 200 K to 2 MEGO

(c) Grounded Cathode Triode

G_p : 10,000 to 100,000
 R_{in} : Up to 2 MEGO (determined by permissible R_g)
 R_o : 5 K to 80 K

(d) Grounded Cathode Pentode or Tetrode

G_p : 20,000 to 200,000
 R_{in} : up to 2 MEGO
 R_o : 100 K to 2 MEGO

4.6.3.2 Transistors

The manufacturer's data sheets most frequently quote the 'h' or hybrid transistor parameters. These are defined by the equations:

$$V_{in} = h_i \cdot I_{in} + h_r \cdot V_o \quad (96)$$

$$I_o = h_f \cdot I_{in} + h_o \cdot V_o \quad (97)$$

where (referring to Figure 20):

h_i = input resistance at 1, 1' with 2, 2' short-circuited

h_r = reverse voltage transfer ratio from 2, 2' to 1, 1' with terminals 1, 1' open-circuited

h_f = forward current transfer ratio from 1, 1' to 2, 2' with 2, 2' short-circuited

h_o = input resistance at 2, 2' with 1, 1' open-circuited

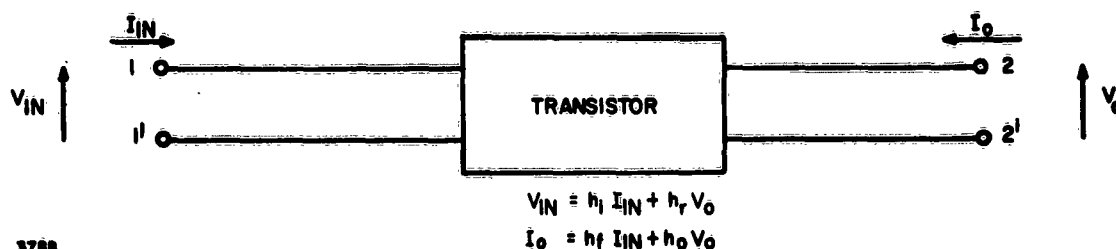


Figure 20. Transistor "Black Box"

Figure 20 defines the current and voltage relationships.

Additional subscripts b, e, or c specify whether the parameters are those for the common base, common emitter, or common collector configuration, respectively. For the purpose of design calculation, these parameters may be regarded as purely resistive in the frequency range under discussion. The base-emitter and base-collector capacitances have only a limited effect which can be remedied if necessary during the experimental stage of the oscillator design.

Typical values of these parameters in the grounded base configuration are usually quoted in the transistor data sheets. These values are normally specified at a particular value of DC emitter or collector current, and for a particular value of DC voltage between collector-base or collector-emitter. In addition, graphs are given showing the change of the parameter values with emitter or collector current,

collector-base or collector-emitter voltage, and with temperature. By using these graphs and the quoted typical parameter values, it is possible to estimate the typical parameter values over a wide range of current, voltage, and temperature.

The data sheets also usually specify the maximum and minimum values of h_{fe} ; the common emitter current gain, and frequently include this and the term $(1 + h_{fb})$ in the graphical information. For a given transistor type, the range of h_{fe} between minimum and maximum values is typically 3:1, and comparable variations of h_{ib} , h_{rb} , and h_{ob} can be expected.

4.6.3.2.1 Power Gain, Input and Output Resistance

The formulae for power gain, input resistance, and output resistance of a transistor in terms of the 'h' parameters are:

$$G_p = \frac{h_f^2 \cdot R_T}{(1 + h_o \cdot R_T) [h_i + (h_i \cdot h_o - h_f \cdot h_r) R_T]} \quad (98)$$

where

R_T = total load resistance

$$R_{in} = h_i - \frac{h_r \cdot h_f \cdot R_T}{1 + h_o \cdot R_T} \quad (99)$$

$$R_o = \frac{h_i + R_G}{h_i \cdot h_o - h_f \cdot h_r + h_o \cdot R_G} \quad (100)$$

where

R_G = driving source resistance

4.6.3.2.2 Common Base to Common Emitter 'h' Parameter Conversions

The transistor data sheets normally give the common base parameters. To convert these to the common emitter parameters, the following formulae are used:

$$h_{ie} = \frac{h_{ib}}{1 + \Delta b + h_{fb} - h_{rb}} \approx \frac{h_{ib}}{1 + h_{fb}} \quad (101)$$

$$h_{re} = \frac{\Delta b - h_{rb}}{1 + \Delta b + h_{fb} - h_{rb}} \approx \frac{\Delta b - h_{rb}}{1 + h_{fb}} \quad (102)$$

$$h_{fe} = \frac{(h_{fb} + \Delta b)}{1 + \Delta b + h_{fb} - h_{rb}} \approx \frac{-h_{fb}}{1 + h_{fb}} \quad (103)$$

$$h_{oe} = \frac{h_{ob}}{1 + \Delta b + h_{fb} - h_{rb}} \approx \frac{h_{ob}}{1 + h_{fb}} \quad (104)$$

where

$$\Delta b = h_{ib} \cdot h_{ob} - h_{rb} \cdot h_{fb} \quad (105)$$

The approximate formulae indicate the dependence of the common emitter parameters on the term $(1 + h_{fb})$. The value of h_{fb} is within a few percent of -1. Consequently, when converting the parameters, small changes in the assumed value can radically affect the values obtained. Therefore, the power gain and impedance level calculations should only be regarded as indicative of the actual performance of the transistor, and experimental checks are desirable.

4.6.3.2.3 Typical Transistor Amplifier Operating Characteristics

The typical operating characteristics of small signal transistor amplifiers suitable for low-frequency oscillator service are:

(a) Common Base Amplifier

G_p = Up to 30 to 35 DB, depending on the degree of input and output matching

R_{in} = 30 to 150 ohms, depending on the total load resistance

R_o = 100 K to 2 MEGΩ, depending on the value of R_G

(b) Common Emitter Amplifier

G_p = Up to 45 DB, depending on the degree of input and output matching

R_{in} = 500 ohms to 5 K, depending on the total load resistance

R_o = 10 K to 100 K, depending on the value of R_G

4. 6. 3. 2. 4 Simplifications of G_p , R_{in} , and R_o Formulae

Various simplifications of these formulae can be made under certain conditions.
If:

$$R_T \ll \frac{1}{h_o} \quad (106)$$

then

$$G_p \approx h_f^2 \cdot \frac{R_T}{h_i} \quad (107)$$

and

$$R_{in} \approx h_i \quad (108)$$

These equations are usually applicable when $R_T \leq 60$ K for common base operation and $R_T \leq 5$ K for common emitter operation. Also, if:

$$R_G \gg h_i \quad (109)$$

then

$$R_o \approx \frac{1}{h_o} \quad (110)$$

Equation (110) is usually applicable when $R_G > 1$ K for common base operation and $R_G > 15$ K for common emitter operation.

4. 6. 4 Possible Oscillator Configurations

Because of the large frequency range covered here and the drastic change in the characteristics of quartz crystals in the vicinity of 100 KC, it is convenient to consider the possible oscillator configurations before discussing impedance transforming networks. It is also convenient to consider the oscillator configurations in two parts, referring to oscillators below and above 100 KC.

4. 6. 4. 1 Oscillator Configurations Below 100 KC

The major factors influencing the possible oscillator configurations are:

- (a) The high resonance resistance of the crystal
- (b) The large size of variable capacitors and inductors suitable for use as tuning elements

Item (b) does not constitute a problem, provided the oscillator size is of little consequence. Under these circumstances, the series configuration discussed in paragraph 4.5 can be employed, with suitable modifications to account for the large value of R_T .

If the oscillator package size must be small, it will be necessary to consider other circuit configurations. The following discussion is intended to show which configurations can be profitably employed.

4.6.4.1.1 Single-Stage Untuned Oscillators

The factors that will determine the practicality of this configuration are:

- (a) **Oscillator Load.** The following stages will normally be an amplifier or mixer. For a tube, the typical load resistance will, therefore, be in the region of 1 MEGΩ for an amplifier and somewhere between 1 K and 50 K for a mixer, depending on the circuit operation. In the first case, the load power will be on the order of 1 UW; in the second, the load power requirements will normally be in the 1 MW to 20 MW region. For a transistor the typical load resistance will be between 1 K and 3 K for an amplifier, and between 50 ohms and 3 K for a mixer or power amplifier. The input power requirements will range from microwatts for a linear power amplifier to a few milliwatts for a mixer or power amplifier.
- (b) **Expected available power gain G_p .** For a tube in grounded grid connection, a realistic value of G_p will be between 30 and 400 (the lower value refers to triodes, the higher value to pentodes or tetrodes). For a tube in grounded cathode connection, G_p will be in the region of 1000 to 100,000, depending on the grid leak resistor value employed. For a transistor in grounded base connection, G_p will be between 100 and 1000, and in the grounded emitter connection between 5000 and 20,000.
- (c) **Active device input resistance.** For a tube in grounded grid connection, the input resistance will be between 100 ohms and 2 K. In the grounded cathode connection, the input resistance will be any value up to 1 MEGΩ. For a transistor in grounded base connection, the input resistance will be between 30 ohms and 200 ohms; in grounded emitter connection, between 500 ohms and 5 K.
- (d) **Active device loading requirements for high power gain.** For a tube in either connection, the desirable load will be in the range of 20 K to 200 K. For a transistor in grounded base connection, loads of 100 K or greater are desirable. In the grounded emitter connection, loads of 10 K to 50 K are desirable.

- (e) Crystal characteristics (CR-50A/U). The maximum resonant resistance is 100 K with a possible minimum of 10 K. Q degradation considerations suggest that a total terminating resistance in the region of 35 K or less will be desirable, giving a feedback efficiency E of 0.26 for an upper limit crystal.

4.6.4.1.2 Grounded Grid or Grounded Base Connections

Consideration of the data of Items (c) and (e), Paragraph 4.6.4.1.1, shows that impedance transformation will be required between the crystal and the active device input if the feedback efficiency is to approach 0.26. Furthermore, this order of efficiency will be required if reasonable power output is to be obtained because of the low available gain in these connections.

Consideration of Items (a) and (d) shows that, with one exception (the load being a vacuum tube amplifier, $R_{in} = 1 \text{ MEGO}$), impedance transforming will be required between the active device and the load.

These considerations show that at least two impedance matching devices will be required because of the low gain available. Impedance transformation at these frequencies requires inductive transformers, and this suggests the possibility of phase inversion. Clearly, if a transformer has to be employed, its phase inverting property can be used to take advantage of the higher available power gain of the grounded cathode or grounded emitter connections.

This leaves only one case worthy of further consideration; that is, a grounded grid oscillator feeding a grounded cathode amplifier. Figure 21 shows a schematic of such an oscillator.

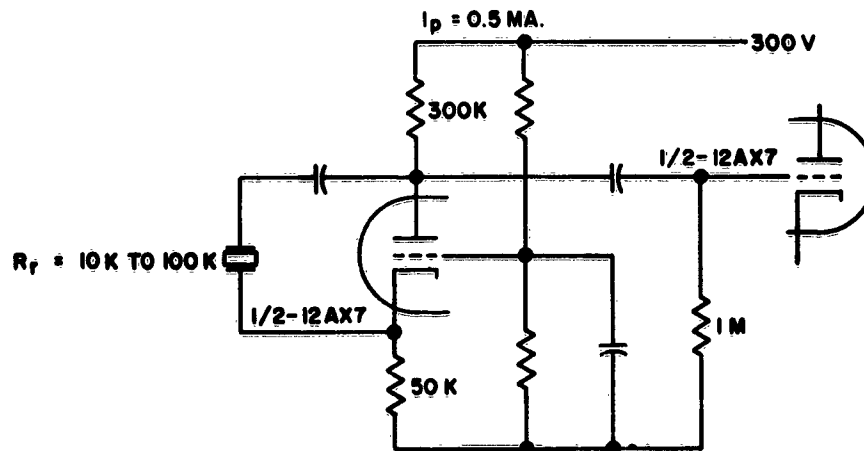


Figure 21. Low Frequency Grounded Grid Oscillator

Using the following characteristics of the 12AX7:

$$U = 100$$

$$R_p = 80 \text{ K}$$

and $R_r = 100 \text{ K},$

the following can be calculated:

$$\text{Load resistance} = 70 \text{ K (300 K, 1 MEG, and 100 K in parallel)}$$

$$G_p = \frac{100 \times 70}{150} = 47$$

$$R_{in} = \frac{150 \times 10^3}{100} = 1.5 \text{ K}$$

$$E = \frac{1.5 \times 10^3}{102 \times 10^3} \approx 0.015$$

$$E \times G_p = 0.7$$

Thus, the loop gain is less than one, and oscillation will not occur using a crystal with $R_r \rightarrow 100 \text{ K}$. With a pentode or tetrode having a g_m of 5000 UA/V, a power gain of 350 would be obtained; however, $R_{in} (\frac{1}{g_m})$ would be 200 ohms, giving $E = 0.002$ or again $E \times G_p = 0.7$.

This shows that single-stage untuned oscillators without matching transformers are not practical, and from the previous discussion there appears to be no point in using grounded grid or grounded base connections with a matching transformer. The use of a transformer alone does not void the initial discussion of this section concerning circuit bulk, since large values of inductance can be packed into relatively small volume. For example, 10 H in 1 to 2 cubic inches is possible.

4.6.4.1.3 Grounded Cathode or Grounded Emitter Connections

Tuned output oscillators and oscillators employing an untuned matching transformer in the output circuit can be considered together because of their similarity of operation. The following discussion is given in terms of the tuned output oscillators, but is also applicable to the untuned case, provided the transformer inductance does not introduce excessive phase shift in the loop. In the untuned case, it may also be necessary to use a frequency selective network to prevent possible oscillation at higher frequencies.

4.6.4.1.4 Triode Oscillator

The circuit to be analyzed is shown in Figure 22. Assuming that the total load R_T is matched to the tube output resistance, the applicable power gain formula is:

$$G_p \text{ max} = \frac{U^2 R_g}{4 R_p} \quad (111)$$

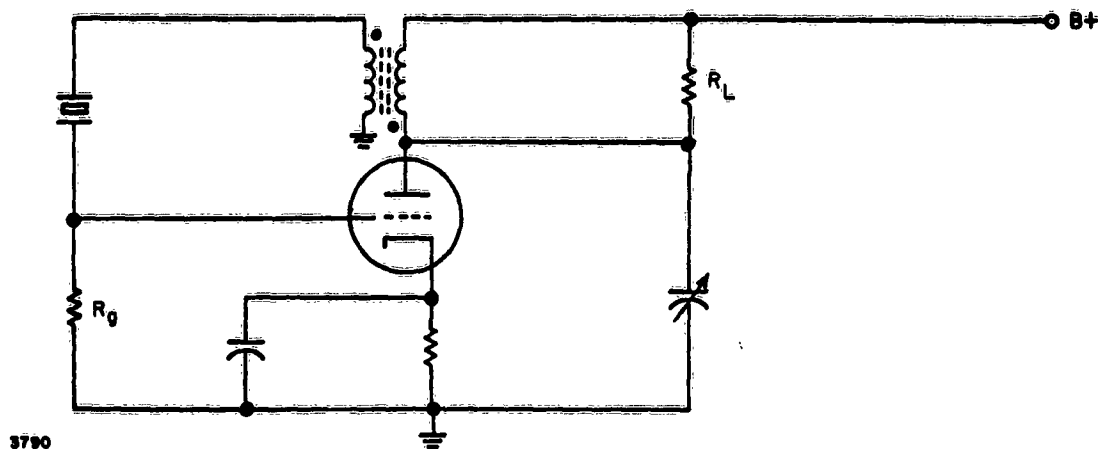


Figure 22. Grounded Cathode Tuned Oscillator

Because R_g will be one of the crystal terminating resistors, its value should be less than 30 K and preferably no more than 20 K.

Fixing the value of R_g determines the type of tube which will give the greatest gain. The desirable characteristics are an $R_p \leq 10$ K and a U as large as possible. Table 8 presents examples of such tubes.

TABLE 8. TWIN TRIODE CHARACTERISTICS

Twin Triode	R_p (K)	g_m (UA/V)	U
6201	10	5500	60
6414	9	5000	45
6829	7	6500	47

$$\text{The feedback efficiency, } E = \frac{20 \text{ K}}{120 \text{ K}} = \frac{1}{6} \quad (R_g = 20 \text{ K}) \quad (112)$$

Therefore

$$G'_{p \text{ max}} = \frac{U^2 R_g}{4 R_p} \cdot \frac{1}{6} \quad (113)$$

$$R_L = \frac{G'_{p \text{ max}}}{G'_{p \text{ max}} - 1} \cdot R_p \approx R_p \quad (114)$$

$$R_{FB} \approx G'_{p \text{ max}} \cdot R_L = \frac{U^2 R_g}{24} \quad (115)$$

$$\text{The Transformation Ratio, } T_r = \frac{R_{FB}}{R_g + R_r \text{ max}} = \frac{U^2 R_g}{24(20 + 100) \times 10^3} \quad (116)$$

Substituting in these equations the values $U = 45$, $R_p = 9 \text{ K}$, and $R_g = 20 \text{ K}$ gives:

$$R_L = 9 \text{ K}$$

$$G'_{p \text{ max}} = 1125$$

$$R_{FB} = 1690 \text{ K}$$

$$T_r \approx 14$$

The output circuit appears to the crystal as:

$$\frac{9 \times 10^3}{2 \times 14} = 320 \text{ ohms}$$

The values of the maximum permissible output voltage and power can be obtained by considering the feedback circuit when $R_r = 20 \text{ K}$ (see Paragraph 4.2.1.4). Since R_r and R_{in} are in series, their power dissipations are equal. Therefore, the total feedback power before crystal overdrive is:

$$2P_{c \text{ max}} = 0.2 \text{ MW (CR-50A/U)} \quad (117)$$

R_{FB} is now changed to:

$$R_{FB} = T_r (R_r + R_{in}) = 560 \text{ K} \quad (118)$$

This is the load that the feedback network presents to the tube output and which appears effectively in parallel with R_L . Therefore, the power into R_L is:

$$P_L = \frac{R_{FB}}{R_L} \times 2P_{c \text{ max}} = 12.5 \text{ MW} \quad (119)$$

The output voltage is approximately 10 VRMS.

The power output calculation is based on the assumption that perfect limiting occurs in the tube output circuit. This is not justifiable in practice, and the power output would have to be decreased. This calculation is also based on a loop gain of 1; a more realistic loop gain of 2 would reduce the permissible output power to below 6 MW.

4.6.4.1.5 Transistor Oscillator

The circuit to be analyzed is shown in Figure 23. For the 2N336 transistor, the following parameters are quoted at the current and voltage levels assumed:

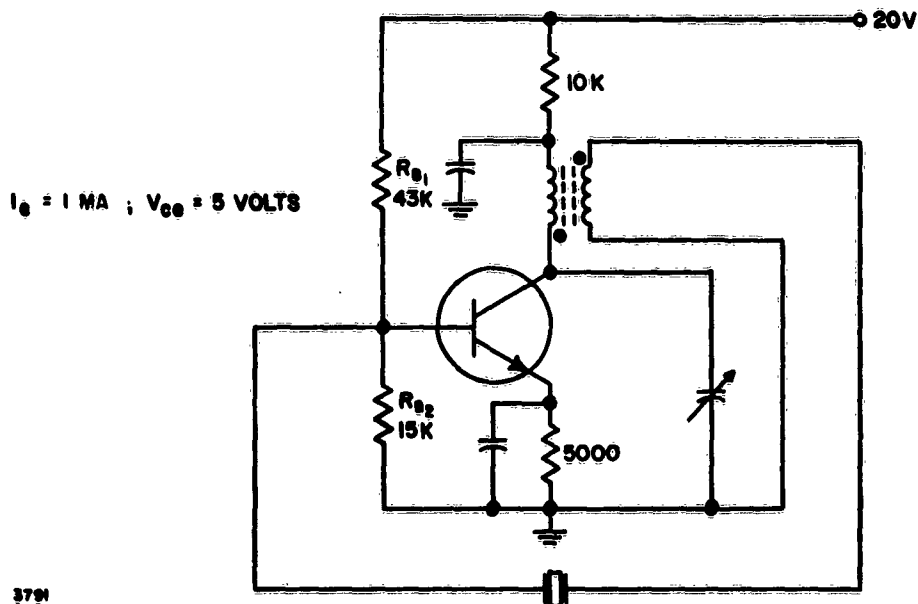


Figure 23. Grounded Emitter Tuned Oscillator

$$h_{ib} = 55 \text{ ohms}$$

$$h_{ob} = 0.25 \times 10^{-6} \text{ mho}$$

$$h_{rb} = 700 \times 10^{-6}$$

$$h_{fb} = -0.99$$

Conversion to the common emitter parameters gives:

$$h_{ie} = 5.5 \times 10^3 \text{ ohms}$$

$$h_{oe} = 0.25 \times 10^{-4} \text{ mho}$$

$$h_{re} = 7 \times 10^{-4}$$

$$h_{fe} = 99$$

Substituting these values in Equations (98) and (99) with $R_T = 10 \text{ K}$ gives:

$$G_p = 12,700$$

$$R_{in} = 5 \text{ K}$$

With the biasing network shown, the value of R_{in} is shunted by R_{B1} and R_{B2} in parallel, and with the values shown, this reduces R_{in} to 3.5 K and G_p to 8700.

$$G'_p = G_p \cdot \frac{R_{in}}{R_{in} + R_r} = 294 \quad (R_r = 100 \text{ K}) \quad (120)$$

$$R_L = \frac{G'_p}{G'_p - 1} \cdot R_T \approx R_T = 10 \text{ K} \quad (121)$$

$$R_{FB} = G'_p \cdot R_T = 2.9 \text{ MEGOHM} \quad (122)$$

$$\text{Transformation Ratio, } T_r = \frac{R_{FB}}{R_{in} + R_r} = 28 \quad (123)$$

giving a transformer turns ratio of 5.3 if unity coupling is assumed.

The values of the maximum permissible output voltage and power can be obtained by considering the feedback circuit when $R_r = 10\text{K}$, the assumed minimum value.

Then:

$$E = \frac{R_{in}}{R_{in} + R_r} = 0.26 \quad (124)$$

Therefore,

$$P_{FB} = \frac{P_{c \max}}{1 - E} = 0.14 \text{ MW} \quad (125)$$

$$R_{FB} = T_r (R_{in} + R_r) = 380 \text{ K} \quad (126)$$

$$P_L = \frac{R_{FB}}{R_L} \cdot P_{FB} = 5.3 \text{ MW} \quad (127)$$

This gives an output voltage of approximately 7 VRMS. This is a larger power output than the transistor is capable of giving under the assumed bias conditions, and there is no danger of crystal overdrive. A larger power output could be obtained by re-designing the oscillator at a higher transistor dissipation level. No transformer losses are accounted for, and, therefore, the effective load would actually be somewhat lower than 10 K. Also, the calculation is based on a loop gain of 1; a more realistic output power based on a loop gain of 2 would give a power output of 2.5 MW.

The impedance level seen by the crystal at the secondary terminals of the feedback transformer is approximately:

$$\frac{R_L}{T_r} = 360 \text{ ohms} \quad (128)$$

The crystal, therefore, sees a total terminating resistance of approximately 3.9 K.

These two examples show that single-stage oscillators employing only one impedance transforming network are feasible. The power output capability of the tube oscillator is twice that of the transistor oscillator. However, it would be difficult to limit the output voltage swing to the level indicated. This problem will not be as severe in the transistor oscillator because of the limited output voltage swing.

4.6.4.1.6 Single-Stage Oscillator Using the Crystal to Give Phase Inversion

As stated in Paragraph 4.6.2, the crystals used below 16 KC can be obtained with the four electrical connections to the crystal brought out individually from the holder. By connecting the crystal as a two-terminal pair network, a phase inverting bandpass filter centered at the crystal resonance frequency is formed (see Reference 3, Paragraph 7.0).

Only preliminary work has been performed using the crystal as described above, and the data gathered is insufficient to form the basis of a design procedure. Only one design evaluation was performed, but the results obtained were so promising that this circuit warrants serious consideration for oscillator design at very low

frequencies.

The evaluation of this oscillator is contained in the Design Data Sheets along with the design approach used.

4. 6. 4. 1. 7 Two-Stage Untuned Oscillators

The impedance transforming network of the single-stage oscillator can be replaced by an additional active device, enhancing the power gain, thereby making impedance matching less critical. There are nine possible cascaded combinations of two tubes or transistors, all of which will increase the overall gain and, in some cases, give a degree of impedance matching between the crystal and the active device. However, when considered relative to the crystal resonance resistance, its desirable terminating resistance level, and the zero phase inversion requirement, the cascaded grounded cathode and grounded emitter configurations have the most desirable characteristics.

In this configuration, the power gain of cascaded triodes with an input grid resistor, $R_g = 20 \text{ K}$, is of the order of 10^5 to 10^6 . The power gain of two cascaded grounded emitter transistors is also of the order of 10^5 to 10^6 . For the maximum power output, the crystal should be placed at the lowest power point of the amplifier; that is, the configuration of Figure 24, which gives the highest power output relative to crystal dissipation.

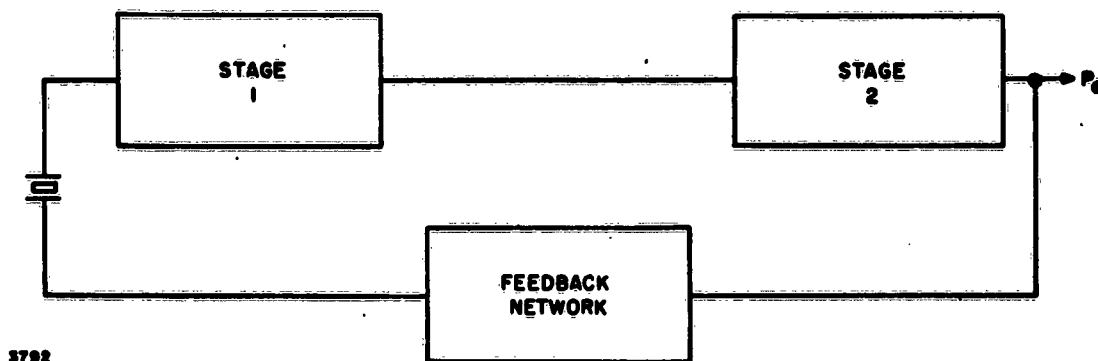


Figure 24. Crystal Position in Two Stage Oscillator

Because of the increased available power gain when using cascaded stages, the impedance transformer can be in the form of a resistive divider network. The values of the network are arranged to terminate the crystal correctly, while giving sufficient loop gain for oscillation. However, in many cases, a simple divider network is inadequate because of its lack of selectivity. Oscillation is likely to occur

either in an overtone mode of the crystal or due to positive feedback through C_0 . The necessary selectivity can be introduced by using a frequency selective RC network in place of the resistive divider. A Wien bridge network serves this purpose admirably; examples of its use are given in the Design Data Sheets.

4. 6. 4. 2 Oscillator Configurations Above 100 KC

Due to the considerably smaller values of R_r max and the smaller inductors and capacitors required for tuning and impedance transforming, only single-stage oscillators need be considered. Allowing for the different crystal characteristics, the grounded cathode and grounded emitter configurations still have the best characteristics both from the standpoint of impedance matching and power gain. These configurations were analyzed in Paragraphs 4. 6. 4. 1. 4 and 4. 6. 4. 1. 5 for tube and transistor, respectively, for low frequency oscillators. Crystals designed for resonant operation in this frequency band have R_r max of the order of 2 K to 7 K, which suggests a desirable terminating resistance of 1 K and 2 K. Inspection of the two calculations shows that for this condition the transistor will have superior gain capabilities due to its inherently low input resistance when operating at high gain. However, either tube or transistor oscillators should be capable of 50 MW to 100 MW output power in this connection with these crystals.

Pierce type oscillators using tubes are also feasible in this frequency band. References 1 and 3, Paragraph 7. 0, deal extensively with tube oscillators of this type.

Field effect transistors should also function well in this configuration at these frequencies.

4. 6. 5 Impedance Transforming Networks

The previous paragraphs note the difficulties of constructing tunable impedance transforming networks at frequencies much below 100 KC and the consequent need for alternative types. The untuned inductive transformer appears to have possible application for this purpose (see Paragraph 4. 7); however, if used solely to supply feedback power, careful design is necessary to prevent phase sensitivity to the value of the crystal resonance resistance. Also, because of its wide bandwidth, it may be necessary to introduce additional selectivity to prevent parasitic oscillation. No designs of this type have been evaluated and, therefore, this is pure conjecture.

Another alternative would be to fix-tune the transformer, the transformer being designed to be uncritical with regard to the tuning.

One partially satisfactory alternative to the tuned transformer is to use a two-stage amplifier in conjunction with a selective feedback network. The disadvantage is the relative complexity of the oscillator circuit.

Below 16 KC an entirely satisfactory alternative for a tube oscillator is the crystal phase-inverting circuit. The design evaluation circuit of this type was the least complex of all those evaluated below 100 KC.

Above 100 KC, conventional tuned impedance transforming networks are applicable. The π network, capacitive divider, tuned transformer, or auto-transformer should all work satisfactorily, providing the network design conditions are satisfied.

4. 6. 6 Design Procedure

An actual design procedure applicable to the entire frequency band is difficult to formulate because of the large variety of possible circuit conditions and the changing characteristics of crystals and impedance transforming networks. One approach to this problem is to divide each step of the procedure into three sections, each section covering a particular frequency band. The frequency breakdown selected is:

- (a) Below 16 KC
- (b) 16 KC to 100 KC
- (c) Above 100 KC

4. 6. 6. 1 Step 1, Crystal Operation

- (a) Below 16 KC. These crystals may be operated at resonance or at parallel resonance with a series capacitor. They can also be operated as two terminal pair filters.
- (b) 16 KC to 100 KC. These crystals may be operated at resonance or at parallel resonance with a series capacitor.
- (c) 100 KC to 500 KC. Resonance operation or parallel resonance with either a series or parallel loading capacitor is possible.

4. 6. 6. 2 Step 2, Selection of Crystal Type

- (a) Below 16 KC. If a design using the crystal as a filter is contemplated (applicable to tube oscillators only), the crystal should be purchased as a resonance crystal with the four connections brought out individually. If the crystal is to be used as a series feedback element, operation at parallel resonance with a series capacitor is recommended because of the small frequency tuning range available in this connection.

- (b) 16 KC to 100 KC. Parallel resonance with a series tuning capacitor is recommended because of the frequency tuning range capability.
- (c) Above 100 KC. All three methods of using the crystal appear possible. However, no experimental evaluations have been made and, consequently, no recommendations are made.

Table 7 shows the military standard low frequency crystals. This table shows that no choice exists unless the special types are considered.

4.6.6.3 Step 3, Oscillator Configuration

- (a) Below 16 KC. For a tube oscillator, a grounded cathode amplifier in conjunction with a phase inverting crystal filter is the recommended choice. The second choice is the grounded cathode amplifier with output tuning if oscillator size is inconsequential. Thirdly, the two-stage amplifier with a frequency selective feedback network. These recommendations are based on circuit simplicity, since the performance of all three types is comparable with the exception of power output.

No evaluations have been made using a phase inverting crystal filter in a transistor circuit, and therefore no recommendations concerning this type of oscillator can be given. From the remaining possible configurations, a grounded emitter amplifier with output tuning is the recommended choice if oscillator size is unimportant. The next choice is a two-stage grounded emitter amplifier with a frequency selective feedback network.

- (b) 16 KC to 100 KC. For a tube oscillator, the recommended choice is a grounded cathode tuned output oscillator. The two-stage grounded cathode amplifier with frequency selective feedback is the second choice.

For a transistor oscillator, the grounded emitter tuned output circuit oscillator is recommended if oscillator size is unimportant. The second choice is two grounded emitter transistors with frequency selective feedback.

- (c) Above 100 KC. Because no experimental evaluations were performed, no recommendations can be given regarding anti-resonant oscillators. With regard to the other alternatives, the practical difficulties of tuning are eased and single-stage-tuned output circuits should present no problems.

4.6.6.4 Step 4, Desired Active Device Characteristics

The requirements are:

- (a) High gain at the circuit impedance levels of the selected configuration
- (b) Power output limiting capability compatible with the crystal dissipation rating
- (c) The active device characteristics should not be frequency sensitive at the desired oscillator frequency

4. 6. 6. 5 Step 5, Selection of Active Device

Tubes should be selected on the basis of:

- (a) High U .
- (b) R_p compatible with desired load.
- (c) R_p and tube stray capacitance compatible with operating frequency.
- (d) If the tube is to provide power output limiting action, the operating power level of the tube should also form a basis for selection. This is not completely necessary, since limiting diodes suitable for operation at these frequencies are inexpensive.

For a transistor the requirements are:

- (a) A high common emitter current gain
- (b) A current gain cutoff frequency f_B of approximately three times the desired operating frequency

4. 6. 6. 6 Step 6, Determination of Active Device Characteristics

At the frequencies under discussion, the active device power gain, input resistance, and output resistance can be calculated from the formulae of Paragraph 4. 6. 3 and the manufacturer's data sheet information. The calculations should be made for power levels compatible with the crystal dissipation. The biasing levels should be such that output limiting will prevent crystal overdrive.

4. 6. 6. 7 Step 7, Calculation of Oscillator Component Values

Various examples of the calculations involved are given in this report and in the Design Data Sheets. These examples should be referred to as possible methods of implementing this process.

4. 6. 6. 8 Step 8, Design of Impedance Transforming Network

Reference should be made to Paragraph 4. 7 for impedance transforming network design formulae.

4. 6. 6. 9 Step 9, Experimental Adjustments

Before connecting the feedback loop, it is helpful to check the actual amplifier power gain and the phase angle between input and output voltage. The latter is easily determined using an oscilloscope. The output limiting action of the amplifier can also be checked by overdriving the amplifier and viewing the output waveform.

4. 7 Impedance Transforming Networks

Several impedance transforming networks are analyzed in the following discussion. In addition to deriving the transformation ratio, the analyses also show the phase relationships between input and output voltages of the networks. From the results of the analyses, design equations or methods are presented which enable impedance transforming networks to be designed for a specific transformation ratio with a given phase shift between input and output.

4. 7. 1 π Network

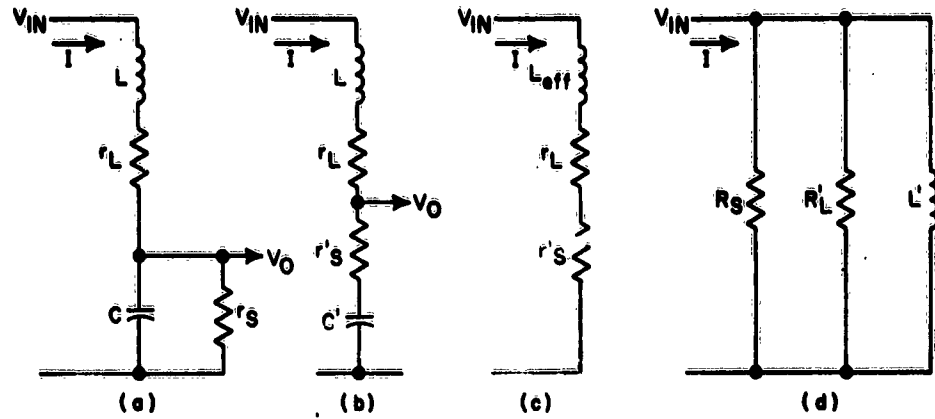
4. 7. 1. 1 π Network Analysis

The following analysis is based on the practical circuit aspects of the network. This is not the most presentable approach mathematically, but it is believed to yield a better practical appreciation of the transforming action of the network.

The useful properties of the π network from the oscillator design viewpoint are:

- (a) The impedance transforming properties between input and output
- (b) The phase inverting action between input and output when the component values are chosen appropriately

The analysis of the impedance transforming portion of the network is developed through the transformations shown in Figure 25. The required network transformation equations are given in Table 3. Figure 25 shows only that part of the network active in the impedance transforming function; the second capacitor used to tune with L' is not shown.

Figure 25. π Network Transformation

Transforming from (a) to (b), Figure 25, the relationships between r'_s and r_s and C' and C (Table 3, c) are:

$$r'_s = r_s \cdot \left(\frac{1}{1 + \omega^2 C^2 r_s^2} \right) \quad (129)$$

and

$$C' = C \cdot \left(1 + \frac{1}{\omega^2 C^2 r_s^2} \right) \quad (130)$$

Transforming from (b) to (c), Figure 25, gives:

$$L_{\text{eff}} = L - \frac{1}{\omega^2 C'} \quad (131)$$

Transforming from (c) to (d), Figure 25 (Table 3, b):

$$\frac{R_s \cdot R'_L}{R_s + R'_L} = (r'_s + r_L) \left[1 + \frac{\omega^2 L_{\text{eff}}^2}{(r'_s + r_L)^2} \right] \quad (132)$$

$$\text{and} \quad L' = L_{\text{eff}} \left[1 + \frac{(r'_s + r_L)^2}{\omega^2 L_{\text{eff}}^2} \right] \quad (133)$$

The value R'_L can be obtained separately by equating r'_s to zero in Equation (132).

The phase angle of the current I relative to V_{in} is:

$$\phi_1 = \tan^{-1} \frac{\omega L_{eff}}{r'_s + r_L} \quad (\text{Lagging}) \quad (134)$$

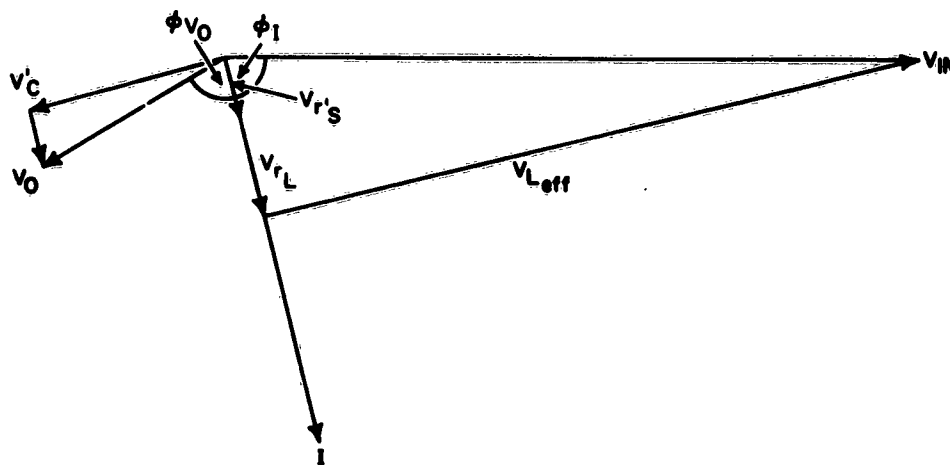
The phase angle of V_o relative to I is:

$$\phi_{V_o} = \tan^{-1} \frac{1}{\omega C r'_s} \quad (\text{Lagging}) \quad (135)$$

The phase lag of V_o relative to V_{in} is, therefore:

$$\phi_1 + \phi_{V_o} = \tan^{-1} \frac{\omega L_{eff}}{r'_s + r_L} + \tan^{-1} \frac{1}{\omega C r'_s} \quad (136)$$

Figure 26 illustrates the vector relationships between the various quantities, and shows that for any practical network there will exist a phase lag of V_o relative to V_{in} which can approach, but never exceed, 180 degrees. The difference from 180 degrees is due to the finite Q of the coil and of the Cr_s circuit elements.



3794

Figure 26. π Network Vector Relationships

4.7.1.2 π Network Design

When used with phase inverting amplifiers, the known requirements for the network are:

- (a) The value of \bar{R}_s . The known ratio of output power to feedback power determines \bar{R}_s .
- (b) The value of r_s . This is the value of the amplifier input resistance in series with the crystal resonant resistance.
- (c) The desired phase shift deviation from 180 degrees may be known. This is mostly applicable to high frequency design.
- (d) At high frequencies, the value of L' is fixed. This is the value of inductance which will tune with the total output capacitance, and includes the tube or transistor output capacitance and the tuning capacitance. At low frequencies, the value of L' becomes a design variable.

The network unknowns are \bar{R}_L , C , r_L , and L . The value of resistance, \bar{R}_L , is not normally of major importance in itself, since its effect can usually be incorporated into the oscillator load by appropriately reducing the total load dissipation. The difficulty is that the values of the other unknowns are all related to \bar{R}_L , except that when \bar{R}_L is greater than $5\bar{R}_s$, its effect will be relatively small.

With this number of unknowns the network design becomes involved, especially when phase requirements have to be met. A relatively rapid method that enables the designer to pay constant attention to the design requirements is the graphical approach outlined below. This is based on the vector diagram of Figure 26.

Since r_s and \bar{R}_s are known and represent the same power dissipation, the ratio of V_o/V_{in} can be calculated as follows:

$$\frac{V_{in}}{V_o} = \sqrt{\frac{\bar{R}_s}{r_s}} \quad (137)$$

Using suitable scaling, draw a line of length V_{in} on the reference axis. From the origin of the vector V_{in} , draw a partial circle of radius V_o in the third quadrant. Bisect V_{in} and, using this point as origin, draw a semicircle in the fourth quadrant of diameter V_{in} . These two circular segments are the loci of V_o and $V(r'_s + r_L)$, respectively. If the required phase angle between V_o and V_{in} is known, the vector V_o can be drawn; if not, a value must be assumed.

Specifying any one of the remaining four vector quantities will automatically complete the design, since V_{Leff} and V'_c are in opposition to each other and mutually perpendicular to $V_{r'_s}$ and $V(r'_s + r_L)$. The choice resolves into the assumption of a value for ϕ_I , and the following factors may influence this choice. For a fixed phase angle between V_o and V_{in} , the value of ϕ_I used determines the power transfer efficiency P_e , since:

$$P_e = \frac{r'_s}{r'_s + r_L} = \frac{V_{r'_s}}{V(r'_s + r_L)} \quad (138)$$

As ϕ_I approaches 90 degrees, the efficiency increases. This is the same as saying the coil losses approach zero. This may be an important factor in the design of low gain amplifier circuits. Another effect as ϕ_I approaches 90 degrees is that the effective Q of the output tuning circuit increases and may be important from the point of view of harmonic rejection.

Using these factors as a design basis, a value for ϕ_I can be selected; and the values of C, L, and r_L can be calculated, using Equations (139) through (143). It should be noted that in these equations $V_{r'_s}$, $V_{c'}$, $V_{L_{eff}}$ and V_{r_L} are voltage magnitudes.

$$r'_s = r_s \cdot \frac{V_{r'_s}^2}{V_o^2} \quad (139)$$

$$X_{c'} = r'_s \cdot \frac{V_{c'}}{V_{r'_s}} \quad (140)$$

$$X_c = X_{c'} \left[1 + \frac{r'_s{}^2}{X_{c'}^2} \right] \quad (\text{Table 3, part (d)}) \quad (141)$$

$$X_{L_{eff}} = X_L' \cdot \frac{1}{1 + \left[\frac{V(r'_s + r_L)}{V_{L_{eff}}} \right]^2} \quad (\text{Table 3, Part (b)}) \quad (142)$$

$$X_L = X_{L_{eff}} + X_{c'} \quad (143)$$

$$r_L = r'_s \cdot \frac{V_{r_L}}{V_{r'_s}} \quad (144)$$

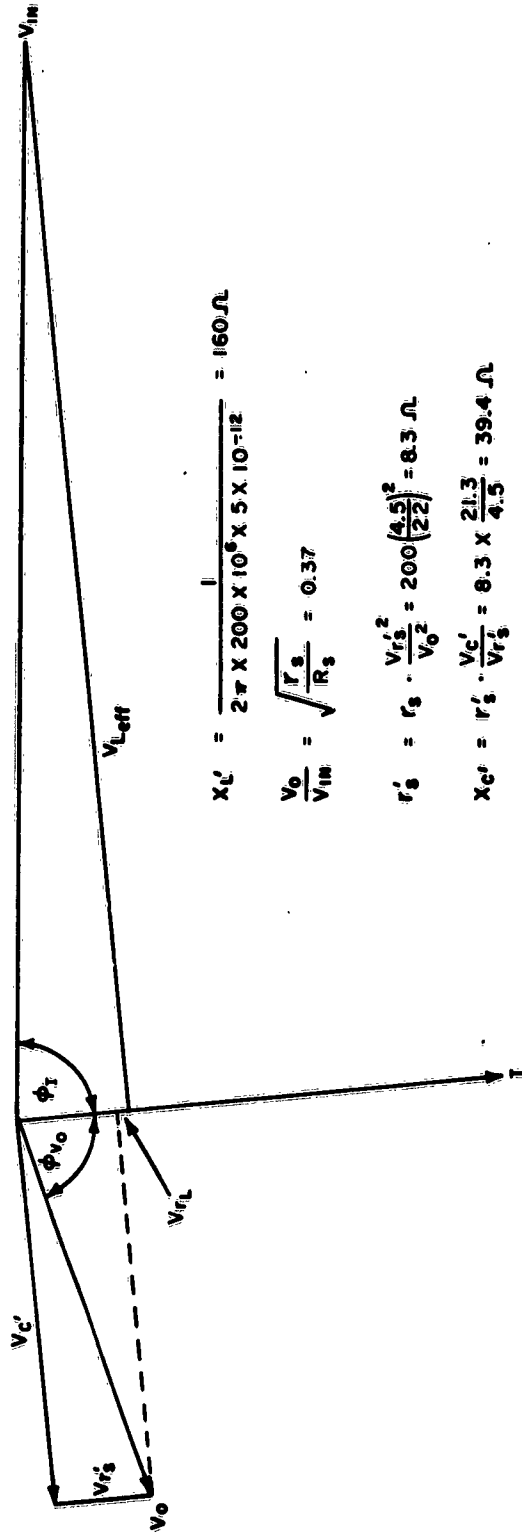
$$\text{The Q of inductance L} = \frac{X_L}{r_L} \quad (145)$$

If this Q is not a feasible value (either too small or too large), the design can be optimized by recalculating, using a new value of ϕ_I . Increasing ϕ_I will require a higher Q for the coil and vice-versa. A typical design is shown in Figure 27.

DESIGN INFORMATION:

$r_s = 200 \Omega$; $R_s = 1.5 K$; TO BE USED AT 200 MC WITH APPROXIMATELY 5pF TUNING CAPACITANCE

PHASE ANGLE OF V_o RELATIVE
TO V_{in} TO BE 160° (LAGGING)



$$X_L' = \frac{1}{2\pi \times 200 \times 10^6 \times 5 \times 10^{-12}} = 160 \Omega$$

$$\frac{V_o}{V_{in}} = \sqrt{\frac{r_s}{R_s}} = 0.37$$

$$r_s' = r_s \cdot \frac{V_{r_s}^2}{V_o^2} = 200 \left(\frac{4.5}{22} \right)^2 = 8.3 \Omega$$

$$X_C' = r_s' \cdot \frac{V_c'}{V_{r_s}} = 8.3 \times \frac{21.3}{4.5} = 39.4 \Omega$$

$$X_C = X_C' \left[1 + \frac{r_s'}{X_C'} \right] = 39.4 \left[1 + \frac{8.3}{39.4} \right] = 48 \Omega$$

$$X_{Leff} = X_L' \cdot \frac{1}{1 + \left[\frac{V(r_s' + r_L)}{V_{Leff}} \right]^2} = 160 \cdot \frac{1}{1 + \left(\frac{0.64}{6} \right)^2} = 120 \Omega$$

$$X_L = X_{Leff} + X_C' = 160 \Omega$$

$$r_L = r_s' \cdot \frac{V_{r_L}}{V_{r_s}} = 8.3 \times \frac{0.5}{5} = 0.83 \Omega$$

$$Q = \frac{X_L}{r_L} = \frac{160}{0.83} = 190$$

Figure 27. Example of π Network Design

4.7.2 Capacitive Divider Network

4.7.2.1 Analysis of Capacitive Divider Network

Referring to Figure 28, it is assumed that the reactive elements are at resonance at angular frequency ω , and that a voltage V_{in} is present across the series combination of C_1 and C_2 . r_s is the load applied across C_2 , and V_{out} is the voltage across r_s . Then:

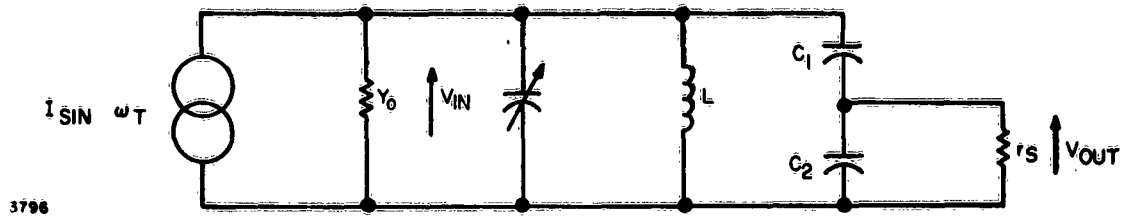


Figure 28. Capacitive Divider Coupling Network

$$\begin{aligned} \frac{V_o}{V_{in}} &= r_s \cdot \frac{j \omega C_1}{1 + j \omega (C_1 + C_2) r_s} \\ &= \frac{\omega C_1 r_s}{\sqrt{1 + \omega^2 (C_1 + C_2)^2 r_s^2}} \angle 90^\circ = \tan^{-1} \omega (C_1 + C_2) r_s \quad (146) \end{aligned}$$

When $\omega^2 (C_1 + C_2)^2 r_s^2 \gg 1$, i.e., $r_s \gg X_{C_1 + C_2}$

$$\frac{V_o}{V_{in}} = \frac{C_1}{C_1 + C_2} \quad (147)$$

Now $\frac{|V_o|^2}{r_s}$, the output power, must be equal to $\frac{|V_{in}|^2}{R_s}$, where R_s is that value of resistance which, if connected across V_{in} with r_s disconnected, would dissipate the same power that r_s does with voltage V_o across it. That is, R_s represents r_s transferred to the input side of the network. Therefore:

$$\frac{|V_o|^2}{r_s} = \frac{|V_{in}|^2}{R_s} \quad (148)$$

and

$$\frac{|V_o|^2}{|V_{in}|^2} = \frac{r_s}{R_s} \quad (149)$$

Substituting for $\frac{|V_o|^2}{|V_{in}|^2}$:

$$\frac{r_s}{R_s} = \frac{\omega^2 C_1^2 r_s^2}{1 + \omega^2 (C_1 + C_2)^2 r_s^2} \quad (150)$$

$$R_s = \frac{1 + \omega^2 (C_1 + C_2)^2 r_s^2}{\omega^2 C_1^2 r_s} \quad (151)$$

Therefore, for the particular case where $\omega^2 (C_1 + C_2)^2 r_s^2 \gg 1$, Equation (151) becomes:

$$R'_s = \left(\frac{C_1 + C_2}{C_1} \right)^2 \cdot r_s \quad (152)$$

For ease of calculation, it is convenient to obtain the relationship, $\frac{R_s}{R'_s}$:

$$\frac{R_s}{R'_s} = \frac{1 + \omega^2 (C_1 + C_2)^2 r_s^2}{\omega^2 (C_1 + C_2)^2 r_s^2} = 1 + \frac{X_{(C_1 + C_2)}^2}{r_s^2} \quad (153)$$

Where

$$X_{C_1 + C_2} = \frac{1}{\omega (C_1 + C_2)}$$

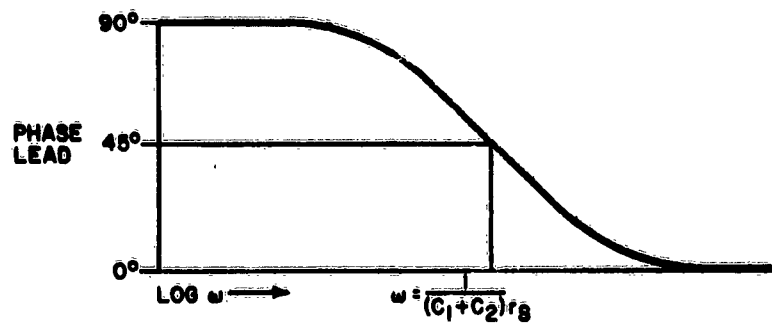
If $r_s = 2 X_{(C_1 + C_2)}$, then $R_s = 1.25 R'_s$

and if

$r_s = 3 X_{(C_1 + C_2)}$, then $R_s = 1.11 R'_s$

This shows that for $r_s \geq 3 X_{(C_1 + C_2)}$, $R_s \approx R'_s$, and Equation (152) adequately describes the circuit insofar as transformation ratio is concerned.

The phase shift occurring between input and output of the network is also of interest. The general phase shift characteristic is shown in Figure 29.



2917

Figure 29. Phase Shift Characteristics

Calculations using the formula $\phi = 90^\circ - \tan^{-1} \omega (C_1 + C_2) r_s$ (see Equation (146)) show that for:

$$r_s = 2 X(C_1 + C_2), \quad \phi = 27^\circ$$

$$r_s = 3 X(C_1 + C_2), \quad \phi = 18^\circ$$

$$r_s = 6 X(C_1 + C_2), \quad \phi = 10^\circ$$

It should be noted that this phase shift is independent of any phase shift due to mistuning of the tank circuit.

An additional effect, which is not brought out in the analysis, is the effective capacitance C_n presented by the C_1 , C_2 , and r_s combination to the input source:

$$C_n = \frac{C_1 \left[1 + \omega^2 C_2 (C_1 + C_2) r_s^2 \right]}{1 + \omega^2 (C_1 + C_2)^2 r_s^2} \quad (154)$$

for the condition $\omega^2 (C_1 + C_2)^2 r_s^2 \gg 1$. This reduces to

$$C_n' = \frac{C_1 \cdot C_2}{C_1 + C_2} \quad (155)$$

If this condition does not apply, then:

$$C_n < \frac{C_1 \cdot C_2}{C_1 + C_2} \text{ since } C_2 < C_1 + C_2$$

The capacitive divider network is useful in oscillator design because of the simplicity of the design equations and the design accuracy obtainable. All the high-frequency oscillators evaluated for this program used this type of feedback network because of these good features.

The analysis assumes that losses in the capacitors have no effect on the network performance. This is a justified assumption when high-quality capacitors are used.

4.7.3 Untuned Inductive Transformer

4.7.3.1 Inductive Transformer Analysis

The circuit to be analyzed is shown in Figure 30,

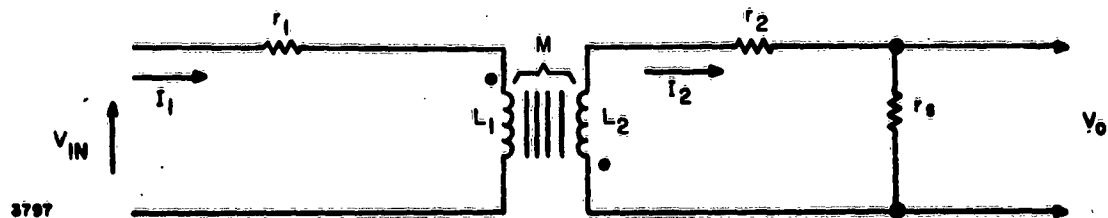


Figure 30. Inductive Transformer

where

L_1 = The primary winding inductance

r_1 = The primary winding resistance

L_2 = The secondary winding inductance

r_2 = The secondary winding resistance

r_s = The load resistance in the secondary circuit

M = The mutual inductive coupling between the two windings defined by:

$$M = K \sqrt{L_1 \cdot L_2} \quad (156)$$

The dots indicate winding polarities. As shown, the transformer has nominal phase inverting properties.

The equations describing this circuit are:

$$V_{in} = I_1 (r_1 + j \omega L_1) + I_2 \cdot j \omega M \quad (157)$$

$$0 = I_1 (j \omega M) + I_2 (r_2 + r_s + j \omega L_2) \quad (158)$$

Substituting for I_2 in Equation (157) gives:

$$V_{in} = I_1 \left[r_1 + j \omega L_1 + \frac{\omega^2 M^2 (r_2 + r_s - j \omega L_2)}{(r_2 + r_s)^2 + \omega^2 L_2^2} \right] \quad (159)$$

Two conditions of operation are considered:

- (a) When the secondary winding is heavily loaded. This would be the case when the oscillator load is connected to the secondary, the assumption being that the feedback power can also be derived from the secondary winding without the need for additional inductive transformers.
- (b) When the secondary is used solely to supply feedback power and the term $E \times G_p$ is large, say larger than 30. In this case the transformer is lightly loaded.

These extreme loading conditions have considerable effect on the transformer operation and are separately analyzed.

4.7.3.1.1 Untuned Transformer, Heavy Secondary Load

For this loading condition, the object is to make the impedance at the primary winding terminals almost purely resistive in order to minimize the phase shift between I_1 and V_{in} . The phase shift between V_o and V_{in} should be as close to 180 degrees as possible.

Assuming that $\omega L_2 \geq 3(r_2 + r_s)$, Equation (159) simplifies to:

$$V_{in} = I_1 \left[r_1 + j \omega L_1 + \frac{M^2}{L_2^2} (r_2 + r_s - j \omega L_2) \right] \quad (160)$$

Substituting for M gives:

$$V_{in} = I_1 \left[r_1 + k^2 \cdot \frac{L_1}{L_2} (r_2 + r_s) + (1 - k^2) \cdot j \omega L_1 \right] \quad (161)$$

The phase angle of V_{in} with respect to I_1 is:

$$\phi_1 = \tan^{-1} \left[\frac{(1 - k^2) \cdot \omega L_1}{r_1 + k^2 \cdot \frac{L_1}{L_2} \cdot (r_2 + r_s)} \right] \quad (162)$$

Typical vector relationships for the transformer primary are shown in Figure 31. Equation (158) establishes the conditions in the secondary of the transformer. The phase angle between the induced voltage $-I_1 \cdot (j \omega M)$ and I_2 is given by:

$$\phi_2 = \tan^{-1} \frac{\omega L_2}{r_2 + r_s} \quad (163)$$

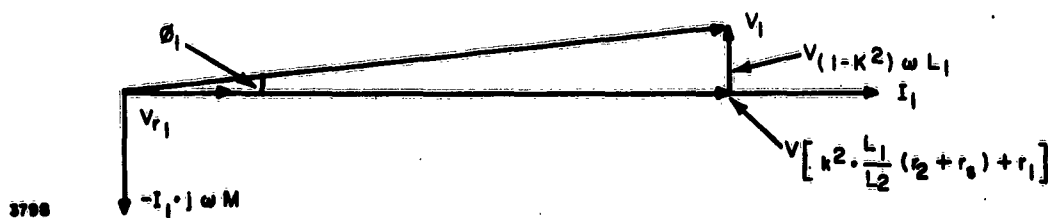


Figure 31. Primary Vector Diagram

Figure 32 shows typical vector relationships for the transformer secondary, remembering that $\omega L_2 \geq 3(r_2 + r_s)$. Combining Figures 31 and 32 gives the vector diagram of the loaded transformer shown in Figure 33. The total phase angle between V_{in} and V_o is:

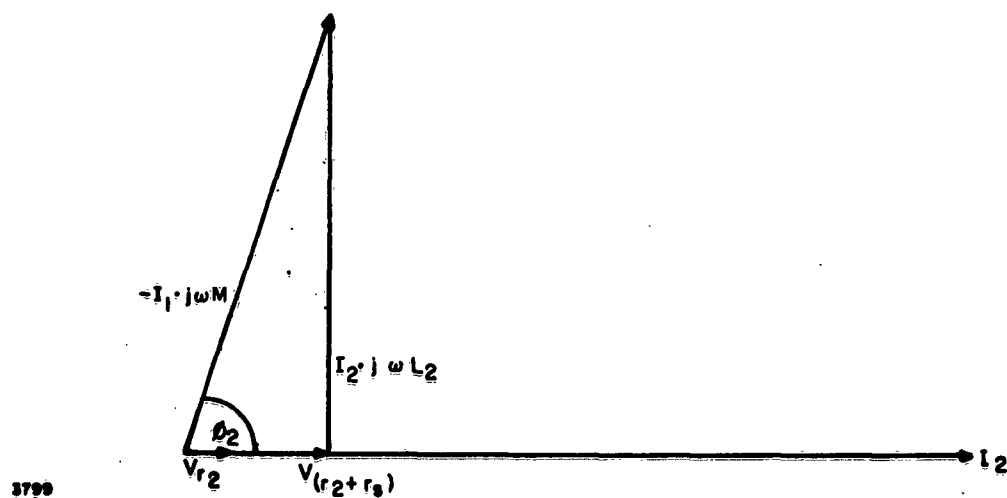


Figure 32. Secondary Vector Diagram

$$\phi_T = \phi_1 + \phi_2 + 90^\circ$$

$$\phi_T = \tan^{-1} \left[\frac{(1 - k^2) \cdot \omega L_1}{r_1 + k^2 \cdot \frac{L_1}{L_2} \cdot (r_2 + r_s)} \right] + \tan^{-1} \left[\frac{\omega L_2}{r_2 + r_s} \right] + 90^\circ \quad (164)$$

Various points may be noted, as follows:

- (a) If ϕ_1 is less than 18 degrees, the voltage across the resistive component of the transformer input impedance is greater than 95 percent of V_{IN} , and the load reflected from the secondary can, for all practical purposes, be regarded as:

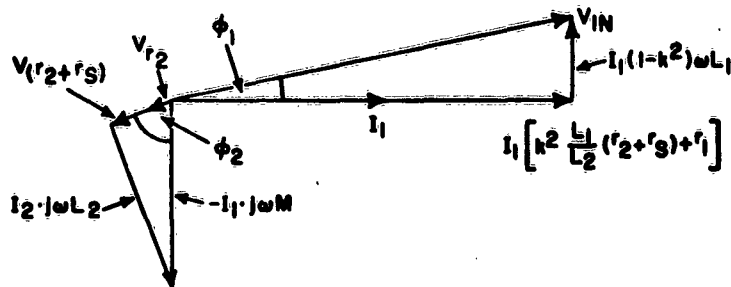


Figure 33. Transformer Vector Diagram

$$R_s = k^2 \cdot \frac{L_1}{L_2} \cdot (r_2 + r_s) \quad (165)$$

Further, if $r_2 \ll r_s$, this reduces to:

$$R_s = k^2 \cdot \frac{L_1}{L_2} \cdot r_s \quad (166)$$

Equation (166) is the well known transformation ratio.

- (b) The power transfer efficiency of the transformer is:

$$E_T = \frac{k^2 \cdot \frac{L_1}{L_2} \cdot r_s}{r_1 + k^2 \cdot \frac{L_1}{L_2} \cdot (r_2 + r_s)} \quad (167)$$

- (c) Small variations of ϕ_1 and ϕ_2 from their ideal values of 0 and 90 degrees tend to compensate each other in maintaining a phase angle approaching 180 degrees between V_{in} and V_o . However, if fed from a resistive source, the source voltage will lag V_{in} because of the inductive nature of the load. This will increase the deviation from 180 degrees of the phase angle of V_o relative to the source voltage. For example, if the source is a grounded cathode vacuum tube, it appears as a power source consisting of R_p in series with a voltage generator, $-uV_g$. In oscillator design, the phase angle of V_o relative to V_g is the important relationship.

4.7.3.1.2 Untuned Transformer Design, Heavy Secondary Load

Figure 34 is representative of a transformer driven by an active device, the latter being shown as a voltage generator in series with its output resistance R_o .

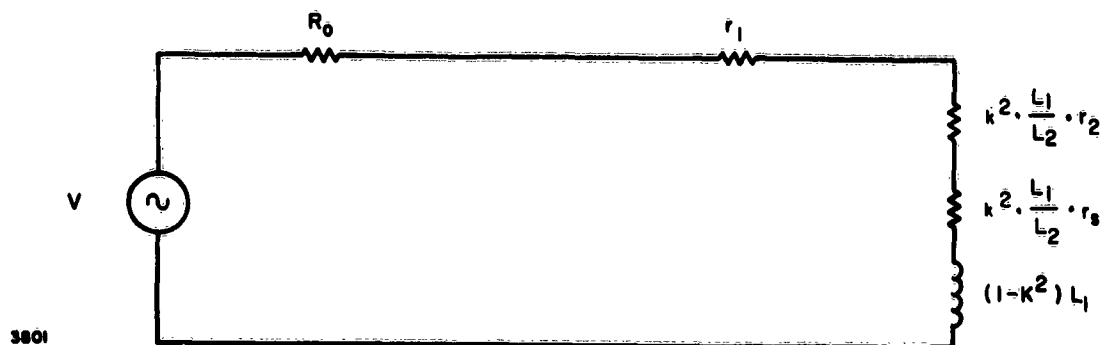


Figure 34. Driven Transformer, Heavy Secondary Load

At frequencies where untuned transformers are likely to be used (say, below 100 KC), it is not difficult to obtain coupling coefficients greater than 0.9 and winding Q's greater than 100 using ferrite or laminated iron cores. Assuming these values as minimum conditions, $r_1 + k^2 \cdot \frac{L_1}{L_2} \cdot r_2$ will normally be small compared to $R_o + k^2 \cdot \frac{L_1}{L_2} \cdot r_s$ and will, therefore, have negligible effect on the value of ϕ'_1 . In any case, the effect of r_1 and $k^2 \cdot \frac{L_1}{L_2} \cdot r_2$ is to reduce ϕ'_1 , and ignoring them will add a safety factor in the design. ϕ'_1 is the modified primary phase angle due to the presence of R_o .

With these assumptions,

$$Z_{in} = R_o + R_s + 0.2 \cdot j \omega L_1 \quad (k = 0.9) \quad (168)$$

$$\text{and} \quad \tan \phi'_1 = \frac{0.2 \omega L_1}{R_o + R_s} \quad (169)$$

$$\text{or} \quad L_1 = \frac{R_o + R_s}{0.2 \omega} \cdot \tan \phi'_1 \quad (170)$$

and assuming a value for ϕ'_1 determines L_1 . The value of ϕ'_1 should be small (say, 10 to 15 degrees) to avoid the need for excessive phase correction elsewhere in the oscillator circuit.

Using $K = 0.9$ and the known values of R_s and r_s , the value of L_2 can be calculated by substituting for L_1 in Equation (166):

$$L_2 = 0.8 \times L_1 \times \frac{r_s}{R_s} \quad (171)$$

At this point in the calculation the following condition should be checked:

$$\omega L_2 \geq 3r_s$$

If not, the value L_2 should be increased to satisfy this condition and the new values of L_1 and ϕ'_1 determined from Equations (171) and (170), respectively.

Calculate the secondary phase angle using the equation:

$$\phi_2 = \tan^{-1} \frac{\omega L_2}{r_s} \quad (172)$$

Calculate ϕ_T from:

$$\phi_T = \phi'_1 + \phi_2 + 90^\circ \quad (173)$$

The resulting ϕ_T should be within 10 or 15 degrees of 180 degrees, since phase shifts of this magnitude can be uncritically introduced at other points in the circuit. One particularly easy method is to add a fixed capacitor across the transformer primary winding. In this case, the transformer is actually tuned. However, the Q is less than 1 and the capacitor value is uncritical and, therefore, is not required to be variable. This method also serves to limit the amplifier bandwidth, thereby reducing the possibility of parasitic oscillation.

The original assumption concerning the effect of r_1 and r_2 can now be checked and corrections made, if necessary.

4.7.3.1.3 Untuned Transformer, Light Secondary Load

If the transformer is solely employed to give phase-inverted feedback power, the transformer operation is radically changed. The oscillator load is in parallel with the transformer primary winding, and the secondary of the transformer operates under essentially open circuit conditions; that is, $\omega L_2 < r_s$.

Under these conditions, consideration of Equation (158) shows that the voltage across r_s will lag the induced voltage $-I_1 \cdot j \omega M$ by a small phase angle ϕ_2 as shown in Figure 35, where:

$$\phi_2 = \tan^{-1} \frac{\omega L_2}{r_s + r_2} \quad (174)$$

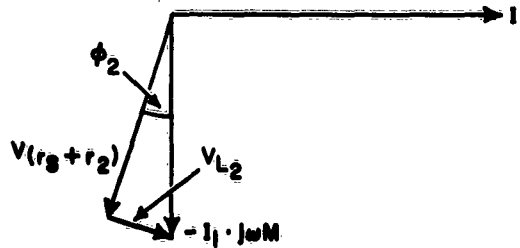


Figure 35. Secondary Vector Diagram, Lightly Loaded

It is evident from Figure 35 that the impedance looking into the transformer primary must have a large inductive component compared to its resistive component in order that the phase angle between input and output voltages approaches 180 degrees. Referring to Equation (159) and approximating for the condition $(r_2 + r_s) \geq 3 \omega L_2$ gives:

$$V_{in} = I_1 \left[r_1 + j \omega L_1 + \frac{\omega^2 M^2 (r_s + r_2 - j \omega L_2)}{(r_2 + r_s)^2} \right] \quad (175)$$

This equation simplifies further to:

$$V_{in} = I_1 \left[r_1 + \frac{k^2 \cdot \omega^2 L_1 L_2}{r_2 + r_s} + j \omega L_1 \right] \quad (176)$$

and, seeing that $\omega L_2 \leq \frac{1}{3} r_s$, any reasonable value of secondary winding $Q \left(\frac{\omega L_2}{r_2} \right)$

will make r_2 negligible in comparison to r_s . Equation (176) then simplifies to:

$$\frac{V_{in}}{I_1} = Z_{in} = r_1 + \frac{k^2 \cdot \omega^2 L_1 L_2}{r_s} + j \omega L_1 \quad (177)$$

When driven by an active device with the active device load across the transformer primary, the circuit is as shown in Figure 36(a), which reduces to the Thevenin equivalent of Figure 36(b). The phase angle of I_1 with respect to V is:

$$\phi_1' = -\tan^{-1} \frac{\omega L_1}{\frac{R_o \cdot R_L}{R_o + R_L} + r_1 + \frac{k^2 \omega^2 L_1 L_2}{r_s}} \quad (178)$$

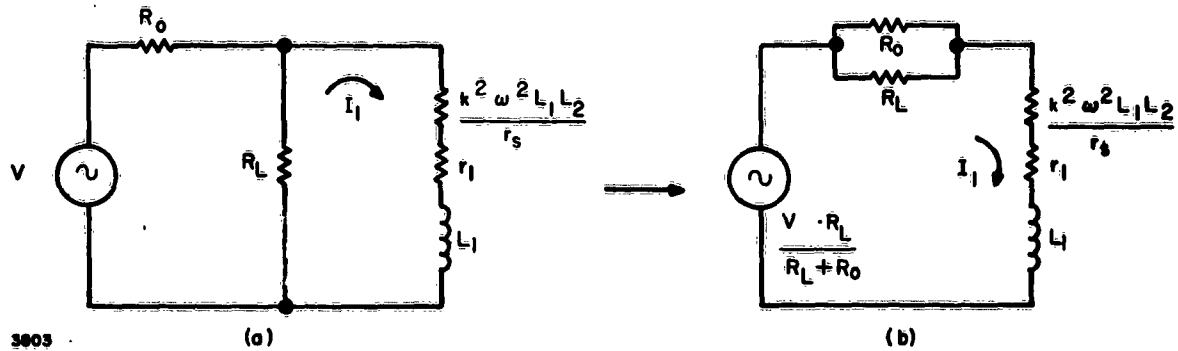


Figure 36. Driven Transformer, Lightly Loaded

A ϕ_1' of 80 degrees is the approximate maximum value that will be required, since for $\phi_2 = 0$ this will result in a 10-degree phase deviation from 180 degrees. For values of ϕ_2 up to that set by the condition $\omega L_2 = 3r_s$, the value of ϕ_1' can be correspondingly reduced while maintaining a small phase error. Therefore:

$$\frac{\omega L_1}{\frac{R_o \cdot R_L}{R_o + R_L} + r_1 + \frac{k^2 \omega^2 L_1 L_2}{r_s}} \leq 5.7 \quad (\tan 80^\circ = 5.67) \quad (179)$$

The Q of the primary winding will be greater than 100 at the frequencies under consideration, provided that a suitable iron core is used. Therefore r_1 is approximately 20 times smaller than the remainder of the denominator of Equation (179) and can be ignored. Furthermore, the desired value of R_{FB} will be at least one order of magnitude greater than R_L ; and, therefore, $k^2 \omega L_1 L_2$, which is the equivalent series

resistance of R_{FB} , will be negligible in comparison with R_0 and R_L in parallel. Consequently, the input circuit phase angle is given with sufficient accuracy by the formula:

$$\phi'_1 = \tan^{-1} \omega L_1 \cdot \frac{R_0 + R_L}{R_0 \cdot R_L} \quad (180)$$

The effective parallel resistance seen at the primary winding terminals with the secondary loaded is (Table 3 (b)):

$$R_s = \left(r_1 + \frac{k^2 \omega^2 L_1 L_2}{r_s} \right) \left[1 + \frac{\omega^2 L_1^2}{\left(r_1 + \frac{k^2 \omega^2 L_1 L_2}{r_s} \right)^2} \right] \quad (181)$$

From the previous discussion:

$$\frac{\omega^2 L_1^2}{\left(r_1 + \frac{k^2 \omega^2 L_1 L_2}{r_s} \right)^2} \gg 1$$

Therefore:

$$R_s = \frac{\omega^2 L_1^2}{r_1 + \frac{k^2 \omega^2 L_1 L_2}{r_s}} \quad (182)$$

For the particular case where $r_1 \ll \frac{k^2 \omega^2 L_1 L_2}{r_s}$, this simplifies to:

$$R_s = \frac{L_1}{k^2 L_2} \cdot r_s \quad (183)$$

The effective parallel coil loss resistance is:

$$R_{L1} = \frac{\omega^2 L_1^2}{r_1} \quad (184)$$

4.7.3.1.4 Transformer Design, Light Secondary Load

Substitute $\tan \phi'_1 = 5.7$ into Equation (180) to determine L_1 :

$$L_1 = \frac{5.7}{\omega} \cdot \frac{R_o \cdot R_L}{R_o + R_L} \quad (185)$$

Assume a value for the primary winding Q (Q_p) to determine r_1 from:

$$r_1 = \frac{\omega L_1}{Q_p} \quad (186)$$

Calculate:

$$R_{L1} = Q_p \cdot \omega L_1 \quad (187)$$

Combining this value of R_{L1} in parallel with the known value of R_{FB} gives:

$$R_s = \frac{R_{L1} \times R_{FB}}{R_{L1} + R_{FB}} \quad (188)$$

L_2 can now be determined from Equation (182) if a value for K is assumed.

$$L_2 = \left[\frac{\omega^2 L_1^2}{R_s} - r_1 \right] \frac{r_s}{k^2 \omega^2 L_1} \quad (189)$$

A suitable K value will be 0.9.

Check to see that the following condition exists:

$$\omega L_2 \leq 3r_s \quad (190)$$

If not, decrease L_2 accordingly. The simplest method possibly is to recalculate Equations (186) through (184) using a smaller L_1 value. The reduction in the L_1 value required is estimated from the reduction in L_2 required.

The phase shift between input and output can be estimated from:

$$\begin{aligned} \phi_T &= \phi_2 + \phi'_1 + 90^\circ \\ &= \tan^{-1} \frac{\omega L_2}{r_s} + \tan^{-1} \frac{(R_o + R_L) \omega L_1}{R_o \cdot R_L} + 90^\circ \end{aligned} \quad (191)$$

4.7.4 Wien Bridge Network

4.7.4.1 Wien Bridge Network Analysis

The Wien Bridge network has frequency selective properties that are useful in untuned oscillators. The network is shown in Figure 37.

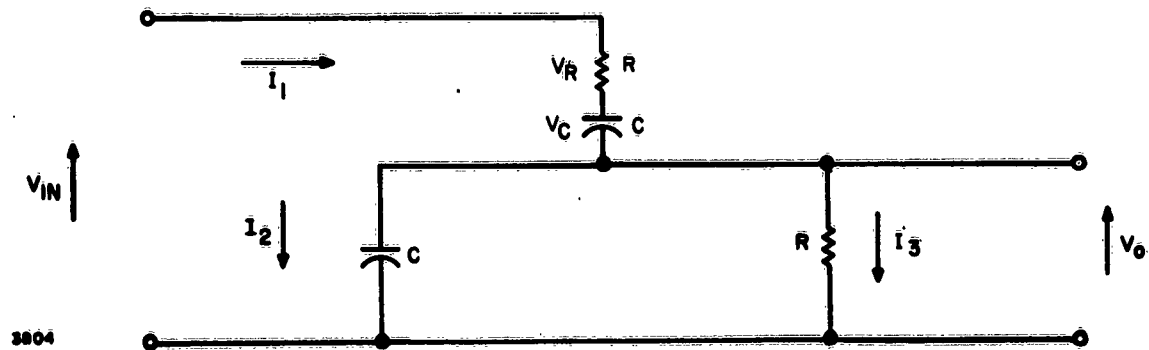


Figure 37. Wien Bridge Network Circuit.

The equations for this circuit are:

$$V_{in} = I_1 \left[R + \frac{1}{j \omega C} + \frac{R}{1 + j \omega CR} \right] \quad (192)$$

$$V_o = I_1 \cdot \frac{R}{1 + j \omega CR} \quad (193)$$

$$\frac{V_o}{V_{in}} = \frac{R}{(1 + j \omega CR) \left(R + \frac{1}{j \omega C} + \frac{R}{1 + j \omega CR} \right)} \quad (194)$$

$$= \frac{1}{3 + j \left(\frac{\omega}{\omega'} - \frac{\omega'}{\omega} \right)} \quad (195)$$

where $\omega' = \frac{1}{CR}$

At $\omega = \omega'$, the reactive component in the denominator falls to zero and:

$$\frac{V_o}{V_{in}} = \frac{1}{3} \quad (196)$$

At angular frequencies in the vicinity of ω' , the response is similar to that of a tuned circuit.

The vector relationships within the network at angular frequency ω' can be determined by noting that:

$$R = \frac{1}{j \omega' C} \quad (197)$$

and therefore:

$$|I_2| = |I_3| \quad (198)$$

Figure 38 shows the vector diagram for the network at $\omega = \omega'$.

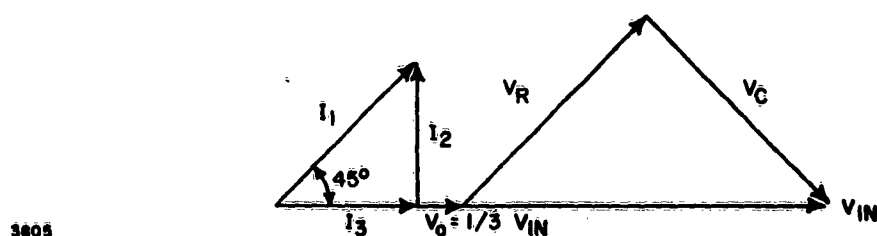


Figure 38. Wien Bridge Network Vector Diagram

The input impedance is:

$$Z_{in} = \frac{V_{in}}{I_1} = \frac{3}{2} \cdot R (1 - j) \quad (199)$$

Or transforming to parallel elements, the parallel resistance is:

$$R' = 3R \quad (200)$$

and the parallel capacitive reactance is

$$X'_C = 3R \quad (201)$$

The Wien Bridge network is only one case of this type of network. If the network is analyzed in its general form where R_1 and C_1 are the series elements and R_2 and C_2 are the parallel elements, the input and output voltages are in phase when:

$$\omega^2 = \frac{1}{C_1 C_2 R_1 R_2} \quad (202)$$

The relationship between $\frac{V_o}{V_{in}}$ at zero phase angle is:

$$\frac{V_o}{V_{in}} = \frac{R_2}{R_1 + R_2 \left(1 + \frac{C_2}{C_1}\right)} \quad (203)$$

5.0 CONCLUSIONS AND RECOMMENDATIONS

5.1 Conclusions

Background data applicable to the design and operation of both high and low frequency oscillators has been presented. The data that is applicable to high frequency oscillators has been combined with experimentally gathered data to form a design procedure for the frequency range of 30 MC to 200 MC.

This design procedure is simple in form and should present few difficulties in execution. The most complex part of the procedure is the determination of the active device characteristics, and this is straightforward once the techniques have been mastered. An active device evaluation normally requires less than one hour to complete. This compares favorably with the time required to calculate 2 or 3 values of power gain and input impedance, using the complex parameters of an active device. In addition, the data obtained by measurement is more reliable, since it is obtained under actual operating conditions.

The low-frequency design procedure offered is somewhat vague because of the limited number of evaluations obtained of any one type of oscillator, and also because of the large number of feasible oscillator configurations. Nevertheless, when used in conjunction with the background data and the Design Data Sheets, it supplies the information necessary for low frequency oscillator design.

5.2 Recommendations

5.2.1 High-Frequency Oscillators

The high frequency oscillator design procedure is limited by its failure to consider alternative active device configurations. Areas of investigation that would make the procedure more universal would be:

- (a) Grounded grid pentodes or tetrodes at all frequencies
- (b) Grounded cathode pentodes and tetrodes in the 20 MC to 100 MC region
- (c) Grounded emitter transistors in the 20 MC to 50 MC region

Other areas that could profitably be investigated are:

- (d) Methods of reducing oscillator frequency instability with temperature, due to the active device and oscillator components other than the crystal. This is particularly applicable to the transistor.

- (e) Extending the frequency range above 200 MC. Judging by the experiences of the design evaluation program, 200 MC does not appear to be the upper limit of performance. In fact, one 200-MC oscillator operated quite well on the next higher crystal overtone mode at a frequency of 244 MC. Oscillator operation up to at least 300 MC should be investigated.
- (f) The operation of the oscillator under typical loading conditions. The majority of oscillators will be loaded by a mixer or other non-linear circuit which may influence performance considerably. The limited information obtained during this program suggests that the non-linear loading effect is negligible. However, a fuller investigation would be desirable.

5.2.2 Low-Frequency Oscillators

The low-frequency oscillator design procedure is limited by the lack of sufficient evaluation data, due to the limited number of circuits evaluated. To correct this, it is recommended that the following circuits be further evaluated:

- (a) Oscillators below 16 KC using the crystal as a two-terminal pair filter network.
- (b) Antiresonant Oscillators in the 100-KC to 500-KC frequency band. It appears that field effect transistors could be effectively used in this application.

6.0 IDENTIFICATION OF PERSONNEL

The following personnel devoted the indicated amount of time to this project:

- | | | |
|-----|--|-----------------------|
| (a) | Donald Firth, Electrical Engineer, | 7.13 MM (1235 hours) |
| (b) | John R. Yope, Electrical Engineer, | 10.76 MM (1864 hours) |
| (c) | Gregory J. Bittner, Electrical Engineer, | 4.59 MM (795 hours) |
| (d) | Alan O. Plait, Electrical Engineer, | 1.48 MM (257 hours) |
| (e) | H. Rex Meadows, Senior Staff Engineer, | Time not chargeable |

NOTE

1 man-month (MM) = 173.3 hours

7.0 BIBLIOGRAPHY

- (1) "A Study of Crystal Oscillator Circuits, " Armour Research Foundation; Contract No. DA-36-039-SC-64609, Final Report; August 1957.
- (2) "Transistor Crystal Oscillator Circuitry, " Motorola, Inc. ; Contract No. DA-36-039-SC-72837, Final Report; August 1957.
- (3) "Handbook of Piezoelectric Crystals for Radio Equipment Designers, " Philco Corporation; WADC Technical Report 56-156, ASTIA Document No. AD 110448.
- (4) Terman, "Radio Engineer's Handbook"
- (5) MIL-C-3098C, Supplement 1
- (6) Gartner, "Transistors: Principles, Design, and Application"
- (7) Boothroyd and Page, "Instability in Two Port Active Networks"; IRE Transactions on Circuit Theory, Pages 133 - 139; June 1958.
- (8) "Diffused Base Mesa Transistors Type 2N1141, 2N1142, and 2N1143, " Texas Instruments Qualification Report
- (9) "New Method of Measuring High Frequency Transistor Admittance Parameters Using the Boonton RX Meter"; Ampere Tech News; Vol. 2, No. 1

OSCILLATOR DESIGN AND EVALUATION DATA

The oscillator design evaluations contained in these appendices are the results of the evaluation program that was conducted in parallel with the study program. The object of this experimental program was to determine the practical worth of the background data gathered from the literature and, conversely, to modify this background data in accordance with the specific requirements of crystal oscillator design as determined from the evaluations.

The purpose of presenting these design evaluations is to illustrate the use of the techniques described in the Final Report and to show the level of performance likely to be achieved. It is also possible that the designs presented will find use when a general purpose oscillator is required and there is insufficient time available to carry out a design.

This approach has been experimentally substantiated to some extent. The two high-power output transistor oscillators (75 MC and 120 MC) were both used in limited production run equipments with satisfactory results, in spite of considerably different circuit layouts from those of the prototype circuits. The only deviation was that the power output capabilities of the oscillators averaged out at about 20 percent less than that obtained from the prototypes.

The format utilized for each evaluation is as follows:

- (a) A short discussion giving general information concerning the design and any difficulties encountered
- (b) A schematic of the oscillator together with other pertinent circuit information
- (c) The design calculations
- (d) The evaluation data

APPENDIX A

150-MC OSCILLATOR USING 2N917 TRANSISTOR

Object:

This was an early design; the object was to design a 150-MC oscillator and study its performance.

The circuit was designed for true grounded base operation using two DC supplies. This was done to overcome any possible difficulties due to AC grounding the base. This precaution proved unnecessary as shown by later designs. The transistor was also soldered into the circuit; this again proved unnecessary. Later designs used transistor sockets to facilitate transistor changes.

150-MC TRANSISTOR OSCILLATOR DATA

Oscillator Design and Evaluation Sheet

Active Element: Transistor

Manufacturer's Type No.: 2N917

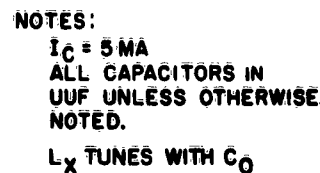
Crystal (s) Used	Resonant Frequency	Series Resistance
Similar to		
<u>CR-56A/U</u>	<u>150.0013 MC</u>	<u>50 ohms</u>
Similar to		
<u>CR-56A/U</u>	<u>150.0018 MC</u>	<u>65 ohms</u>

Description of Oscillator Type

Crystal: Series

Active element configuration: Grounded base

Feedback transformer configuration: Capacitive Divider



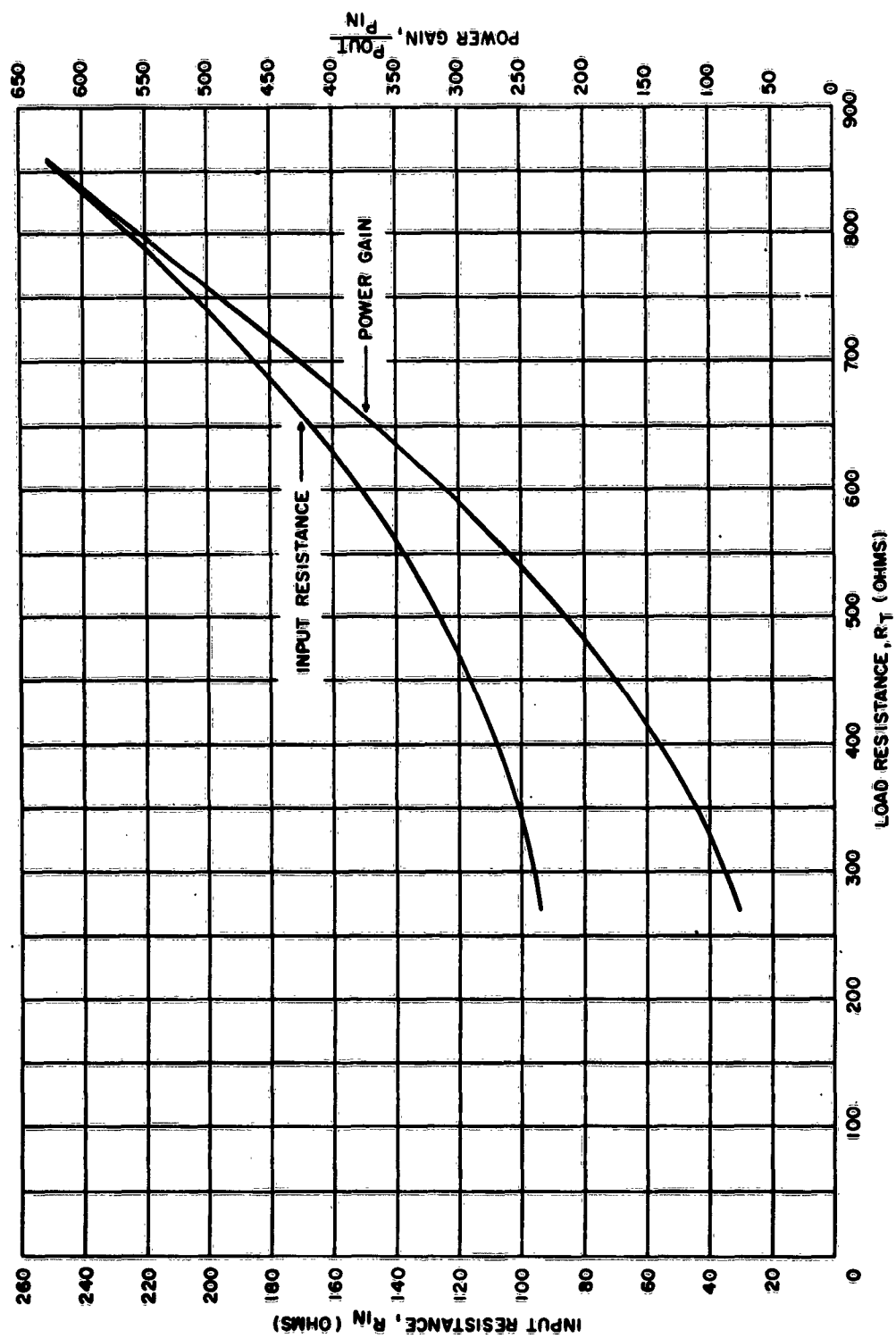


Figure A-2. 2N917 Common Base Transistor Amplifier at 150 MC

The actual value of C_2 used was nominally 5 UUF.

The phase lead introduced by the capacitive divider network is:

$$\theta = 90^\circ - \tan^{-1} \omega (C_1 + C_2) R_s$$

$$= 5^\circ \text{ for } C_2 = 50 \text{ UUF}$$

The effective parallel loss resistance of the tuning coil was 9 K which is negligible compared with 600 ohms. Therefore, $R_L = R_T = 600$ ohms (680 ohms nominal value). The voltage measuring probe loss was also negligible.

This circuit was also evaluated with $C_2 = 25$ UUF.

DESIGN EVALUATION DATA, 150-MC TRANSISTOR OSCILLATOR

Nominal $V_o = 3.5V$ (25 UUF); Oscillator Frequency = 150.0011 MC
 $V_o = 3.1V$ (50 UUF)

EFFECT OF	CHANGE	TEST CONDITIONS
±10% Change in B+ on Oscillator Frequency	±1.4 PPM	$C_2 = 25$ UUF, $R_L = 600$ ohms, $V_e = -5V$, $T_A \approx 25^\circ C$
	±1.5 PPM	$C_2 = 50$ UUF, $R_L = 600$ ohms, $V_e = -5V$, $T_A \approx 25^\circ C$
±10% Change in B+ on Output Voltage	$\Delta V_o = \pm 2\%$	$C_2 = 25$ UUF, $R_L = 600$ ohms, $V_e = -5V$, $T_A \approx 25^\circ C$
	$\Delta V_o = \pm 2\%$	$C_2 = 50$ UUF, $R_L = 600$ ohms, $V_e = -5V$, $T_A \approx 25^\circ C$
±10% Change in R_L on Oscillator Frequency	±1.7 PPM	$C_2 = 25$ UUF, $V_{cc} = 15V$, $V_e = -5V$, $T_A \approx 25^\circ C$
	- - - - -	No oscillation with $C_2 = 50$ UUF for -10% change in R_L
±10% Change in R_L on Output Voltage	$\Delta V_o = \pm 8\%$	$C_2 = 25$ UUF, $V_{cc} = 15V$, $V_e = -5V$, $T_A \approx 25^\circ C$
	- - - - -	No oscillation with $C_2 = 50$ UUF for -10% change in R_L
-50°C to +80°C Variation of T_A on Oscillator Frequency	±35 PPM	$C_2 = 25$ UUF, $V_{cc} = 15V$, $V_e = -5V$, $R_L = 600$ ohms
	±35 PPM	$C_2 = 50$ UUF, $V_{cc} = 15V$, $V_e = -5V$, $R_L = 600$ ohms
-50°C to +80°C Variation of T_A on Output Voltage	$\Delta V_o = \pm 7\%$	$C_2 = 25$ UUF, $V_{cc} = 15V$, $V_e = -5V$, $R_L = 600$ ohms
	$\Delta V_o = \pm 11\%$	$C_2 = 50$ UUF, $V_{cc} = 15V$, $V_e = -5V$, $R_L = 600$ ohms
$T_A =$ Oscillator Ambient Temperature		

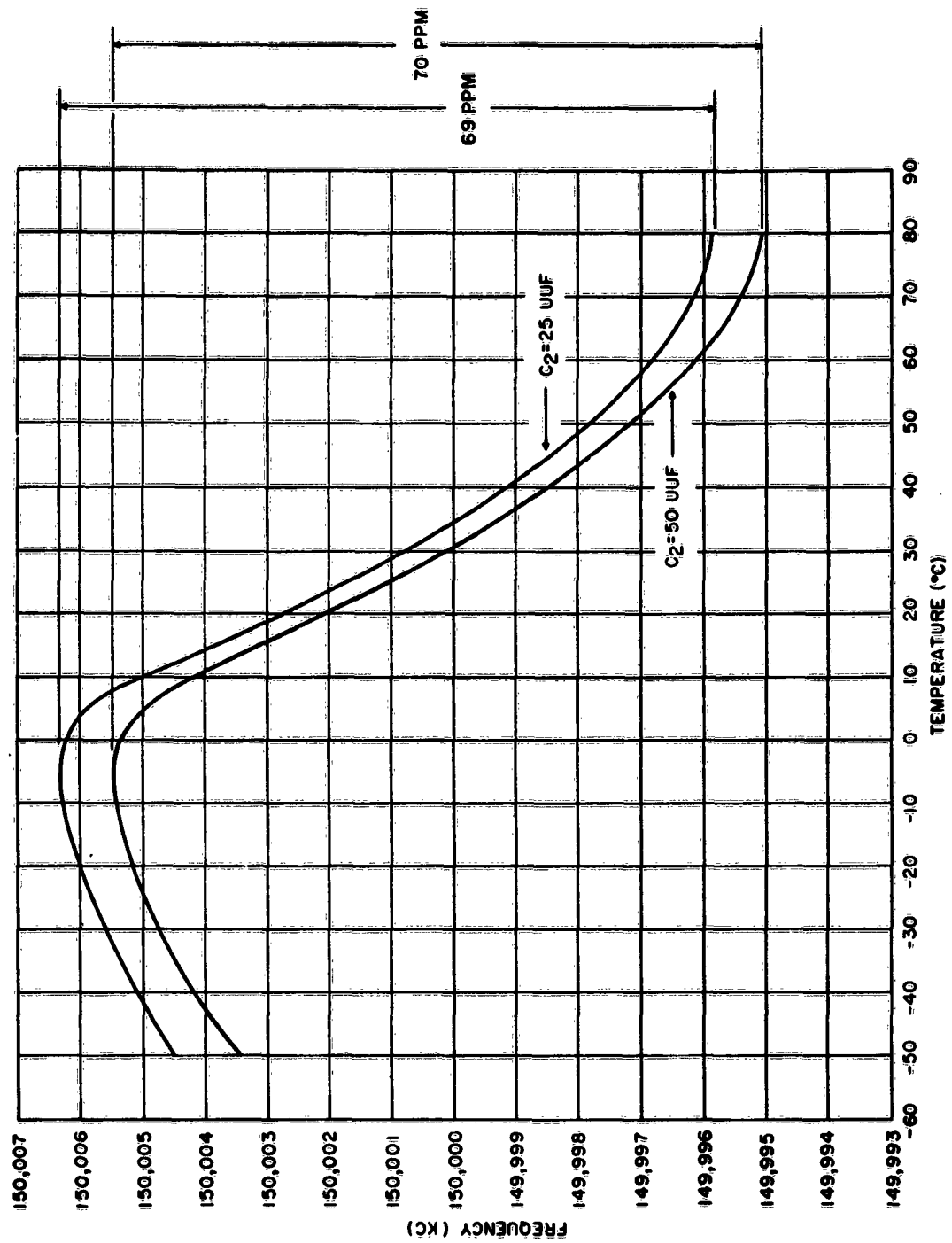


Figure A-3. Frequency vs. Temperature for 150-MC Oscillator

APPENDIX B

193-MC OSCILLATOR USING 2N917 TRANSISTOR

This is essentially the same circuit that was used at 150 MC with tuning and feedback circuit changes. However, a comparison of the power gain and input resistance as a function of load for the two cases shows that the transistor characteristics changed considerably.

The 150-MC crystal was again used in this evaluation by operating it in the 9th overtone mode. Late in the evaluation period the pins of the crystal holder (HC-18) were damaged and it was necessary to transfer the crystal to another holder (HC-6). The repackaged crystal resistance was approximately 20 percent larger and the series resonance frequency decreased 10 KC. No other ill effects were noted.

An attempt was made in this design to separate the temperature effects of the crystal and the remainder of the circuit. The crystal was mounted in an oven which held its temperature at $65^{\circ}\text{C} \pm 5^{\circ}\text{C}$, and the resulting frequency-versus-temperature data showed an improvement from ± 38 PPM to approximately ± 11 PPM (extrapolating the temperature-controlled curve to 80°C).

The peculiar "kinks" in the frequency-versus-temperature curves are probably due to ice melting on the components, since the temperature chamber used at this time was particularly vulnerable to "snowing up."

193-MC TRANSISTOR OSCILLATOR DATA

Oscillator Design and Evaluation Sheet

Active Element: Transistor

Manufacturer's Type No: 2N917

Crystal (s) Used

Resonant Frequency

Series Resistance

Similar to

CR-56A/U

192.8560 MC

78 ohms

Similar to

CR-56A/U (REPACKAGED)

192.8463 MC

96 ohms

Description of Oscillator Type

Crystal: Series

Active element configuration: Grounded base

Feedback transformer configuration: Capacitive Divider

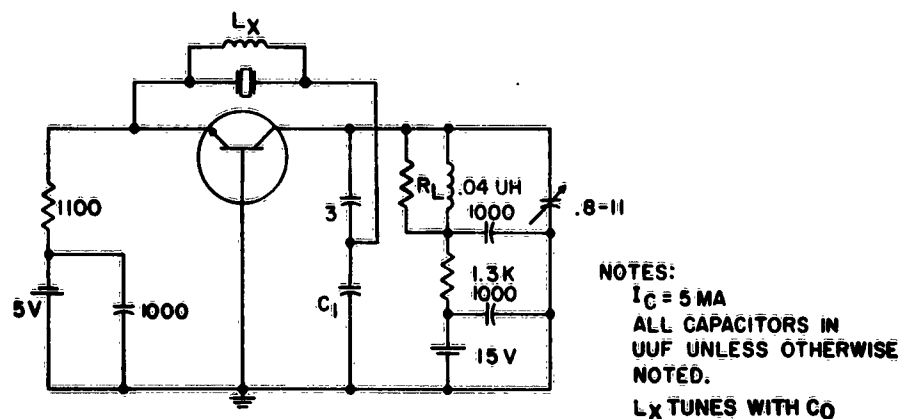


Figure B-1. 193-MC Oscillator Circuit

Details of Design Calculations

Using the notation and design equations of the Final Report and the measured gain and input resistance of the amplifier, the remaining circuit component values are determined as follows:

With the object of keeping the amplifier input resistance relatively low while maintaining adequate gain, the amplifier working point was selected at $R_T = 600 \text{ ohms}$, $G_p = 125$, $R_{in} = 460 \text{ ohms}$. Also, taking $R_{1 \text{ max}} = 100 \text{ ohms}$:

$$R_s = R_{in} + R_{1 \text{ max}} = 560 \text{ ohms}$$

$$G'_p = G_p \cdot \frac{R_{in}}{R_{1 \text{ max}}} = 102$$

and using a safety factor of 2:

$$\frac{G'_p}{2} = 51$$

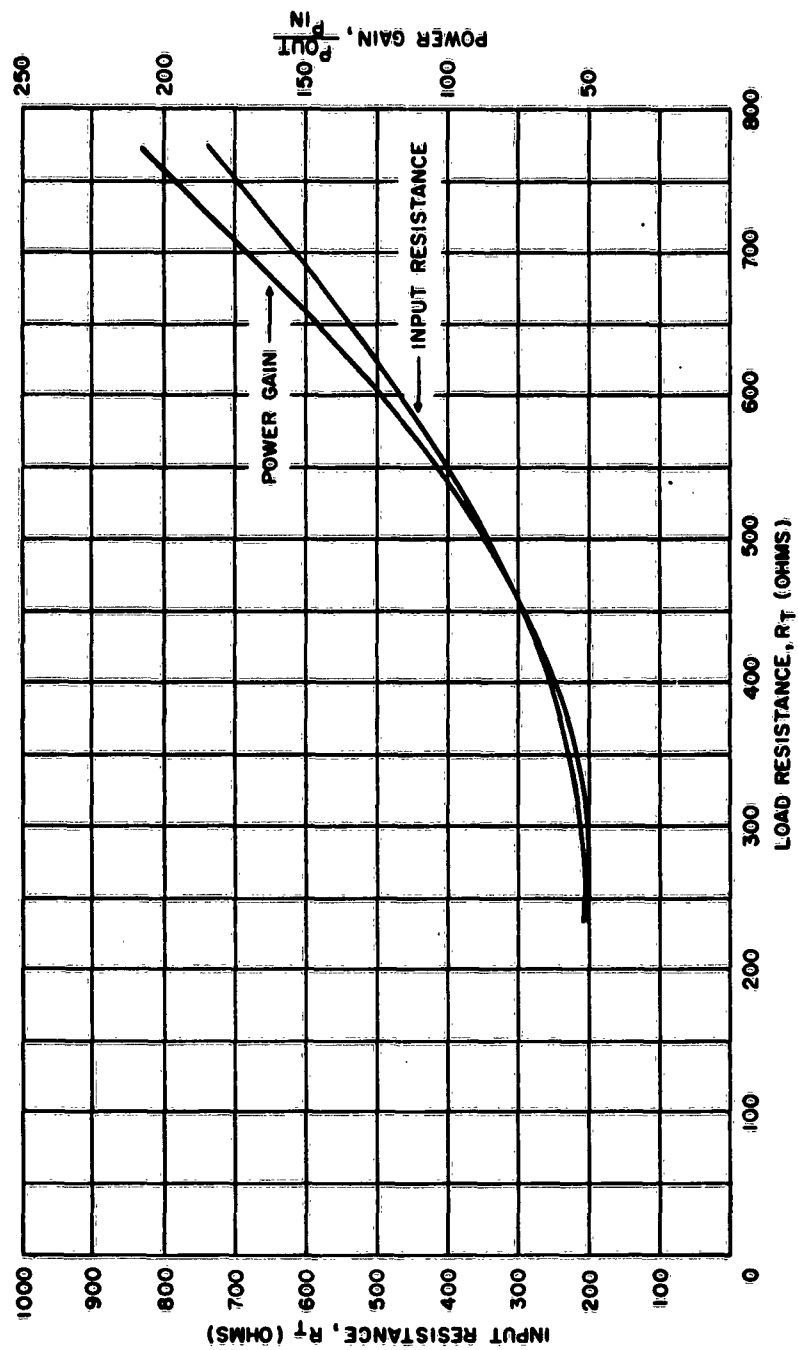


Figure B-2. 2N917 Common Base Transistor Amplifier at 193-MC

$$R_{FB} = \frac{G'_P}{2} \cdot R_T = 31 \text{ K}$$

Using a capacitive divider feedback network, the equations are:

$$T_r = \frac{R_{FB}}{R_s} = 55 = \left(\frac{C_1 + C_2}{C_1} \right)^2$$

$$\text{or } C_2 = 7.4 C_1$$

$$\text{For } C_2 = 25 \text{ UUF, } C_1 = 3.4 \text{ UUF.}$$

The nominal value of C_1 used was 3 UUF.

The loading effect of the voltmeter probe and the coil losses was negligible, and a R_L value of 640 ohms (750 ohms nominal value) was used.

The phase lead introduced by the capacitive divider network is:

$$\theta = 90^\circ - \tan^{-1} w (C_1 + C_2) R_s$$

$$= 3^\circ \text{ for } C_2 = 25 \text{ UUF}$$

An evaluation was also carried out for $C_2 = 15 \text{ UUF}$.

DESIGN EVALUATION DATA, 193-MC TRANSISTOR OSCILLATOR

Nominal $V_o = 3.6V$ (15 UUF) Oscillator Frequency = 192.854 MC
 $V_o = 3.1V$ (25 UUF)

EFFECT OF	CHANGE	TEST CONDITIONS
±10% Change in B+ on Oscillator Frequency	±3.2 PPM ±2.2 PPM	$C_2 = 15$ UUF, $R_L = 640$ ohms, $V_e = -5V$, $T_A \approx 25^\circ C$ $C_2 = 25$ UUF, $R_L = 640$ ohms, $V_e = -5V$, $T_A \approx 25^\circ C$
±10% Change in B+ on Output Voltage	$\Delta V_o = \pm 4\%$ $\Delta V_o = \pm 10\%$	$C_2 = 15$ UUF, $R_L = 640$ ohms, $V_e = -5V$, $T_A \approx 25^\circ C$ $C_2 = 25$ UUF, $R_L = 640$ ohms, $V_e = -5V$, $T_A \approx 25^\circ C$
±10% Change in R_L on Oscillator Frequency	±2 PPM ±1.5 PPM	$C_2 = 15$ UUF, $V_{cc} = 15V$, $V_e = -5V$, $T_A \approx 25^\circ C$ $C_2 = 25$ UUF, $V_{cc} = 15V$, $V_e = -5V$, $T_A \approx 25^\circ C$
±10% Change in R_L on Output Voltage	$\Delta V_o = \pm 13\%$ $\Delta V_o = \pm 15\%$	$C_2 = 15$ UUF, $V_{cc} = 15V$, $V_e = -5V$, $T_A \approx 25^\circ C$ $C_2 = 25$ UUF, $V_{cc} = 15V$, $V_e = -5V$, $T_A \approx 25^\circ C$
-50°C to +80°C Variation of T_A on Oscillator Frequency	±38 PPM ±36 PPM ±11 PPM	$C_2 = 15$ UUF, $V_{cc} = 15V$, $V_e = -5V$, $R_L = 640$ ohms $C_2 = 25$ UUF, $V_{cc} = 15V$, $V_e = -5V$, $R_L = 640$ ohms $C_2 = 15$ UUF, $V_{cc} = 15V$, $V_e = -5V$, $R_L = 640$ ohms Crystal temperature maintained at $65^\circ C \pm 5^\circ C$ for testing temperatures lower than $+50^\circ C$
-50°C to +80°C variation of T_A on Output Voltage	$\Delta V_o = \pm 10\%$ $\Delta V_o = \pm 17\%$ $\Delta V_o = \pm 5\%$	$C_2 = 15$ UUF, $V_{cc} = 15V$, $V_e = -5V$, $R_L = 640$ ohms $C_2 = 25$ UUF, $V_{cc} = 15V$, $V_e = -5V$, $R_L = 640$ ohms $C_2 = 15$ UUF, $V_{cc} = 15V$, $V_e = -5V$, $R_L = 640$ ohms Crystal temperature maintained at $65^\circ C \pm 5^\circ C$ for testing temperatures lower than $+50^\circ C$.

PPM frequency change calculated using the formula: $PPM = \frac{\text{Total frequency change}}{2 \times \text{nominal } f_o \text{ (MC)}}$

% V_o change calculated using the formula: $\Delta V_o \% = \frac{\text{Total } V_o \text{ change}}{2 \times \text{nominal } V_o} \times 100$

T_A = Oscillator Ambient Temperature

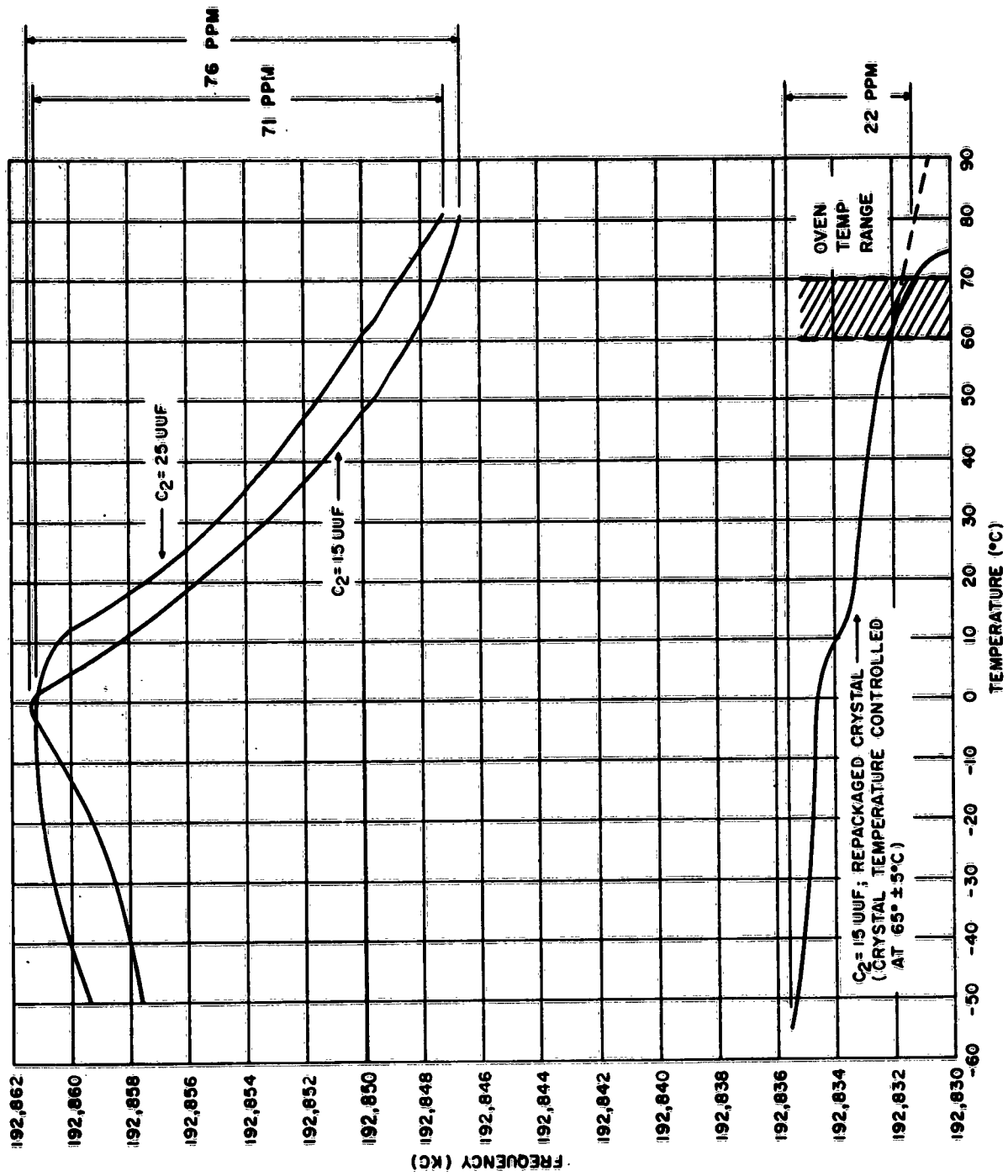


Figure B-3. Frequency vs. Temperature for 193-MC Oscillator

APPENDIX C

120-MC OSCILLATOR USING 2N2217 TRANSISTOR

Object:

The object of this design was to obtain high power output while maintaining crystal dissipation below maximum rating. The power output was in the region of 100 MW to 120 MW at room temperature for a crystal dissipation of 1 to 1.5 MW.

The family of transistors investigated was the 2N2217-19, the only difference between these types being in the values of h_{FE} . Experimental tests showed that the 2N2217 (the lowest gain type) suffered least from the effects of internal feedback at this frequency, and this type was selected for the application.

The experimentally derived power gain and input resistance curves of the amplifier show that the load resistance necessary for stable gain is in the region of 200 to 300 ohms, an undesirable range of values in view of the specified 28-volt supply. This resulted in considerable mismatching of the oscillator to the power supply and, consequently, a poor oscillator efficiency.

Temperature tests of the oscillator resulted in frequency deviations of ± 0.0052 percent using $R_L = 325$ ohms (measured at 120 MC) and ± 0.0044 percent using $R_L = 250$ ohms. These tolerances are 3 to 4 times those expected of the crystal alone and indicate the price paid for the high power output. Similar results were obtained from a temperature test on a production unit when loaded with a Class B power amplifier.

The results obtained with this oscillator should be compared with those of the 75-MC oscillator, which was designed for higher power output using a slightly different approach.

120-MC TRANSISTOR OSCILLATOR DATA

Oscillator Design and Evaluation Sheet

Active Element: Transistor

Manufacturer's Type No: 2N2217

Crystal (s) Used

Resonant Frequency

Series Resistance

CR-56A/U

120.0005 MC

38 ohms

CR-56A/U

119.9977 MC

48 ohms

Feedback transformer configuration: Capacitive Divider



and $\frac{G'_p}{2} = 215$

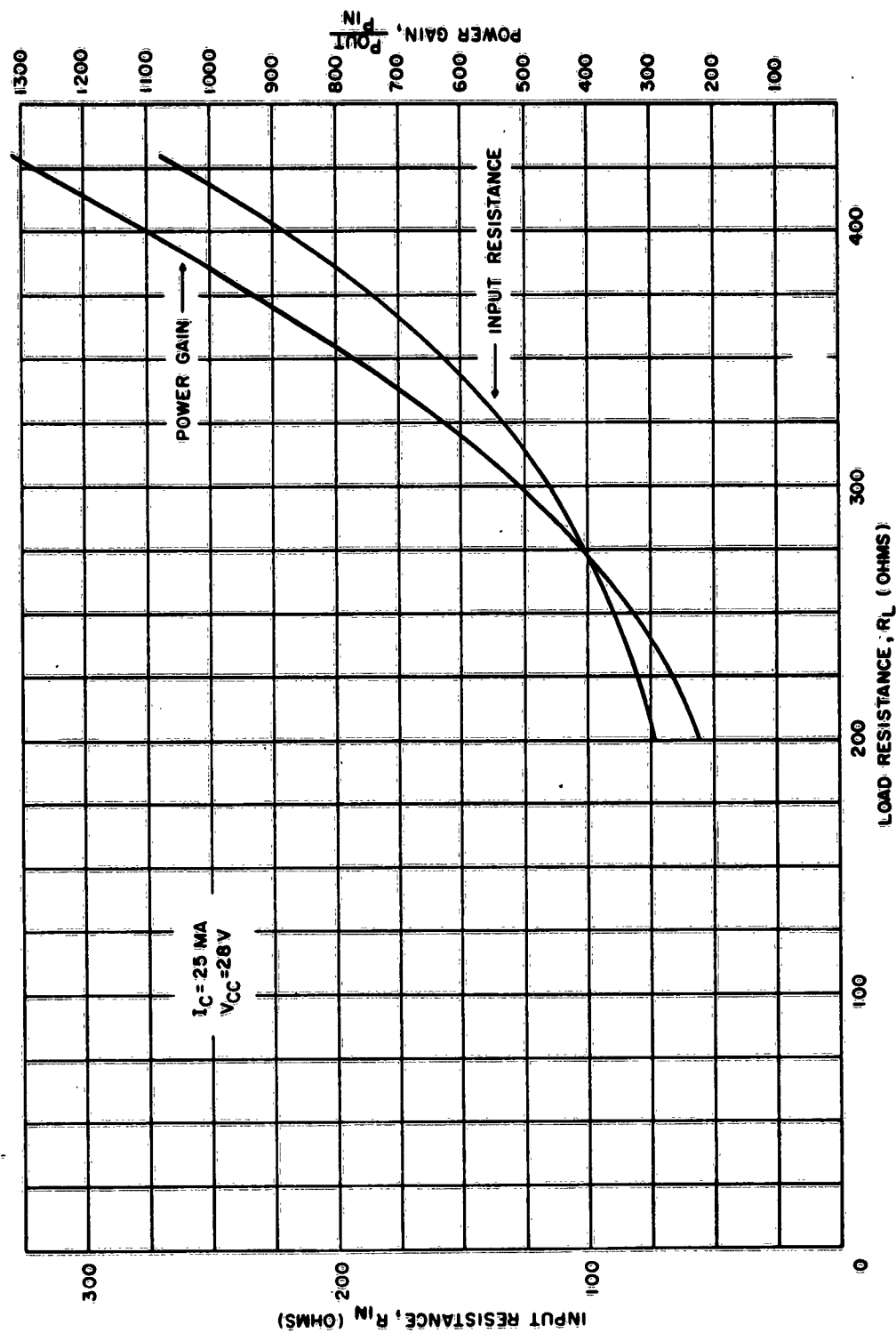


Figure C-2. Input Resistance and Power Gain vs. Load Resistance for 2N2217 Transistor

$$R_{FB} = \frac{G'P}{2} \times R_T = 69 K$$

For a capacitive divider feedback network, the equations are:

$$T_r = \frac{R_{FB}}{R_s} = 362 = \left(\frac{C_1 + C_2}{C_1} \right)^2$$

or $C_2 = 18 C_1$

For $C_1 = 8 \text{ UUF}$, $C_2 = 140 \text{ UUF}$.

To obtain high power output, C_2 was decreased to 50 UUF giving a crystal dissipation of 1 to 1.5 MW.

The phase lead introduced by the capacitive divider is:

$$\begin{aligned} \theta &= 90^\circ - \tan^{-1} w (C_1 + C_2) R_s \\ &= 7^\circ \end{aligned}$$

The loading effects of voltmeter probe and coil losses were negligible in comparison to R_T . Therefore, $R_L = R_T = 320 \text{ ohms}$ (360 ohms nominal value).

This circuit was also evaluated for an $R_L = 250 \text{ ohms}$.

DESIGN EVALUATION DATA, 120-MC TRANSISTOR OSCILLATOR (2N2217)

Nominal $V_o = 6V$ ($R_L = 320 \text{ ohms}$); Oscillator Frequency = 120.0004 MC
 $4.4V$ ($R_L = 250 \text{ ohms}$)

EFFECT OF	CHANGE	TEST CONDITIONS
$\pm 10\%$ Change in $B+$ on Oscillator Frequency	$\pm 3 \text{ PPM}$	$C_2 = 50 \text{ UUF}$, $R_L = 320 \text{ ohms}$, $T_A \approx 25^\circ\text{C}$
$\pm 10\%$ Change in $B+$ on Output Voltage	$\Delta V_o = \pm 7\%$	$C_2 = 50 \text{ UUF}$, $R_L = 320 \text{ ohms}$, $T_A \approx 25^\circ\text{C}$
$\pm 10\%$ Change in R_L on Oscillator Frequency	$\pm 2 \text{ PPM}$	$C_2 = 50 \text{ UUF}$, $V_{cc} = 28V$, $T_A \approx 25^\circ\text{C}$
$\pm 10\%$ Change in R_L on Output Voltage	$\Delta V_o = \pm 12\%$	$C_2 = 50 \text{ UUF}$, $V_{cc} = 28V$, $T_A \approx 25^\circ\text{C}$
-50°C to $+70^\circ\text{C}$ Variation of T_A on Oscillator Frequency	$\pm 52 \text{ PPM}$ $\pm 44 \text{ PPM}$	$C_2 = 50 \text{ UUF}$, $V_{cc} = 28V$, $R_L = 320 \text{ ohms}$ $C_2 = 50 \text{ UUF}$, $V_{cc} = 28V$, $R_L = 250 \text{ ohms}$
-50°C to $+70^\circ\text{C}$ Variation of T_A on Output Voltage	$\Delta V_o = \pm 12\%$ $\Delta V_o = \pm 12\%$	$C_2 = 50 \text{ UUF}$, $V_{cc} = 28V$, $R_L = 320 \text{ ohms}$ $C_2 = 50 \text{ UUF}$, $V_{cc} = 28V$, $R_L = 250 \text{ ohms}$
PPM frequency change calculated using the formula: $\text{PPM} = \frac{\text{Total Frequency Change}}{2 \times \text{nominal } f_o (\text{MC})}$		
$\%V_o$ change calculated using the formula: $\Delta V_o \% = \frac{\text{Total } V_o \text{ Change}}{2 \times \text{nominal } V_o} \times 100$		
$T_A = \text{Oscillator Ambient Temperature}$		

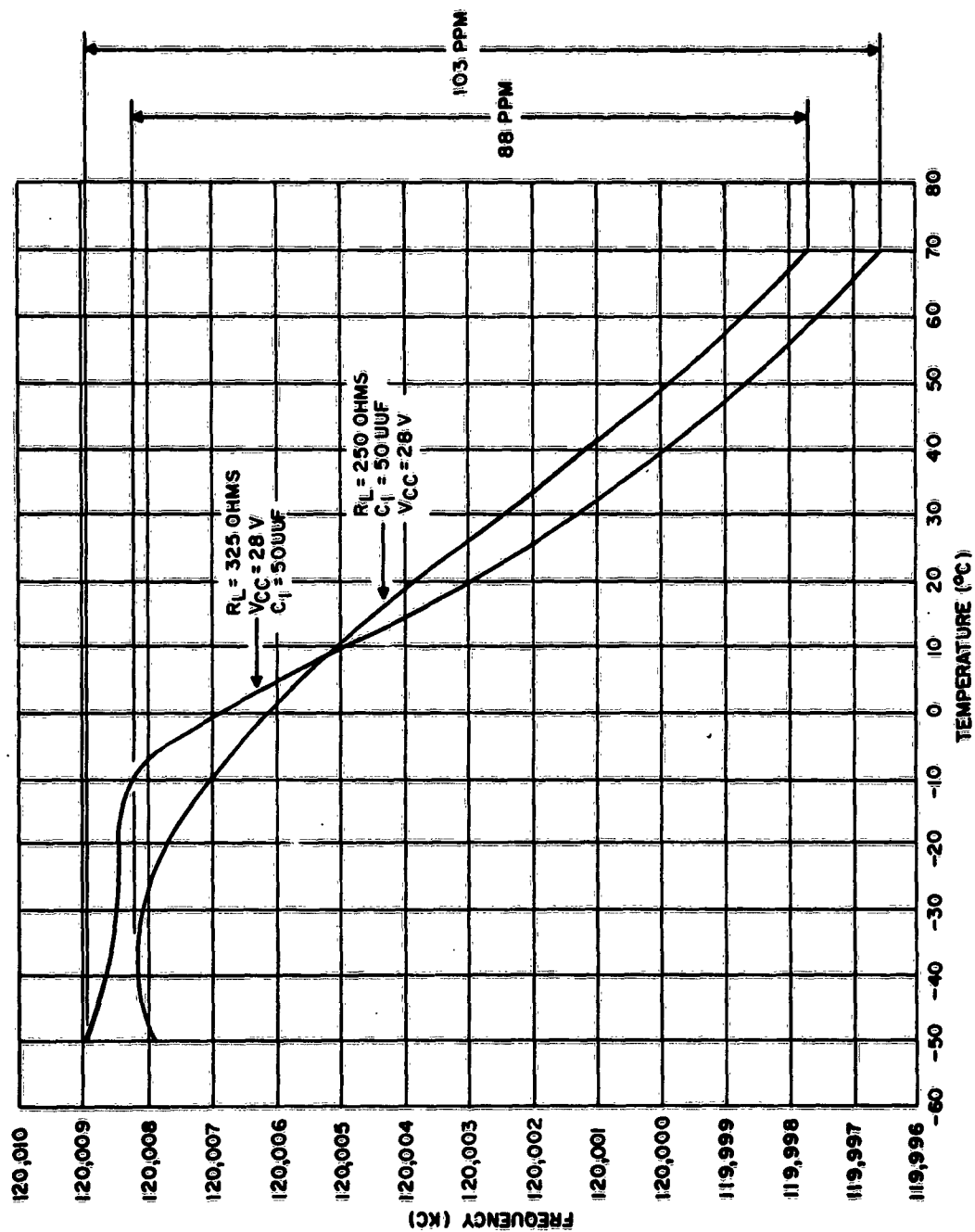


Figure C-3. Frequency vs. Temperature for 120-MC Oscillator

APPENDIX D

120-MC OSCILLATOR USING 2N834 TRANSISTOR

Object:

In view of the wide oscillator frequency tolerance and low efficiency of the 120-MC Oscillator using a 2N2217, the object was to attempt to achieve comparable output power using a transistor of lower power rating. The basis for this approach was that a transistor having smaller junction areas would have equal stability at higher R_L values, thereby improving the efficiency.

The evaluation of the oscillator showed no improvement in efficiency. The power output dropped by 20 percent compared with the previous design, while the DC power input also dropped by 20 percent.

The temperature stability of the oscillator was improved over the previous design having a value of ± 0.0037 percent, an improvement of ± 0.0015 percent. This is possibly due to lower amplifier gain used in this design.

120-MC TRANSISTOR OSCILLATOR DATA

Oscillator Design and Evaluation Sheet

Active Element: Transistor

Manufacturer's Type No.: 2N834

Crystal (s) Used

Resonant Frequency

Series Resistance

CR-56/U

120.0005 MC

38 ohms

Description of Oscillator Type

Crystal: Series

Active element configuration: Grounded Base

Feedback transformer configuration: Capacitive Divider

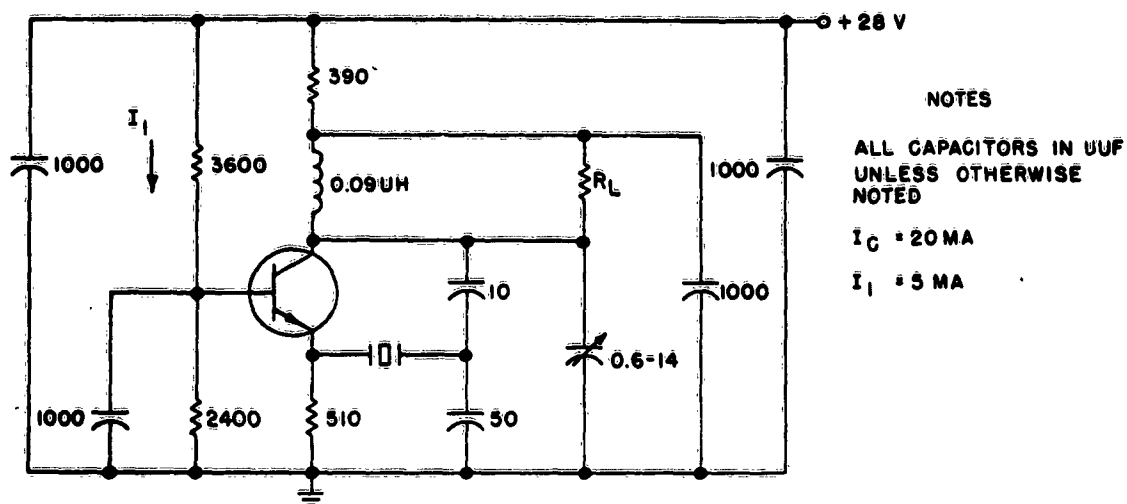


Figure D-1. 120-MC Oscillator Circuit, 2N834 Transistor

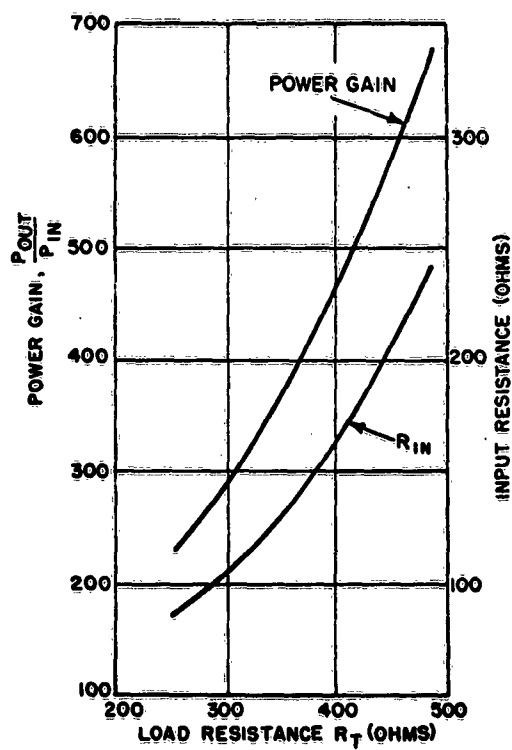


Figure D-2. Input Resistance and Power Gain Versus Load Resistance, 2N834 Transistor at 120 MC

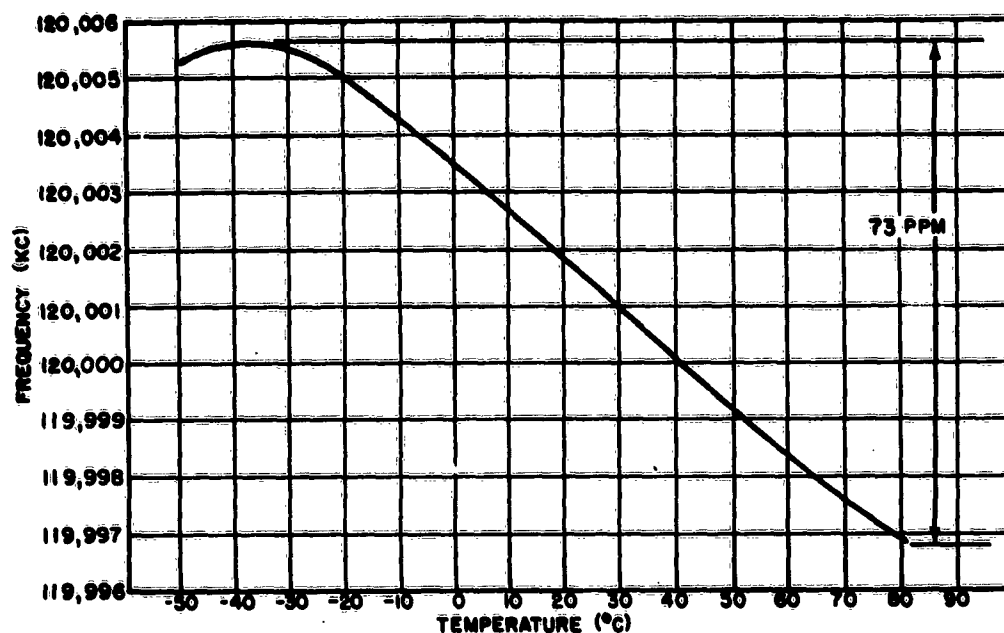


Figure D-3. Frequency Versus Temperature, 2N834 Transistor at 120 MC,
 $C_2 = 50$ UF

Details of Design Calculations

Using the notation and design equations of the Final Report and the measured gain and input resistance of the amplifier, the remaining circuit component values are determined as follows:

A working power gain of 450 was selected corresponding to $R_T = 390$ ohms and $R_{in} = 150$ ohms. The crystal resonance resistance $R_T \text{ max} = 50$ ohms. Therefore:

$$R_s = R_{in} + R_T = 200 \text{ ohms}$$

$$G'_p = G_p \cdot \frac{R_{in}}{R_s} = 340$$

Using a safety factor of 2 gives:

$$\frac{G'_p}{2} = 170$$

$$R_{FB} = \frac{G_p}{2} \cdot R_T = 66 \text{ K}$$

Using a capacitive divider feedback network, the relevant equations are:

$$\text{Transformation Ratio} = \frac{R_{FB}}{R_s} = 330 = \left(\frac{C_1 + C_2}{C_1} \right)^2$$

$$\text{or } C_2 = 17C_1$$

$$\text{Let } C_1 = 10 \text{ UUF, then } C_2 = 170 \text{ UUF}$$

Optimum crystal drive level (1 to 1.5 MW) was obtained with $C_1 = 50 \text{ UUF}$.

The phase lead introduced by the capacitive divider is:

$$\theta = 90^\circ - \tan^{-1} \omega (C_1 + C_2) R_s$$

$$= 7^\circ \text{ for } C_2 = 50 \text{ UUF}$$

DESIGN EVALUATION DATA, 120-MC TRANSISTOR OSCILLATOR (2N834)

Nominal $V_o = 6V$; Oscillator Frequency = 120.0008 MC

EFFECT OF	CHANGE	TEST CONDITIONS
$\pm 10\%$ Change in $B+$ on Oscillator Frequency	± 2.5 PPM	$R_L = 390$ ohms, $T_A \approx 25^\circ C$
$\pm 10\%$ Change in $B+$ in Output Voltage	$\Delta V_o = \pm 11\%$	$R_L = 390$ ohms, $T_A \approx 25^\circ C$
$\pm 10\%$ Change in R_L on Oscillator Frequency	± 2.5 PPM	$V_{cc} = 28V$, $T_A \approx 25^\circ C$
$\pm 10\%$ Change in R_L on Output Voltage	$\Delta V_o = \pm 17\%$	$V_{cc} = 28V$, $T_A \approx 25^\circ C$
$-50^\circ C$ to $+80^\circ C$ Variation of T_A on Oscillator Frequency	± 37 PPM	$V_{cc} = 28V$, $R_L = 390$ ohms
$-50^\circ C$ to $+80^\circ C$ Variation of T_A on Output Voltage	$\Delta V_o = \pm 4\%$	$V_{cc} = 28V$, $R_L = 390$ ohms
PPM frequency change calculated using the formula: $PPM = \frac{\text{Total Frequency Change}}{2 \times \text{Nominal } f_o (\text{MC})}$		
$\%V_o$ change calculated using the formula: $\Delta V_o \% = \frac{\text{Total } V_o \text{ Change}}{2 \times \text{Nominal } V_o} \times 100$		
$T_A =$ Oscillator Ambient Temperature		

APPENDIX E

75-MC OSCILLATOR USING 2N2219 TRANSISTOR

Object:

The object was to develop as much power output as possible while maintaining the crystal dissipation below the 2 MW maximum.

This design followed the 120-MC high power oscillator. The 2N2217 - 2N2219 types were again selected for evaluation. At this frequency the 2N2219 had the best power gain-to-input resistance characteristic. When converted to an oscillator and the feedback network optimized, the performance was surprisingly poor; i.e., the power output was only 100 MW.

After several values of load resistance and feedback network were attempted without any improvement, it was decided to partially neutralize the transistor so that operation with a larger value of load resistor would be possible. The neutralizing scheme consisted of connecting a coil of 0.15 UH across the crystal socket. Re-testing the circuit on the RX Meter (crystal removed) gave the improved curves of Figure E-2. These curves show stable gain characteristics for $R_T = 900$ ohms. In practice the maximum value was 500 ohms before tuning hysteresis occurred.

The neutralized oscillator displayed a much improved power output (170 MW), but the surprising characteristic was a frequency stability with temperature of ± 0.0013 percent. This is approximately one-third of that typically obtained with previous transistor oscillators. No further evaluations were made, and it is undetermined whether this was a freak occurrence or whether the neutralizing was influential in this improvement.

75-MC TRANSISTOR OSCILLATOR DATA

Oscillator Design and Evaluation Sheet

Active Element: <u>Transistor</u>	Manufacturer's Type No.: <u>2N2219</u>	
Crystal (s) Used	Resonant Frequency	Series Resistance
<u>CR-56/U</u>	<u>74.9995 MC</u>	<u>38 ohms</u>

Feedback transformer configuration: Capacitive Divider

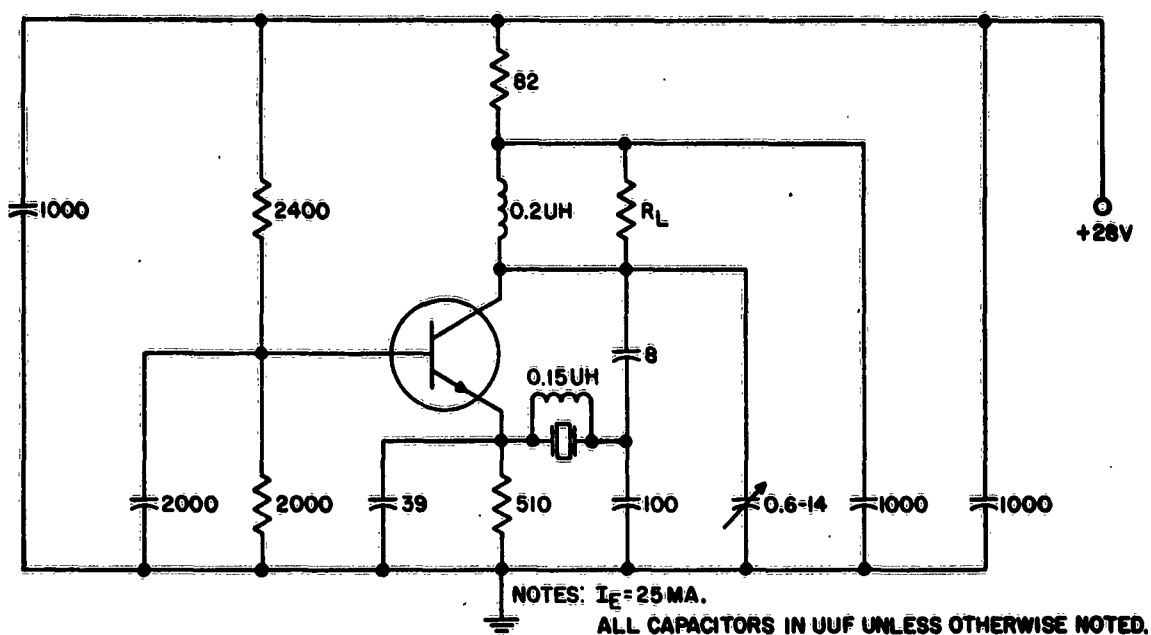


Figure E-1: 75-MC Oscillator Circuit

Details of Design Calculations

Using the notation and design equations of the Final Report and the measured gain and input resistance of the amplifier, the remaining component values were determined as follows for the partially neutralized circuit case:

A power gain of 88 was selected corresponding to:

$$R_T = 470 \text{ ohms}, R_{in} = 45 \text{ ohms}$$

The crystal resonance resistance, $R_T = 50$ ohms max:

$$R_s = R_{in} + R_r = 95 \text{ ohms}$$

$$G'_p = G_p \times \frac{R_{in}}{R_s} = 42$$

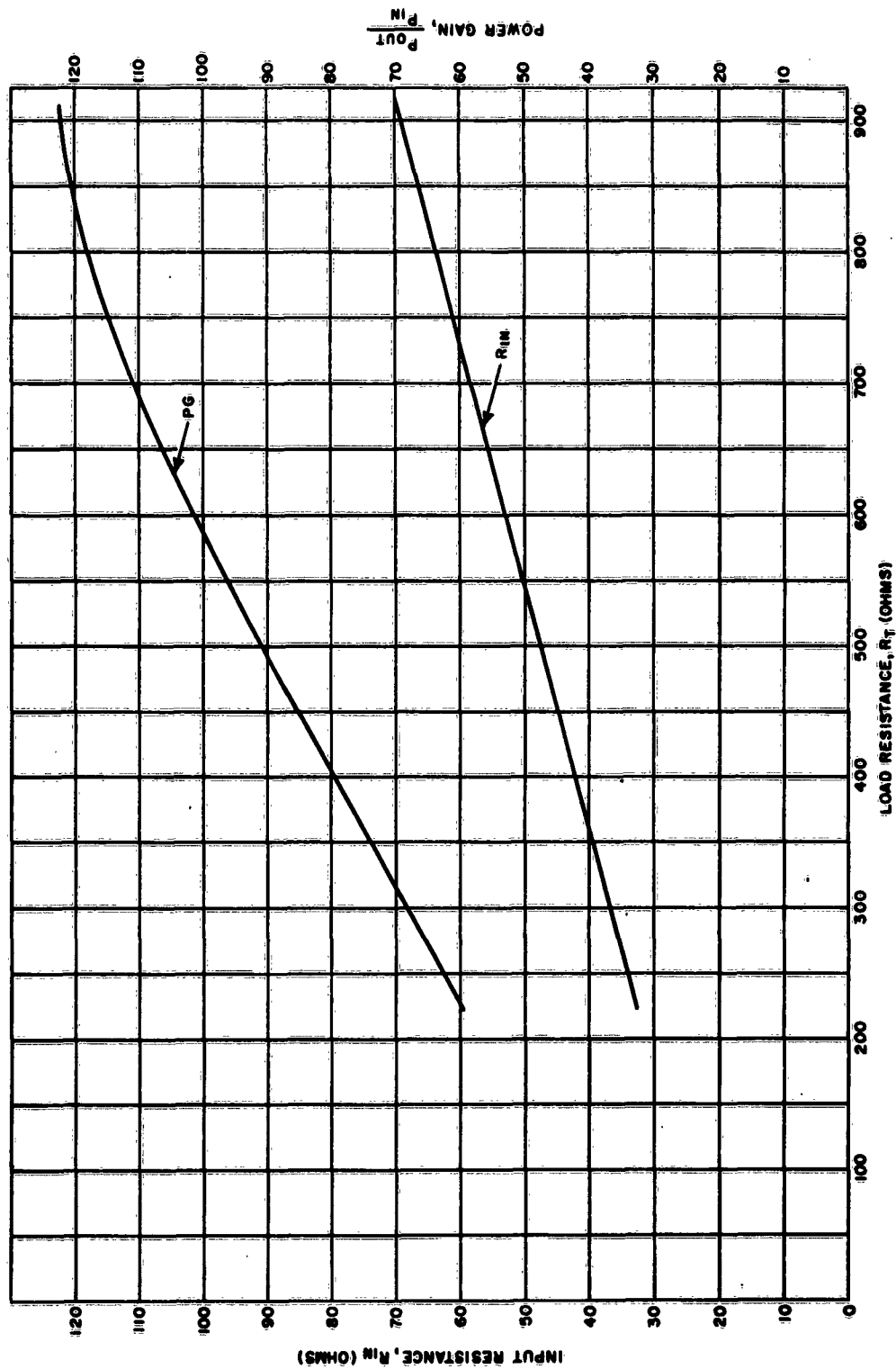


Figure E-2. Power Gain and Input Resistance vs. Load Resistance for 2N2219 Transistor at 75-MC with Neutralization

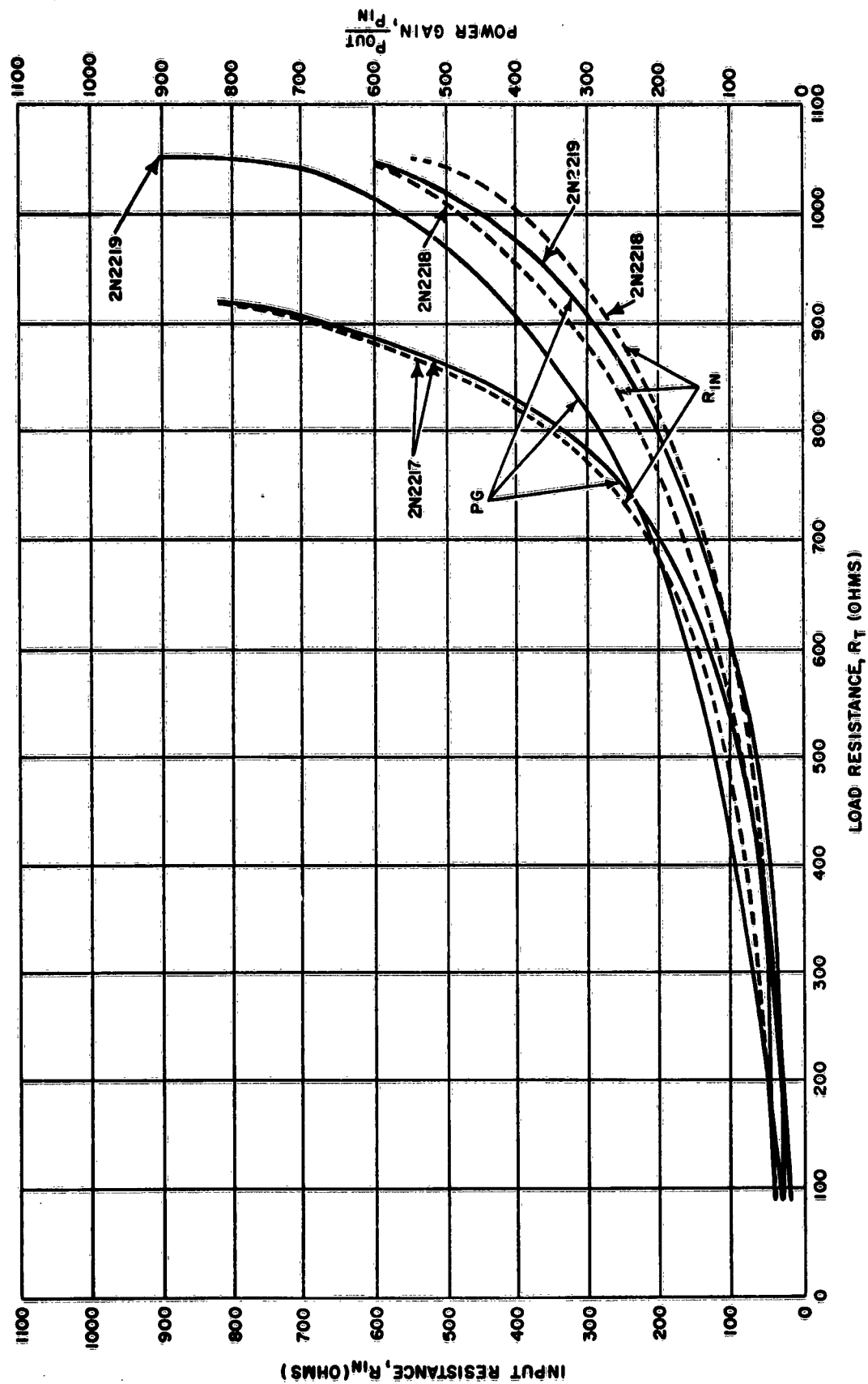


Figure E-3. Input Resistance and Power Gain of 2N2217-19 Transistors at 75 MC

Using a safety factor of 2 gives:

$$\frac{G'_P}{2} = 21$$

$$R_{FB} = 21 \times 470 = 9.9 \text{ K}$$

Using a capacitive divider feedback network, the relevant equations are:

$$T_r = \frac{R_{FB}}{R_s} = 104 = \left(\frac{C_1 + C_2}{C_1} \right)^2$$

$$\text{or } C_2 = 9C_1$$

$$\text{Letting } C_1 = 8 \text{ UUF gives } C_2 = 72 \text{ UUF}$$

Optimum crystal drive level (1 to 1.5 MW) was obtained for $C_2 = 100 \text{ UUF}$.

The phase lead introduced by the capacitive divider is:

$$\theta = 90^\circ - \tan^{-1} \omega (C_1 + C_2) R_s$$

$$= 10^\circ$$

DESIGN EVALUATION DATA, 75-MC TRANSISTOR OSCILLATOR

Nominal $V_o = 9$ V RMS Corresponding to an Output Power of 170 MW; Oscillator Frequency = 75.0000 MC

EFFECT OF	CHANGE	TEST CONDITIONS
$\pm 10\%$ Change in B+ on Oscillator Frequency	± 2.4 PPM	$R_L = 470$ ohms, $T_A \approx 25^\circ\text{C}$
$\pm 10\%$ Change in B+ on Output Voltage	$\Delta V_o = \pm 10\%$	$R_L = 470$ ohms, $T_A \approx 25^\circ\text{C}$
$\pm 10\%$ Change in R_L on Oscillator Frequency	± 1.7 PPM	$V_{cc} = 28$ V, $T_A \approx 25^\circ\text{C}$
$\pm 10\%$ Change in R_L on Output Voltage	$\Delta V_o = \pm 20\%$	$V_{cc} = 28$ V, $T_A \approx 25^\circ\text{C}$
-50°C to $+80^\circ\text{C}$ Variation of T_A on Oscillator Frequency	± 12.5 PPM	$R_L = 470$ ohms, $V_{cc} = 28$ V
-50°C to $+80^\circ\text{C}$ Variation of T_A on Output Voltage	$\Delta V_o = \pm 17\%$	$R_L = 470$ ohms, $V_{cc} = 28$ V
PPM frequency change calculated using the formula: $\text{PPM} = \frac{\text{Total Frequency Change}}{2 \times \text{Nominal } f_o (\text{MC})}$		
$\%V_o$ change calculated using the formula: $\Delta V_o \% = \frac{\text{Total } V_o \text{ Change}}{2 \times \text{Nominal } V_o} \times 100$		
$T_A =$ Oscillator Ambient Temperature		

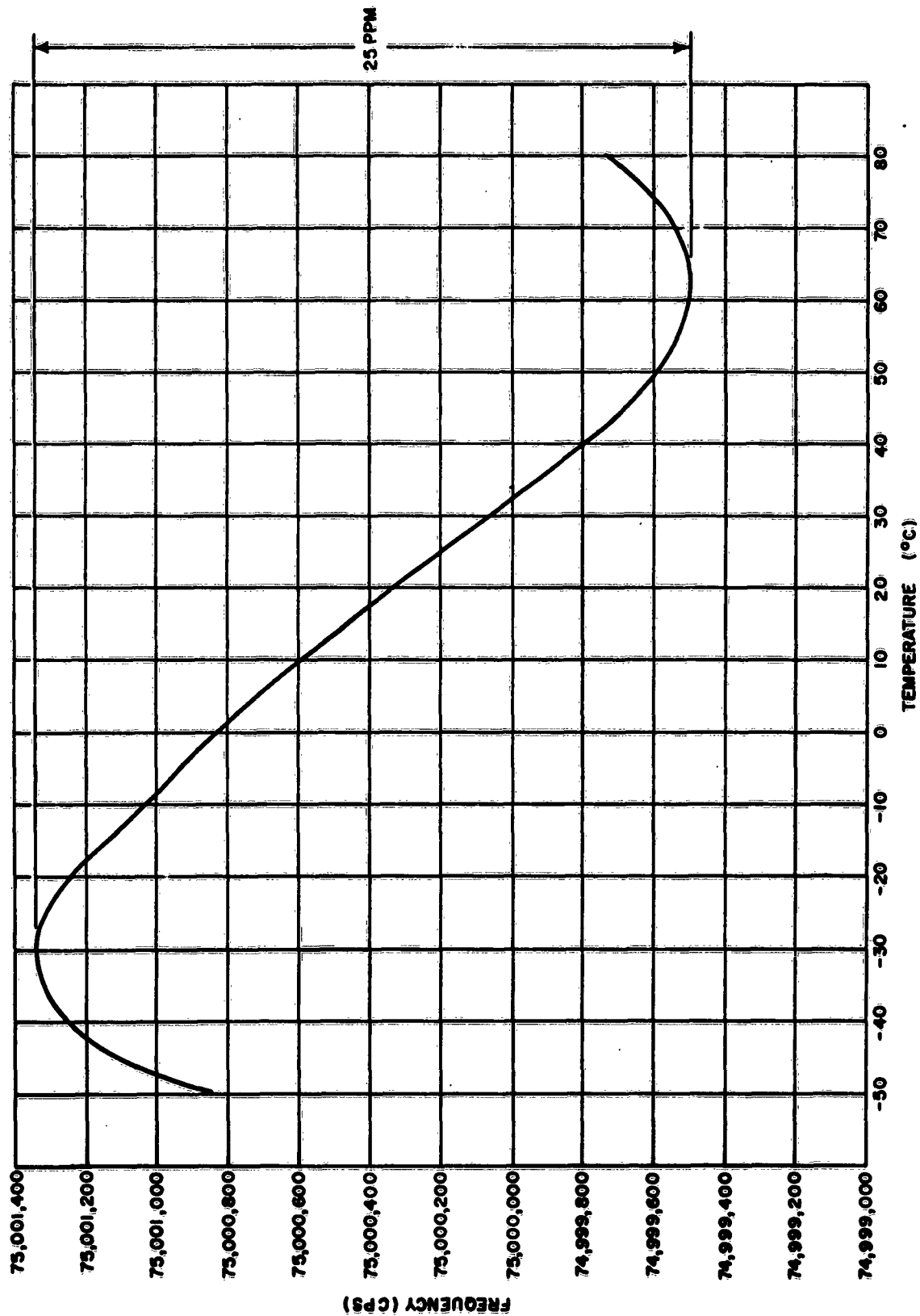


Figure E-4. Frequency vs. Temperature for 2N2219, 75-MC Oscillator with Neutralization

APPENDIX F

100-MC TUBE OSCILLATOR USING 5718A SUB-MINIATURE TRIODE

Object:

This design and the one at 200 MC using the 5718A triode were the first ones attempted using tubes. The object was to determine the difficulties that would be encountered in tube oscillator design at these higher frequencies.

Design Details:

The physical layout followed as closely as possible the one previously used in the transistor oscillators. However, because of the physical bulk of the tube, changes were necessary and the layout shown in Figure F-1 was used.

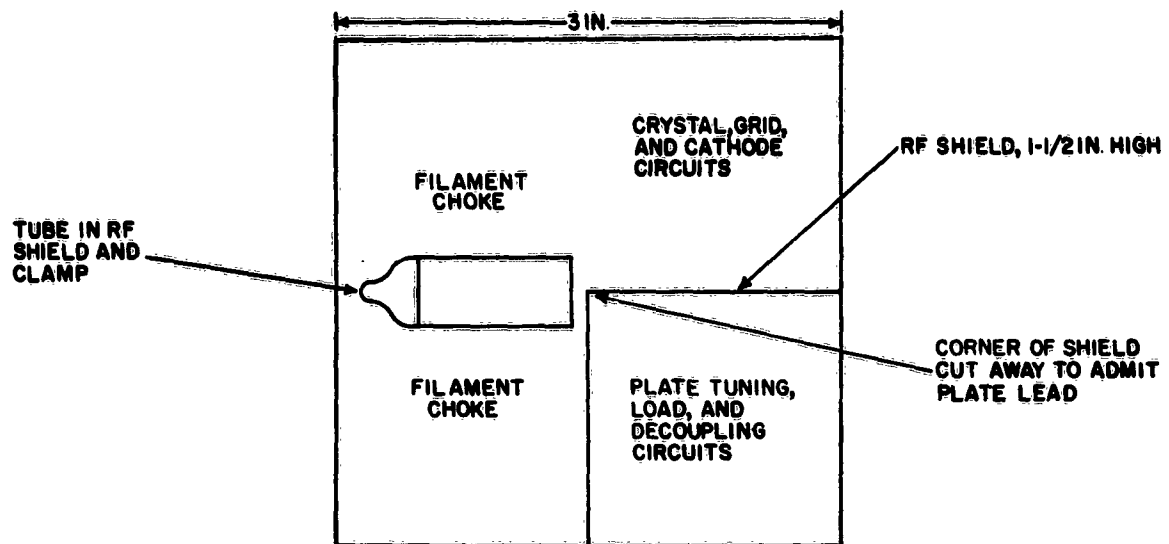


Figure F-1. Chassis Layout

Difficulty was experienced in establishing this design; several redesigns of the grid and cathode circuits were necessary before a successful oscillator was obtained. Initially, the circuit was constructed with the grid directly grounded and the cathode connected to ground via a 1-UH choke. This arrangement was unsatisfactory because of uncontrolled oscillation that could be tuned in, in addition to the desired crystal controlled oscillation. After several grid and cathode circuit redesigns were made, the circuit shown in Figure F-2 was found to give stable crystal controlled oscillation.

Conclusions:

Because of the amount of experimental work involved in developing a satisfactory oscillator, this design cannot be claimed as a successful example of the design procedure. The information obtained from the design measurements, while being sufficient to determine the feedback requirements for the crystal-controlled oscillation at 100 MC, did not predict the instability that occurred at adjacent frequencies.

This possibility is noted in the Final Report. However, it can justifiably be ignored, since these undesired effects did not occur in the majority of the oscillators constructed using the design procedure. This design and the one at 200 MC using the same tube type proved to be exceptions to the rule.

Some of the possible reasons for the uncontrolled oscillation are given below:

- (a) Feedback through the un-neutralized crystal C_0 undoubtedly had some effect, since the circuit was stable with the crystal removed. However, this feedback alone is insufficient to cause oscillation, since a C_0 of 7 PF has a reactance of 230 ohms at 100 MC. This is incompatible with the loop gain requirements for the feedback ratio used.
- (b) Inductive coupling between output tuning coil and the cathode choke. Because of the single-ended layout of the tube, the RF shielding was poor in the vicinity of the tube base. However, the circuit when tested as an amplifier did not show any tendency toward instability.
- (c) The grid circuit had an important bearing on the instability, and there appeared to be positive feedback via this circuit.

100-MC TUBE OSCILLATOR DATA

Oscillator Design and Evaluation Sheet

(Test results obtained with diode limiting)

Active Element: <u>Tube</u>	Manufacturer's Type No.: <u>5718A</u>	
Crystal Used	Resonant Frequency	Resonance Resistance
<u>CR-56/U</u>	<u>99.9998 MC</u>	<u>29 ohms</u>
Description of Oscillator Type		
Active element configuration: <u>Grounded Grid</u>		
Feedback transformer configuration: <u>Capacitive Divider</u>		

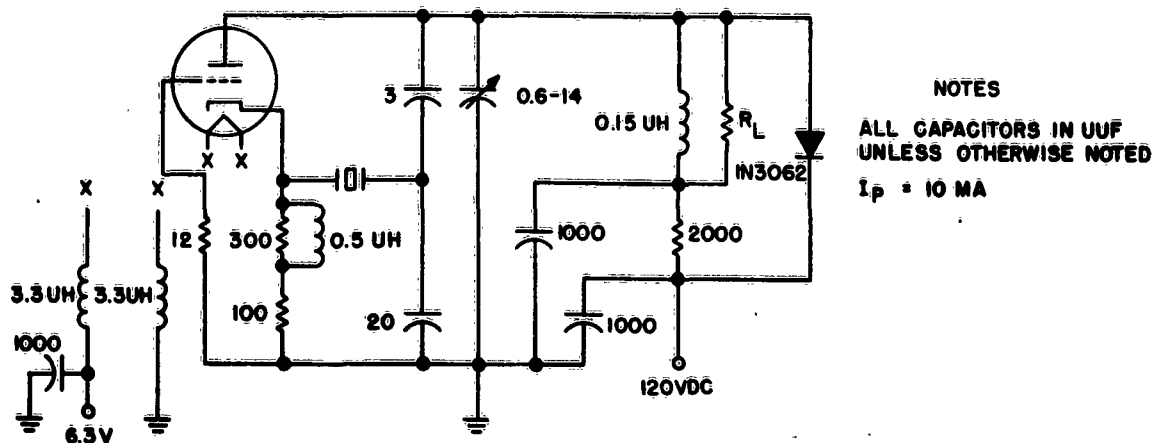


Figure F-2. Oscillator Circuit, 5718A Tube at 100 MC

Details of Design Calculations

Using the notation and design equations of the Final Report and the measured gain and input resistance of the amplifier, the remaining circuit component values are determined as follows:

The working point selected was $G_p = 12$, $R_{in} = 190 \text{ ohms}$, and $R_T = 3K$.

For $R_{r \text{ max}} = 60 \text{ ohms}$:

$$R_s = R_r + R_{in} = 250 \text{ ohms}$$

$$G'_p = G_p \times \frac{R_{in}}{R_s} = 9$$

$$\frac{G'_p}{2} = 4.5$$

$$R_{FB} = \frac{G'_p}{2} \times R_T = 13.5 K$$

$$R_L = \frac{R_{FB}}{\frac{G'_p}{2} - 1} = 3.9 K$$

Using a capacitive divider feedback network, the relevant equations are:

$$\text{Transformation ratio} = \frac{R_{FB}}{R_s} = 54 = \left(\frac{C_1 + C_2}{C_1} \right)^2$$

$$\text{or } C_2 = 6C_1$$

$$\text{For } C_2 = 20 \text{ UUF, } C_1 = 3 \text{ UUF}$$

The phase lead introduced by the capacitive divider is:

$$\theta = \tan^{-1} \omega (C_1 + C_2) R_s = 15 \text{ degrees}$$

The voltage measuring probe parallel resistance was 50 K and the effective parallel loss resistance of the coil was 25 K, giving a parallel combination of 17 K. The load resistance value required to make the total load resistance, $R_L = 3.9 \text{ K}$ was therefore 5 K. The actual load resistance value used was 5.4 K, having a nominal value of 15K.

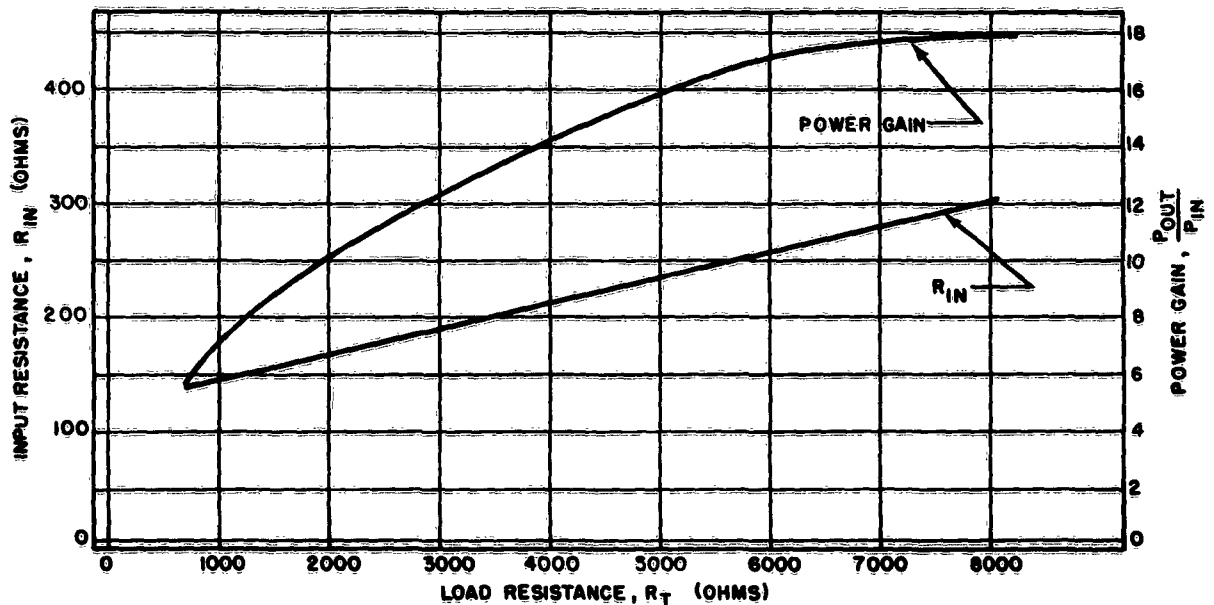


Figure F-3. Input Resistance and Power Gain Versus Load Resistance, 5718A Tube at 100 MC

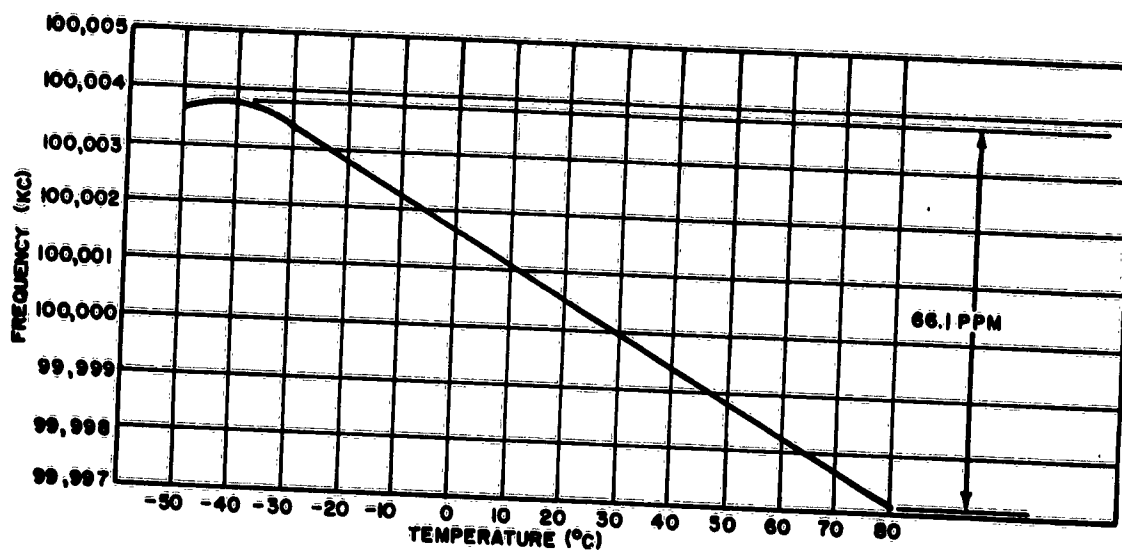


Figure F-4. Frequency Versus Temperature, 5718A Tube at 100 MC, with Diode Limiting

DESIGN EVALUATION DATA, 100-MC TUBE OSCILLATOR

Nominal $V_o = 16$ V; Nominal Oscillator Frequency = 100.0000 MC

EFFECT OF	CHANGE	TEST CONDITIONS
$\pm 10\%$ Change in B+ on Oscillator Frequency	± 1.4 PPM	$E_f = 6.3$ V, $R_L = 15$ K, $T_A \approx 25^\circ$ C
$\pm 10\%$ Change in B+ on Output Voltage	$\Delta V_o = \pm 12\%$	$E_f = 6.3$ V, $R_L = 15$ K, $T_A \approx 25^\circ$ C
$\pm 10\%$ Change in R_L on Oscillator Frequency	± 3.2 PPM	$E_{bb} = 120$ V, $R_L = 15$ K, $T_A \approx 25^\circ$ C
$\pm 10\%$ Change in R_L on Output Voltage	$\Delta V_o = \pm 1\%$	$E_{bb} = 120$ V, $R_L = 15$ K, $T_A \approx 25^\circ$ C
$\pm 10\%$ Change in Filament Supply Voltage on Oscillator Frequency	± 1.2 PPM	$E_{bb} = 120$ V, $R_L = 15$ K, $T_A \approx 25^\circ$ C
$\pm 10\%$ Change in Filament Supply Voltage on Output Voltage	$\Delta V_o = \pm 4\%$	$E_{bb} = 120$ V, $R_L = 15$ K, $T_A \approx 25^\circ$ C
-50° C to $+80^\circ$ C Variation of T_A on Oscillator Frequency	± 33 PPM	$E_{bb} = 120$ V, $E_f = 6.3$ V, $R_L = 15$ K
-50° C to $+80^\circ$ C Variation of T_A on Output Voltage	$\Delta V_o = \pm 6\%$	$E_{bb} = 120$ V, $E_f = 6.3$ V, $R_L = 15$ K

APPENDIX G

150-MC TUBE OSCILLATOR USING 8058 NUUVISTOR

Object:

Alternative tube types were reviewed as a result of:

- (a) The difficulties experienced with the oscillators using the 5718A tube in progressing from the design and measurements stage to a finalized oscillator
- (b) A clearer knowledge of the characteristics required of the tube in an oscillator circuit

The desirable characteristics are discussed in the high-frequency design procedure section of the Final Report and will not be restated here. Based on these considerations, the nuvistor triode, type 8058, was selected for experimental evaluation. The object was to determine if a finalized tube oscillator could be designed by a straightforward application of the design procedure, without recourse to experimental methods.

The physical layout of the circuit is shown in Figure 14 of the Final Report and, as can be seen, the construction of the tube resulted in good shielding between input and output circuits. The only adjustment required to finalize this oscillator consisted of increasing C_2 from 3 UUF to 5 UUF with a corresponding adjustment of the limiter diode biasing resistor. In this case the allowable plate swing before crystal overdrive was 10 VRMS.

Conclusions:

No difficulties were experienced in finalizing this oscillator, and this appears to be due mainly to the better isolation between input and output sections of the tube. Isolation was aided by the considerably better RF shielding that can be applied to the external circuitry of a tube of planar or semi-planar construction.

In comparing the evaluation data of this design with the one at 200 MC using the same type of tube, the following items stand out:

- (a) The frequency stability of this oscillator as a function of temperature is lower by a factor of 2. In view of the similarity of the circuits and circuit components in the two oscillators, it appears that this may be attributable to differences in the crystal temperature characteristics. No verification of this has been made.

- temperature limited conditions, and for many oscillator applications a stabilized heater supply would be required. (Another possibility would be to replace the limiter diode biasing resistor with a zener diode, thereby stabilizing the limiting voltage.)

Oscillator Design and Evaluation Sheet

Manufacturer's Type No. : 8058

Series Resistance

47 ohms

Feedback transformer configuration: Capacitive Divider

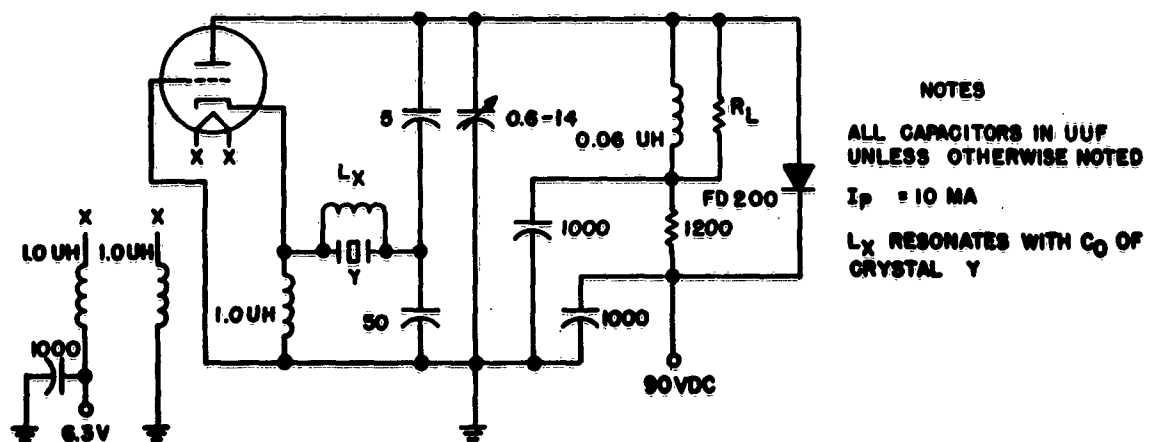


Figure G-1. Oscillator Circuit, 8058 Nuvistor at 150 MC

Details of Design Calculations

Using the notation and design equations of the Final Report and the measured gain and input resistance of the amplifier, the remaining component values are determined as follows:

A working point on the amplifier characteristics was selected corresponding to $G_p = 39$, $R_T = 2.7 \text{ K}$ and $R_{in} = 80 \text{ ohms}$. Using $R_1 \text{ max}$ (crystal series arm resistance) = 100 ohms gives:

$$R_s = 180 \text{ ohms}$$

$$G'_p = 17$$

$$\text{and } \frac{G'_p}{2} = 9$$

$$\text{Therefore, } R_{FB} = 9 \times 2.7 \text{ K} = 24 \text{ K}$$

$$\text{and } R_L = \frac{24\text{K}}{8} = 3 \text{ K}$$

The voltage measuring probe parallel resistance = 50 K and the effective parallel coil loss resistance = 23 K. The actual load resistance required to give $R_L = 3 \text{ K}$ was, therefore, 3.4 K (5.1 K nominal value).

Using a capacitive divider feedback network, the relevant equations are:

$$\text{Transformation Ratio} = \frac{R_{FB}}{R_s} = 135 = \left(\frac{C_1 + C_2}{C_1} \right)^2$$

giving:

$$11C_1 = C_2$$

$$\text{For } C_2 = 50 \text{ UUF, } C_1 = 4.5 \text{ UUF}$$

The actual value of C_1 used was 5 UUF (nominal).

The phase lead introduced by the capacitive divider is:

$$\theta = 6^\circ$$

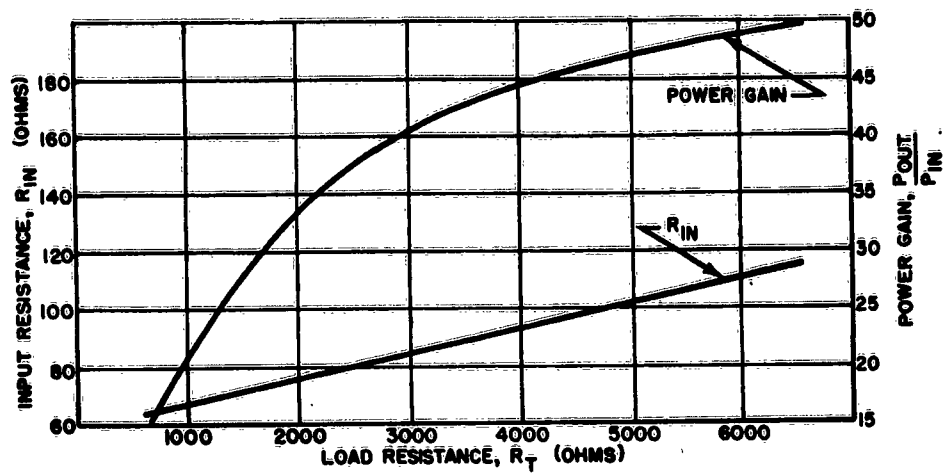


Figure G-2. Input Resistance and Power Gain Versus Load Resistance, 8058 Nuvistor at 150 MC

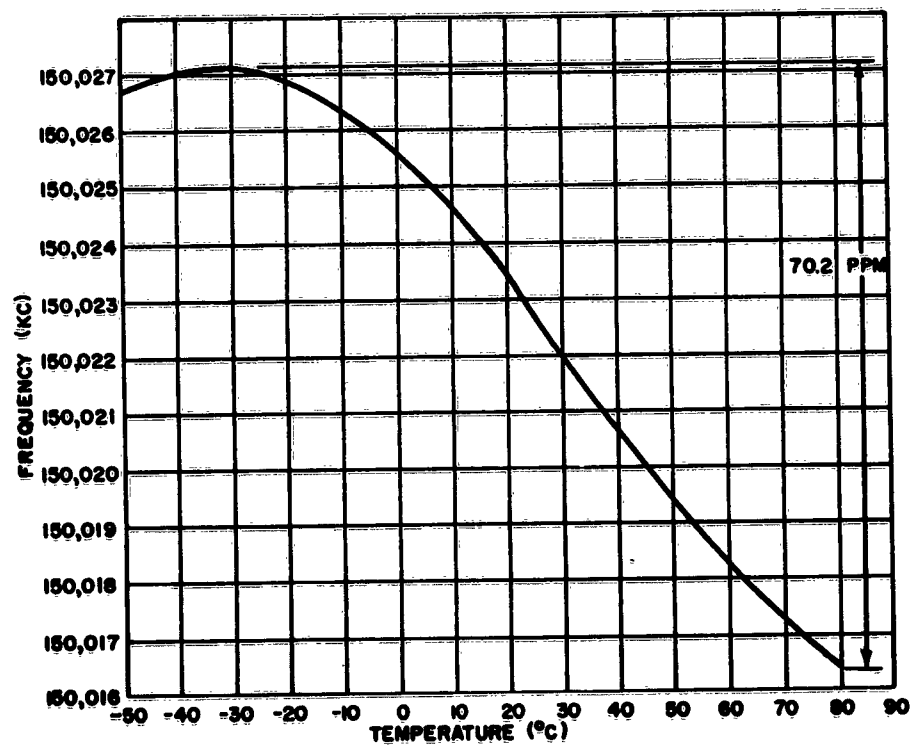


Figure G-3. Frequency Versus Temperature, 8058 Nuvistor at 150 MC

DESIGN EVALUATION DATA, 150-MC TUBE OSCILLATOR

Nominal $V_o = 9$ V; Nominal Oscillator Frequency = 150.0211 MC

EFFECT OF	CHANGE	TEST CONDITIONS
$\pm 10\%$ Change in B+ on Oscillator Frequency	± 1.4 PPM	$R_L = 5.1K, E_f = 6.3V, T_A \approx 25^\circ C$
$\pm 10\%$ Change in B+ on Output Voltage	$\Delta V_o = \pm 10\%$	$R_L = 5.1K, E_f = 6.3V, T_A \approx 25^\circ C$
$\pm 10\%$ Change in R_L on Oscillator Frequency	± 1.4 PPM	$E_{bb} = 90V, E_f = 6.3V, T_A \approx 25^\circ C$
$\pm 10\%$ Change in R_L on Output Voltage	$\Delta V_o = \pm 1\%$	$E_{bb} = 90V, E_f = 6.3V, T_A \approx 25^\circ C$
$\pm 10\%$ Change in Filament Voltage on Oscillator Frequency	± 2.6 PPM	$E_{bb} = 90V, R_L = 5.1K, T_A \approx 25^\circ C$
$\pm 10\%$ Change in Filament Voltage on Output Voltage	$\Delta V_o = \pm 26\%$ (16% for 5% ΔE_f)	$E_{bb} = 90V, R_L = 5.1K, T_A \approx 25^\circ C$
-50°C to +80°C Change in T_A on Oscillator Frequency	± 36 PPM	$E_{bb} = 90V, R_L = 5.1K, E_f = 6.3V$
-50°C to +80°C Change in T_A on Output Voltage	$\Delta V_o = \pm 2\%$	$E_{bb} = 90V, R_L = 5.1K, E_f = 6.3V$

APPENDIX H

200-MC TUBE OSCILLATOR USING 5718A

Object:

This design actually preceded that of the 100-MC oscillator using the same tube type. The object was to determine design difficulties using tube circuits at this frequency.

The physical circuit layout was the same as that used for the 100-MC tube oscillator, as shown in Figure F-1.

Design Details:

Initially, this oscillator was constructed with an RC network in the grid to provide limiting action and with a choke in the cathode to reduce shunt losses in the feedback path. The resulting oscillator was unsatisfactory due to "squegging" (a relaxation type modulation of the oscillator output due to the action of the grid circuit time-constant) and to uncontrolled oscillation. Adjustment of the grid time constant cured the "squegging", but it was necessary to replace the cathode choke with a resistor to prevent the uncontrolled oscillation. The remaining defect in the oscillator was crystal overdrive. It was found impractical to remedy this by B+ and grid circuit adjustments, and the diode limiting circuit was incorporated into the design to give the necessary limiting action. After these changes, the oscillator performed well as shown in the accompanying data sheet.

Conclusions:

Many of the remarks concerning the 100-MC oscillator are applicable to this design. This oscillator exhibited the same tendency to uncontrolled oscillation until circuit changes were made in the grid and cathode circuits. In this case, however, stabilizing the circuit was easier, the amount of experimental adjustment required being far smaller; no explanation is available for this discrepancy.

The difficulty in keeping the crystal drive within permissible limits is due to the low gain in the amplifier portion of the circuit and the relatively large linear signal handling properties of a vacuum tube. In this design, the plate voltage had to be limited to less than 4 VRMS to prevent crystal overdrive. When it is considered that plate voltages of 100V or more are required to optimize the gain, it is easily seen that external limiting methods are necessary.

200-MC TUBE OSCILLATOR DATA

Oscillator Design and Evaluation Sheet

Active Element: <u>Tube</u>	Manufacturer's Type No.: <u>5718A</u>	
Crystal Used	Resonant Frequency	Series Resistance
Similar to		
<u>CR-57/U</u>	<u>199.9990 MC</u>	<u>88 ohms</u>
Description of Oscillator Type		
Crystal: <u>Series</u>		
Active element configuration: <u>Grounded Grid</u>		
Feedback transformer configuration: <u>Capacitive Divider</u>		

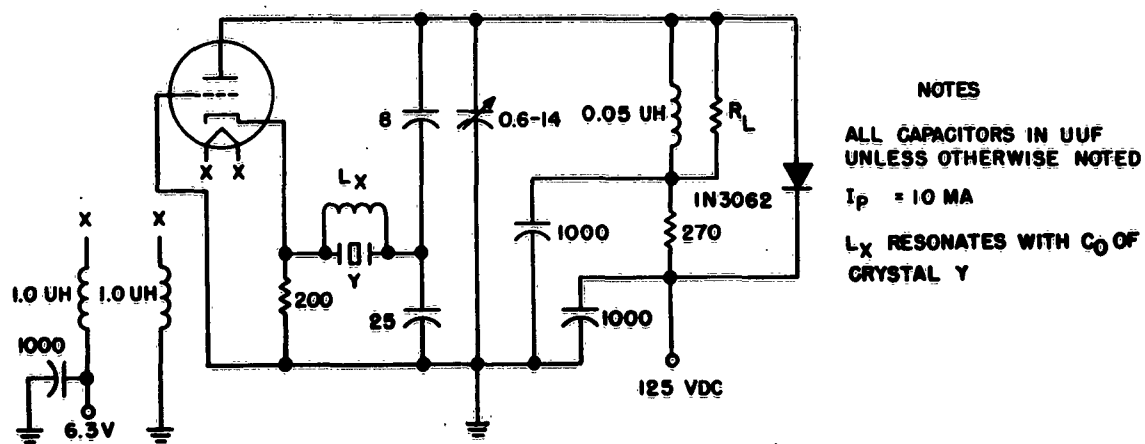


Figure H-1. Oscillator Circuit, 5718A Tube at 200 MC

Details of Design Calculations

Using the notation and design equations of the Final Report and the measured gain and input resistance of the amplifier, the remaining circuit component values are determined as follows:

The working point was selected at $R_T = 1.6 \text{ K}$, $G_p = 12$, $R_{in} = 120 \text{ ohms}$.

Using a crystal series resistance value of 100 ohms gives:

$$R_s = R_{in} + R_1 = 220 \text{ ohms}$$

$$G'_p = 6.6$$

$$\frac{G'_p}{2} = 3.3$$

$$R_{FB} = \frac{G'_p}{2} \times R_T = 5.3 \text{ K}$$

$$R_L \left(\begin{array}{l} \text{including voltage measuring} \\ \text{probe and coil losses} \end{array} \right) = \frac{R_{FB}}{\frac{G'_p}{2} - 1} = 2.3 \text{ K}$$

Using a capacitive divider feedback network, the relevant equations are:

$$\text{Transformation Ratio} = \frac{R_{FB}}{R_s} = 24 = \left(\frac{C_1 + C_2}{C_1} \right)^2$$

$$\text{giving, } C_2 = 4C_1$$

$$\text{For } C_2 = 25 \text{ UUF, } C_1 = 6 \text{ UUF}$$

The actual value of C_1 used was 8 UUF.

The voltage measuring probe parallel resistance was 8 K and the effective parallel loss resistance of the coil was 8 K; that is, a parallel combination of 4 K. The actual loading resistance value required to make the total load resistance, $R_L = 2.3 \text{ K}$ was therefore 5.4 K. The actual value used was 5 K (13 K nominal value). The phase lead introduced by the capacitive divider is 7° .

DESIGN EVALUATION DATA, 200-MC TUBE OSCILLATOR 5718A

Nominal $V_o = 2.7$ V; Operating Frequency = 199.998 MC

EFFECT OF	CHANGE	TEST CONDITIONS
$\pm 10\%$ Change in B+ on Oscillator Frequency	± 1 PPM	$E_f = 6.3$ V, $R_L = 13$ K, $T_A \approx 25^\circ\text{C}$
$\pm 10\%$ Change in B+ on Output Voltage	$\Delta V_o = \pm 11\%$	$E_f = 6.3$ V, $R_L = 13$ K, $T_A \approx 25^\circ\text{C}$
$\pm 10\%$ Change in R_L on Oscillator Frequency	± 2.5 PPM	$E_f = 6.3$ V, $E_{bb} = 125$ V, $T_A \approx 25^\circ\text{C}$
$\pm 10\%$ Change in R_L on Output Voltage	$\Delta V_o = \pm 2\%$	$E_f = 6.3$ V, $E_{bb} = 125$ V, $T_A \approx 25^\circ\text{C}$
$\pm 10\%$ Change in Filament Voltage on Oscillator Frequency	± 2.5 PPM	$E_{bb} = 125$ V, $R_L = 13$ K, $T_A \approx 25^\circ\text{C}$
$\pm 10\%$ Change in Filament Voltage on Output Voltage	$\Delta V_o = \pm 2\%$	$E_{bb} = 125$ V, $R_L = 13$ K, $T_A \approx 25^\circ\text{C}$
-50°C to $+70^\circ\text{C}$ Change in T_A on Oscillator Frequency	± 22 PPM	$E_{bb} = 125$ V, $R_L = 13$ K, $E_f = 6.3$ V
-50°C to $+70^\circ\text{C}$ Change in T_A on Output Voltage	$\Delta V_o = \pm 11\%$	$E_{bb} = 125$ V, $R_L = 13$ K, $E_f = 6.3$ V

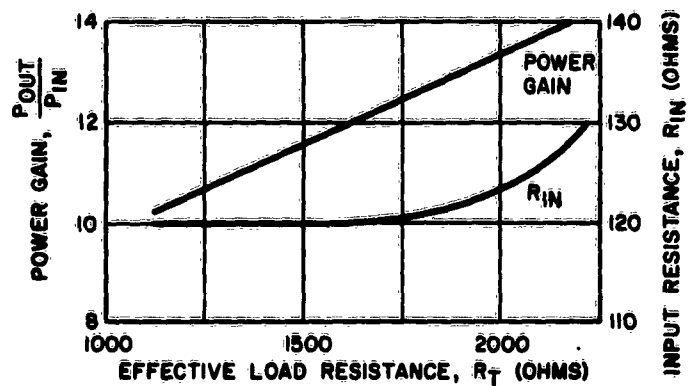


Figure H-2. Input Resistance and Power Gain Versus Load Resistance, 5718A Tube at 200 MC

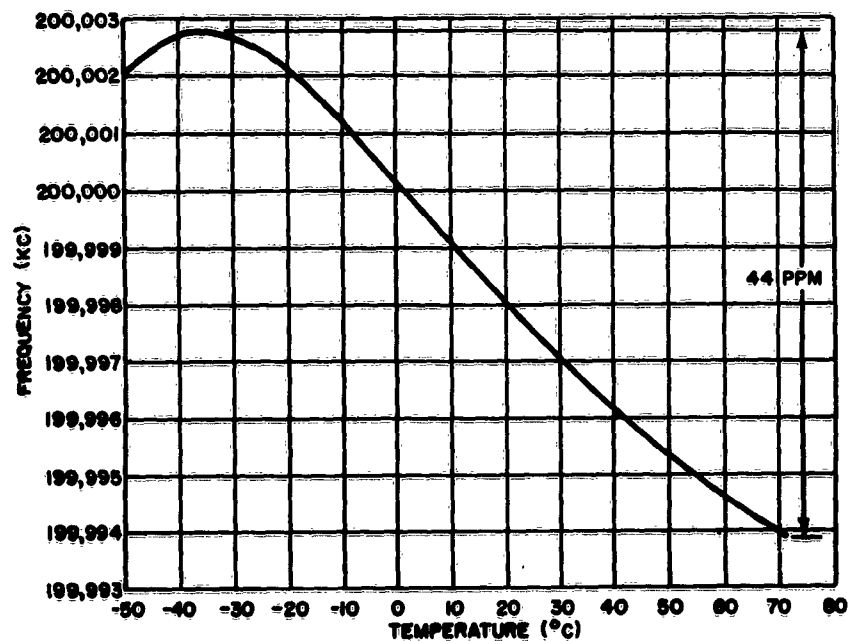


Figure H-3. Frequency Versus Temperature, 5718A Tube at 200 MC

APPENDIX I

200-MC TUBE OSCILLATOR USING 8058 NUVISTOR

This circuit is essentially similar to that used in the 150-MC oscillator (Appendix G), and the comments made concerning the design and performance of that oscillator are directly applicable.

200-MC NUVISTOR OSCILLATOR DATA

Oscillator Design and Evaluation Sheet

Active Element: Nuvistor

Manufacturer's Type No.: 8058

Crystal Used
Similar to

CR-56/U

Resonant Frequency

199.9990 MC

Series Resistance

88 ohms

Description of Oscillator Type

Crystal: Series

Active element configuration: Grounded Grid

Feedback transformer configuration: Capacitive Divider

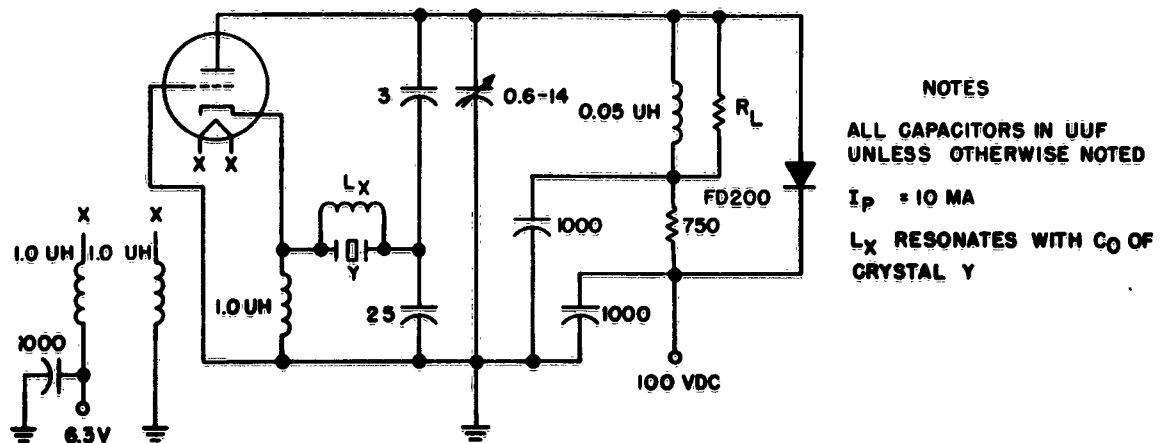


Figure I-1. Oscillator Circuit, 8058 Nuvistor at 200 MC

Details of Design Calculations

Using the notation and design equations of the Final Report and the measured gain and input resistance of the amplifier, the remaining circuit component values are determined as follows for the amplifier characterized by condition No. 1 (see Figure I-2).

A working point was selected at $R'_T = 2.5 \text{ K}$,
 $G_p = 58$, $R_{in} = 75 \text{ ohms}$, $R_{1 \text{ max}} = 100 \text{ ohms}$

$$R_s = 175 \text{ ohms}$$

$$\frac{G'_p}{2} = \frac{R_{in}}{2R_s} \times G_p = 12.5$$

$$R_{FB} = \frac{G'_p}{2} \times R_T = 31 \text{ K}$$

$$R_L = \frac{R_{FB}}{\frac{G'_p}{2} - 1} = 2.7 \text{ K}$$

The coil losses are already accounted for in the amplifier curves, so in this case R_L consists of the actual loading resistor in parallel with the voltmeter probe effective parallel resistance. The value of the latter was 8 K, requiring that the loading resistor be 4.2 K to give $R_L = 2.7 \text{ K}$. The loading resistor used had a nominal 10 K value corresponding to an actual resistance of 4.5 K at this frequency.

Using a capacitive divider feedback network, the relevant equations are:

$$\text{Transformation Ratio} = \frac{R_{FB}}{R_s} = 177 = \left(\frac{C_1 + C_2}{C_1} \right)^2$$

$$\text{or} \quad C_2 = 12C_1$$

Therefore, for $C_2 = 25 \text{ UUF}$, $C_1 = 2 \text{ UUF}$.

The value of C_1 used was 3 UUF.

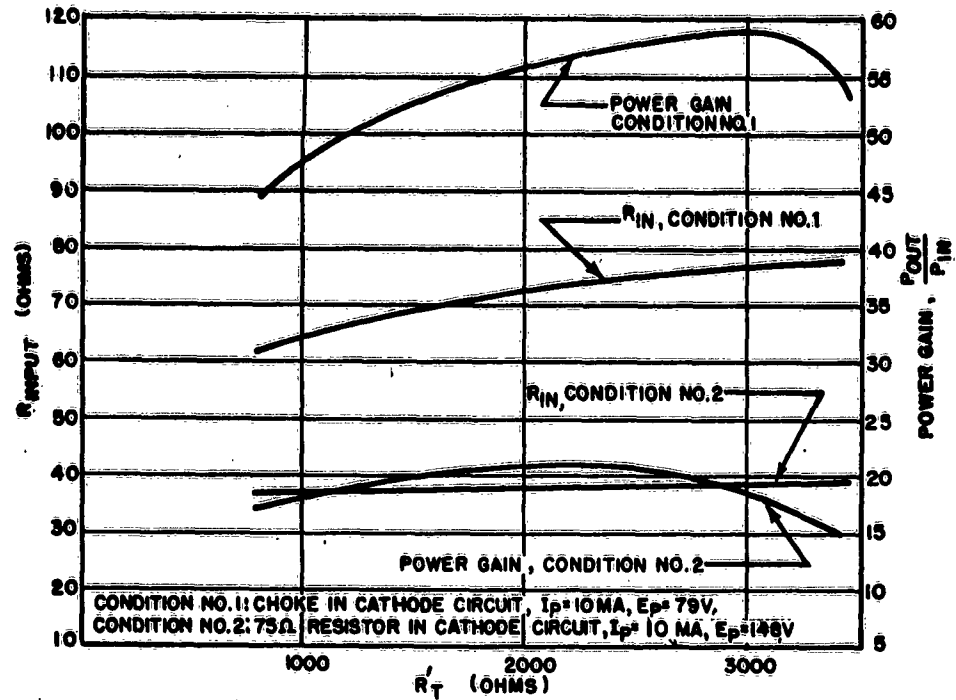


Figure I-2. Input Resistance and Power Gain Versus Total Load Resistance (minus coil losses), 8058 Nuvistor at 200 MC

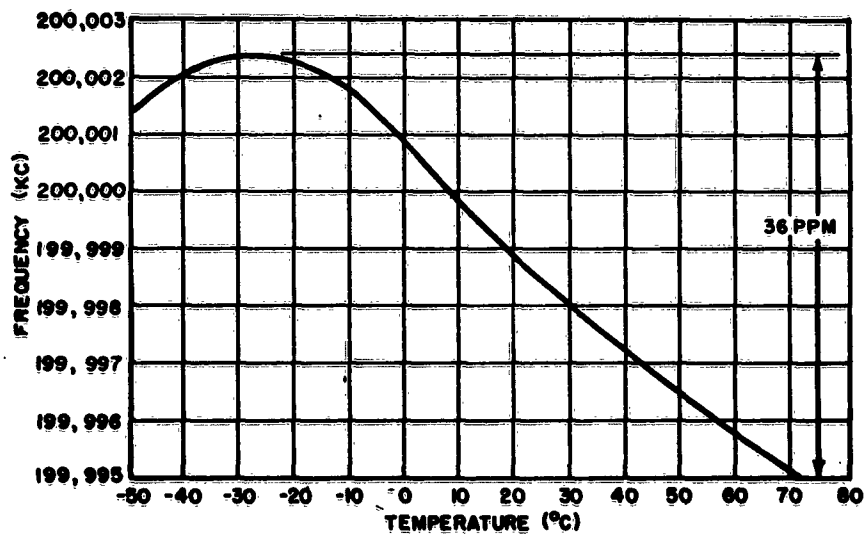


Figure I-3. Frequency Versus Temperature, 8058 Nuvistor at 200 MC

DESIGN EVALUATION DATA, 200-MC TUBE OSCILLATOR 8058

Nominal $V_o = 5.8$ V; Oscillator Frequency = 199.9985 MC

EFFECT OF	CHANGE	TEST CONDITIONS
$\pm 10\%$ Change of $B+$ on Oscillator Frequency	± 1 PPM	$E_f = 6.3$ V, $R_L = 10$ K, $T_A \approx 25^\circ\text{C}$
$\pm 10\%$ Change of $B+$ on Output Voltage	$\Delta V_o = \pm 10\%$	$E_f = 6.3$ V, $R_L = 10$ K, $T_A \approx 25^\circ\text{C}$
$\pm 10\%$ Change of R_L on Oscillator Frequency	± 2.8 PPM	$E_f = 6.3$ V, $E_{bb} = 100$ V, $T_A \approx 25^\circ\text{C}$
$\pm 10\%$ Change of R_L on Output Voltage	$\Delta V_o < 1\%$	$E_f = 6.3$ V, $E_{bb} = 100$ V, $T_A \approx 25^\circ\text{C}$
$\pm 10\%$ Change of E_f on Oscillator Frequency	± 2.5 PPM	$R_L = 10$ K, $E_{bb} = 100$ V, $T_A \approx 25^\circ\text{C}$
$\pm 10\%$ Change of E_f on Output Voltage	$\Delta V_o = \pm 22\%$	$R_L = 10$ K, $E_{bb} = 100$ V, $T_A \approx 25^\circ\text{C}$
-50°C to $+70^\circ\text{C}$ Change of T_A on Oscillator Frequency	± 18 PPM	$R_L = 10$ K, $E_{bb} = 100$ V, $E_f = 6.3$ V
-50°C to $+70^\circ\text{C}$ Change of T_A on Output Voltage	$\Delta V_o = \pm 6\%$	$R_L = 10$ K, $E_{bb} = 100$ V, $E_f = 6.3$ V

APPENDIX J

1-KC TWO-STAGE TUBE OSCILLATOR USING 12AX7 (WIEN BRIDGE)

Object:

In this design the object was to determine the factors influencing the oscillator performance.

The initial plan was to use a resistive divider feedback network to supply the feedback power, but this method proved unusable because of the lack of frequency selectivity. Oscillation at a high audio frequency occurred due to feedback via the crystal C_0 . Replacing the resistive divider with the Wien Bridge network added the selectivity required to prevent this parasitic oscillation. No other difficulties were experienced in finalizing this design.

Conclusions:

The performance of the oscillator as shown by the evaluation data was satisfactory, having a performance approaching that of the high-frequency oscillators.

No difficulties should be met in designs of this type, provided that frequency selectivity is introduced into the oscillator. Crystal overdrive does not constitute a major problem because of the high available gain. The major disadvantage is the circuit complexity.

1-KC TWO-STAGE TUBE OSCILLATOR (WIEN BRIDGE)

Oscillator Design and Evaluation Sheet

Active Element: Vacuum Tube

Manufacturer's Type No.: 12AX7

Crystal Used

Resonant Frequency

Resonance Resistance

T-9J

999.93 CPS

55 K ohms

Description of Oscillator Type

Crystal: Series

Active element configuration: Grounded Cathode

Feedback transformer configuration: Wien Bridge

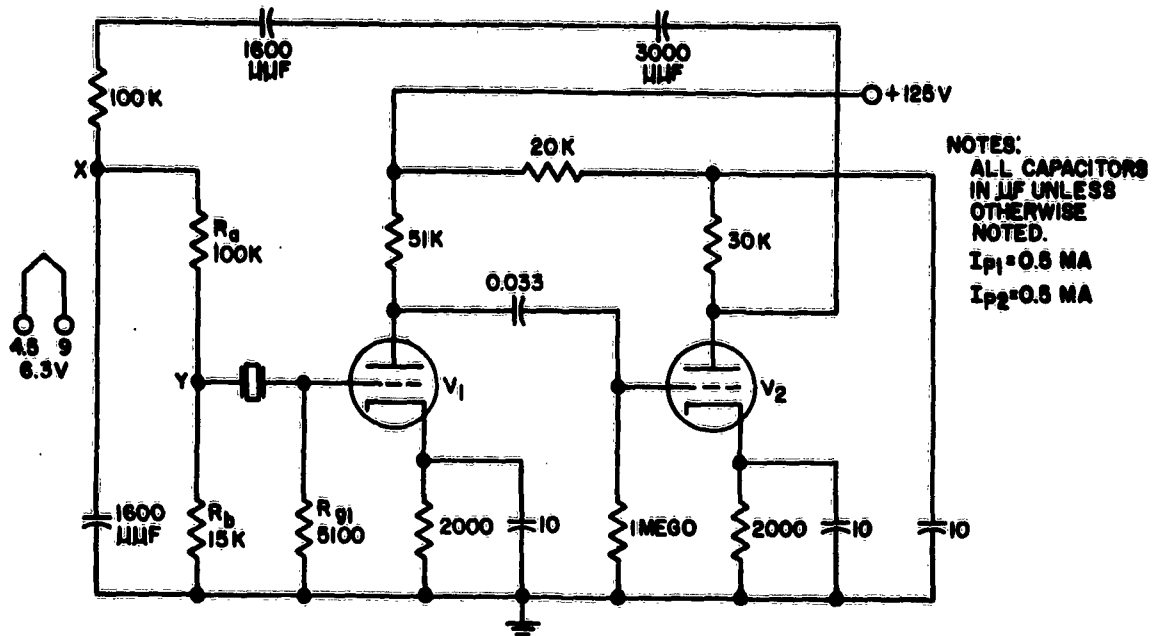


Figure J-1. 1-KC Two-Stage Wien Bridge Oscillator

Details of Design Calculations

With this type of circuit it is convenient to determine the loop voltage gain rather than the power gain. The amplifier voltage gain from the grid of V_1 to the plate of V_2 is:

$$G_v = \frac{U_1 R_{L1}}{R_{L1} + R_{p1}} \times \frac{U_2 R_{L2}}{R_{L2} + R_{p2}}$$

For the biasing conditions shown ($I_p = 0.5 \text{ MA}$, $V_g = -1\text{V}$):

$$U_1 = U_2 = 100, R_{p1} = R_{p2} = 85 \text{ K}$$

$$\frac{V_2}{V_1} = 970$$

This assumes that the loading of the feedback network is negligible (Condition 1).

The voltage attenuation of the feedback network can be calculated as follows:

For this type of crystal, $R_r \text{ max} = 200 \text{ K}$. Therefore, the voltage attenuation between the crystal input and V_1 grid input is:

$$A_c = \frac{R_{g1}}{R_{g1} + 200 \text{ K}}$$

If the loading of $R_r \text{ max} + R_{g1}$ on R_b is assumed small (Condition 2), the attenuation between points X and Y (Figure J-1) is:

$$A_r = \frac{R_b}{R_a + R_b}$$

The attenuation from the plate of V_2 to point X is:

$$A_w = \frac{1}{3} \text{ at the bridge "resonant" frequency.}$$

The total attenuation is therefore:

$$A_T = A_c \times A_r \times A_w$$

To satisfy Condition 1 the feedback network should appear as at least 10 times R_{L2} ; that is, not less than 300 K. Section 4.7.4 of the Final Report shows that the effective parallel resistance of a Wien Bridge network is equal to three times the value of the resistive elements of the bridge. Therefore, a value of 100 K for these elements satisfies Condition 1.

The value of $R_r \text{ max} + R_g$ cannot be less than 200 K, and therefore a value of R_b less than 20 K will satisfy Condition 2.

The loop voltage gain from the input of the Wien Bridge network to the plate of V_2 is therefore:

$$G_{VL} = \frac{1}{3} \times \frac{R_b}{R_a + R_b} \times \frac{R_{g1}}{R_{g1} + 200 \text{ K}} \times 970$$

Letting $R_a + R_b = 100 \text{ K}$, $R_b = 15 \text{ K}$, and equating $G_{VL} = 1.4$ (loop power gain = 2) gives:

$$R_{g1} = 6 \text{ K}$$

The requirement for zero loop phase shift is that:

$$C_1 R_1 C_2 R_2 = \frac{1}{\omega_o^2} \text{ (refer to Wien Bridge analysis)}$$

where the effects of amplifier output resistance and crystal loading are taken into account in the values of R_1 and R_2 , respectively. For the particular feedback network used, the calculation of ω_0 is as follows:

For the crystal used, $R_r = 55$ K and therefore R_b in parallel with $R_r +$

R_{g1} is 12 K.

Therefore, $R_2 = 112$ K.

The output resistance of V_2 is 30 K in parallel with $R_p = 85$ K; that is, 22 K. Therefore $R_1 = 122$ K. C_1 is equal to 1600 UUF in series with 3000 UUF; that is, 1040 UUF and $C_2 = 1600$ UUF. Therefore,

$$\omega_0 = \frac{1}{[C_1 R_1 C_2 R_2]}^{1/2}$$

$$= 6620$$

or $f_0 = 1050$ CPS

The calculated f_0 based on component nominal values agrees to within 5 percent of the actual f_0 which was experimentally adjusted.

The network would be more optimum if the values of R_b and R_{g1} had been interchanged; changes in the value of R_r would then have less effect on loop phase change, since R_2 would be more nearly constant.

The maximum permissible output voltage before crystal overdrive occurs can be determined by considering the feedback network when $R_r = R_r \text{ min}$, which is assumed to be 20 K. For $R_{g1} = 5$ K the crystal dissipation will be 10 UW for an input power of 12.5 UW into R_r and R_{g1} in series. This corresponds to a voltage of 0.56 V at point Y, Figure J-1. The voltage at point X is therefore:

$$V_x = \frac{0.56}{15000} \times 100,000 = 4.1 \text{ V}$$

Since the voltage at the Wien Bridge network is three times V_x , the oscillator output voltage before crystal overload occurs is approximately 12 V. This is not completely accurate, since the network used does not completely satisfy the Wien Bridge conditions.

DESIGN EVALUATION DATA, 1-KC TWO-STAGE TUBE OSCILLATOR

Nominal $V_o = 7.2$ V; Oscillator Frequency = 999.925 CPS

EFFECT OF	CHANGE	TEST CONDITIONS
$\pm 10\%$ Change in B+ on Oscillator Frequency	$\leq \pm 3$ PPM	$E_f = 6.3$ V, $R_L = 30$ K, $T_A \approx 25^\circ$ C
$\pm 10\%$ Change in B+ on Output Voltage	$\Delta V_o = \pm 13\%$	$E_f = 6.3$ V, $R_L = 30$ K, $T_A \approx 25^\circ$ C
$\pm 10\%$ Change in R_L on Oscillator Frequency	$\leq \pm 3$ PPM	$E_f = 6.3$ V, $E_{bb} = 125$ V, $T_A \approx 25^\circ$ C
$\pm 10\%$ Change in R_L on Output Voltage	$\Delta V_o = \pm 7\%$	$E_f = 6.3$ V, $E_{bb} = 125$ V, $T_A \approx 25^\circ$ C
$\pm 10\%$ Change in E_f on Oscillator Frequency	$\leq \pm 3$ PPM	$R_L = 30$ K, $E_{bb} = 125$ V, $T_A \approx 25^\circ$ C
$\pm 10\%$ Change in E_f on Output Voltage	$\Delta V_o = \pm 2\%$	$R_L = 30$ K, $E_{bb} = 125$ V, $T_A \approx 25^\circ$ C
-50°C to +80°C Change in T_A on Oscillator Frequency	± 7 PPM	$R_L = 30$ K, $E_{bb} = 125$ V, $E_f = 6.3$ V
-50°C to +80°C Change in T_A on Output Voltage	$\Delta V_o = \pm 1\%$	$R_L = 30$ K, $E_{bb} = 125$ V, $E_f = 6.3$ V

APPENDIX K

3-KC TWO-STAGE TUBE OSCILLATOR USING 12AX7 (WIEN BRIDGE)

This design was based on the 1-KC oscillator of the same type, the sole adjustment being in the values of capacitance used in the feedback network. All comments concerning the 1-KC Wien Bridge Oscillator are applicable to this oscillator.

3-KC TWO-STAGE TUBE OSCILLATOR (WIEN BRIDGE)

Oscillator Design and Evaluation Sheet

Active Element: Vacuum Tube

Manufacturer's Type No.: 12AX7

Crystal Used

Resonant Frequency

Resonance Resistance

T-9XY

2999.6 CPS

50 Kilohms

Description of Oscillator Type

Crystal: Series

Active element configuration: Common Cathode

Feedback transformer configuration: Wien Bridge

Details of Design Calculations

The design calculations for this oscillator are the same as in Appendix J with the exception of the Wien Bridge network capacitor value. In this case C_1 equals 470 UUF in series with 2400 UUF (390 UUF) and $C_2 = 470$ UUF. Inserting these values into the equation:

$$\omega_o = \left[\frac{1}{C_1 R_1 C_2 R_1} \right]^{1/2}$$

Gives $\omega_o = 18,300$

Or $f_o = 29500$ CPS

The design calculation again gives good agreement between calculated and experimentally adjusted network values.

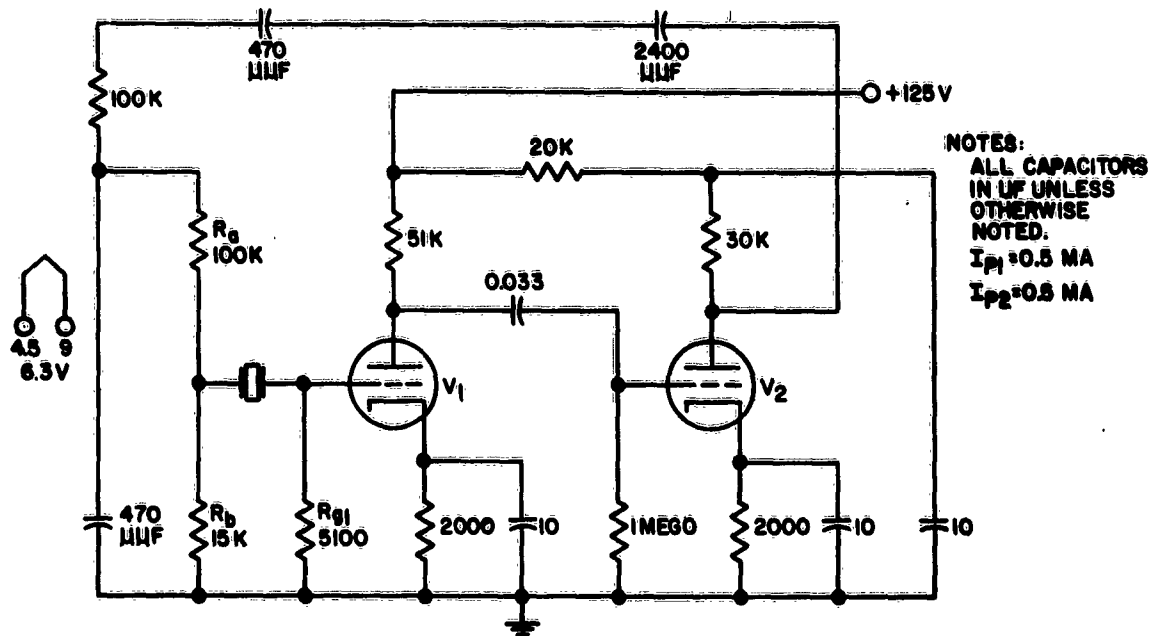


Figure K-1. 3-KC Wien Bridge Oscillator

DESIGN EVALUATION DATA, 3-KC TWO-STAGE TUBE OSCILLATOR

Nominal $V_o = 7V$; Oscillator Frequency = 2999.60 CPS

EFFECT OF	CHANGE	TEST CONDITIONS
$\pm 10\%$ Change in B+ on Oscillator Frequency	$\leq \pm 3$ PPM	$E_f = 6.3V$, $R_L = 30K$, $T_A \approx 25^\circ C$
$\pm 10\%$ Change in B+ on Output Voltage	$\Delta V_o = \pm 13\%$	$E_f = 6.3V$, $R_L = 30K$, $T_A \approx 25^\circ C$
$\pm 10\%$ Change in R_L on Oscillator Frequency	$\leq \pm 3$ PPM	$E_f = 6.3V$, $E_{bb} = 125V$, $T_A \approx 25^\circ C$
$\pm 10\%$ Change in R_L on Output Voltage	$\Delta V_o = \pm 7\%$	$E_f = 6.3V$, $E_{bb} = 125V$, $T_A \approx 25^\circ C$
$\pm 10\%$ Change in E_f on Oscillator Frequency	$\leq \pm 3$ PPM	$R_L = 30K$, $E_{bb} = 125V$, $T_A \approx 25^\circ C$
$\pm 10\%$ Change in E_f on Output Voltage	$\Delta V_o < \pm 2\%$	$R_L = 30K$, $E_{bb} = 125V$, $T_A \approx 25^\circ C$
$-55^\circ C$ to $+80^\circ C$ Change in T_A on Oscillator Frequency	± 150 PPM	$R_L = 30K$, $E_{bb} = 125V$, $E_f = 6.3V$
$-55^\circ C$ to $+80^\circ C$ Change in T_A on Output Voltage	$\Delta V_o < \pm 2\%$	$R_L = 30K$, $E_{bb} = 125V$, $E_f = 6.3V$

APPENDIX L

1-KC SINGLE-STAGE TUBE (12AT7) OSCILLATOR USING THE QUARTZ CRYSTAL TO GIVE PHASE INVERSION

Object:

This type of circuit is discussed briefly in Reference 3, Paragraph 7.0 of the Final Report, and the object of this design was to develop a suitable design method and to determine any disadvantages of the circuit.

Design Details:

The first requirement in establishing a design procedure was to determine the transfer characteristic of a crystal connected as a four-terminal network. The best method found is described in the design calculation discussion and depends on having a signal generator of good short-term frequency stability. The Hewlett-Packard 200CD Signal Generator was adequate for this purpose. Once this information was known, the finalizing of the oscillator was straightforward.

The power transfer efficiency of the crystal varied somewhat depending on the value of the output load resistor used, and the optimum condition of operation was not clear. Several evaluations were therefore run for various values of loading resistor which, in the oscillator, is the grid leak resistor R_g . No feedback network adjustments were made as R_g was varied, and consequently the loop gain increased by a factor of 2.7 for the $R_g = 1$ MEGOhm evaluation over that for $R_g = 200$ K.

Conclusions:

The value of R_g used had negligible effect on the oscillator performance. It would appear that the highest value of R_g consistent with the maximum permissible value for the particular tube type should be used, in view of the improved transfer efficiency for high values of R_g .

The evaluation data indicates a slight improvement in performance for the higher values of R_g , particularly in the effect of B+ changes on power output.

Insufficient data was obtained to determine the influence of the crystal R_r on performance. The tabulated data shows that the crystal input impedance stays consistently approximately 300 K higher than the value of output load resistor used. This value of 300 K, the input resistance with the output short-circuited, is a value 5.5 times greater than the resonance resistance of this particular crystal when connected

as a two-terminal device. This may or may not be coincidental. If the deduction is valid, it may be possible to extrapolate the results of this test. A crystal with $R_r = 200 \text{ K}$ (the assumed maximum value or R_r) could be expected to have an input resistance of 1 MEGO with the output shorted, or 2 MEGO for a load resistance of 1 MEGO. The efficiency would be approximately 40 percent. These assumptions have not been verified.

The work done on this circuit is not sufficient to establish a complete design procedure for the reasons given in the preceding paragraph. Nevertheless, the simplicity of this oscillator circuit makes it the recommended choice for vacuum tube oscillators below 16 KC.

1-KC SINGLE-STAGE TUBE OSCILLATOR USING THE QUARTZ CRYSTAL TO GIVE PHASE INVERSION

Oscillator Design and Evaluation Sheet

Active Element: Tube

Manufacturer's Type No.: 12AT7

Crystal Used

Resonant Frequency

Resonance Resistance

T9J

999.93 CPS

55 K

Description of Oscillator Type

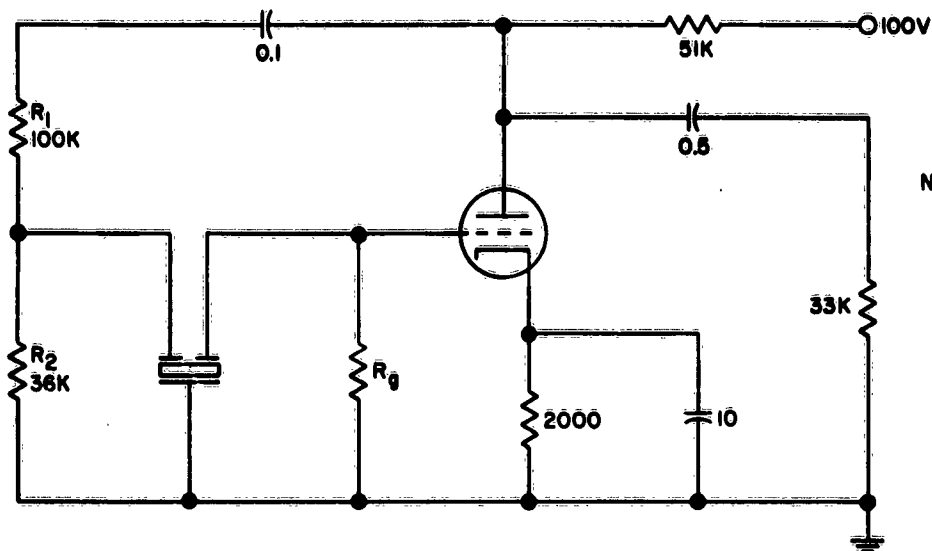
Crystal: Series

Active Element Configuration: Grounded Cathode

Feedback Transformer Configuration: Resistive Divider with crystal providing phase inversion

Details of Design Calculations

Using the circuit shown in Figure L-2, measurements were made of the power transfer efficiency of the crystal connected as a four-terminal network for various values of R . The measuring frequency was adjusted to give phase inversion of V_o with respect to V_{c1} , as measured with a dual beam oscilloscope. The results of these measurements are tabulated below:



NOTES:
ALL CAPACITORS
IN μF UNLESS
OTHERWISE NOTED.
 $I_p = 0.75 \text{ MA}$

Figure L-1. 1-KC Crystal Phase-Inverting Oscillator

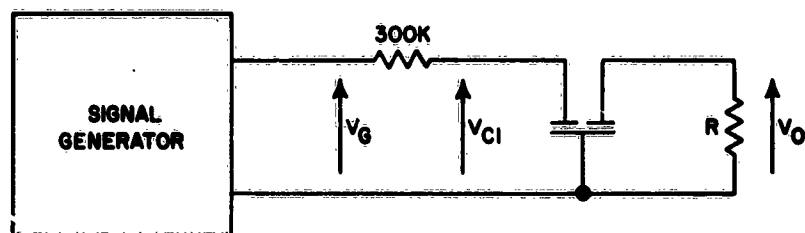


Figure L-2. Crystal Test Circuit

R	$\frac{V_o}{V_{c1}}$	$\frac{V_{c1}}{V_G}$	Crystal Input Resistance, R'_r	Efficiency (P_o/P_{in})
20K	0.063	0.50	300K	0.06
200K	0.420	0.63	510K	0.45
510K	0.540	0.75	900K	0.51
750K	0.610	0.78	1.1 MEGO	0.54
1 MEGO	0.690	0.81	1.3 MEGO	0.62

The characteristics of a 12AT7 at $I_p = 0.75$ MA are:

$$U = 35$$

$$R_p = 35 \text{ K}$$

Using a value of $R_T = 17 \text{ K}$ gives a voltage gain of:

$$G_V = \frac{U \cdot R_T}{R_T + R_p} = 12.4$$

Introducing a loop power gain safety factor of 2 gives:

$$G'_V = 8.7$$

The crystal filter voltage attenuation for $R = R_g = 200 \text{ K}$ is given in the table as 0.42. Therefore, the voltage gain from the input of the crystal to the tube output is:

$$G''_V = G'_V \times 0.42 = 3.7$$

To reduce the loop gain to unity, the attenuation introduced by the feedback divider network (assuming the loading of this network by the crystal is negligible) must be:

$$A_r = \frac{R_2}{R_1 + R_2} = \frac{1}{G''_V} = 0.27$$

giving $\frac{R_2}{R_1} = 0.37$

Therefore, for $R_1 = 100 \text{ K}$, $R_2 = 36 \text{ K}$

Since the crystal input resistance is 510 K, its effect on A_r is negligible. R_T consists of the output load, the feedback load, and the plate supply resistor. The plate supply resistor was determined previously from plate voltage limiting considerations as 51 K, and the feedback load is approximately 130 K. The load resistor value is therefore 33 K.

The crystal power dissipation relative to the power into the crystal is:

$$P_c = 0.55 P_{in}$$

and if P_c max is 10 UW, then:

$$P_{in} = 18 \text{ UW}$$

$$\text{or } V_{c1} = (P_{in} \cdot R'_r)^{1/2} = 3 \text{ V}$$

The oscillator output voltage before crystal overload is:

$$V_o = \frac{V_{c1}}{A_r} = 11 \text{ VRMS}$$

DESIGN EVALUATION DATA, 1-KC VACUUM TUBE OSCILLATOR (FOUR-TERMINAL CRYSTAL)

	Value of R_g			
	200K	510K	750K	1 MEG
Oscillator Frequency (CPS)	999.910	999.905	999.910	999.905
Nominal V_o	5.2	5.9	5.9	5.8
Influence of $\pm 10\%$ Change in $B+$ on Oscillator Frequency	$< \pm 10$ PPM	$< \pm 10$ PPM	$< \pm 10$ PPM	$< \pm 10$ PPM
Influence of $\pm 10\%$ Change in $B+$ on Output Voltage	$\Delta V_o = \pm 22\%$	$\Delta V_o = \pm 20\%$	$\Delta V_o = \pm 20\%$	$\Delta V_o = \pm 14\%$
Influence of $\pm 10\%$ Change in R_L on Oscillator Frequency	$< \pm 4$ PPM	$< \pm 4$ PPM	$< \pm 4$ PPM	$< \pm 4$ PPM
Influence of $\pm 10\%$ Change in R_L on Output Voltage	$\Delta V_o = \pm 6\%$	$\Delta V_o = \pm 5\%$	$\Delta V_o = \pm 5\%$	$\Delta V_o = \pm 4\%$
Influence of $\pm 10\%$ Change in E_f on Oscillator Frequency	$< \pm 3$ PPM	$< \pm 3$ PPM	$< \pm 3$ PPM	$< \pm 3$ PPM
Influence of $\pm 10\%$ Change in E_f on Output Voltage	$\Delta V_o = \pm 3\%$	$\Delta V_o = \pm 2\%$	$\Delta V_o = \pm 2\%$	$\Delta V_o = \pm 2\%$
Influence of -50°C to $+80^\circ\text{C}$ Change in T_A on Oscillator Frequency	± 60 PPM	± 50 PPM	± 55 PPM	± 50 PPM
Influence of -50°C to $+80^\circ\text{C}$ Change in T_A on Output Voltage	$\Delta V_o = \pm 6\%$	$\Delta V_o = \pm 2\%$	$\Delta V_o = \pm 2\%$	$\Delta V_o < \pm 2\%$

APPENDIX M

1-KC TWO-STAGE TRANSISTOR OSCILLATOR (TUNED OUTPUT)

In this circuit the amplifier gain is well in excess of 10^6 . Consequently, there was no difficulty in providing adequate loop gain. In fact, it was necessary to severely mismatch the crystal to limit the loop gain sufficiently (note the 2-K resistor in the resistive divider feedback network).

No difficulty occurred in finalizing the design. Other methods could have been used to give the necessary selectivity. For example, a Wien Bridge network could have been used in place of the tuned circuit and resistance divider network. Furthermore, because of the high available power gain, the sacrifice in output power using the Wien Bridge would not be unduly large, since the total load resistance could be reduced appreciably by appropriately increasing the feedback power.

1-KC TWO-STAGE TRANSISTOR OSCILLATOR (TUNED OUTPUT)

Oscillator Design and Evaluation Sheet

Active Element: Transistor

Manufacturer's Type No.: 2N336

Crystal Used

Resonant Frequency

Resonance Resistance

T-9J

999.93 CPS

55 Kilohms

Description of Oscillator Type

Crystal: Series

Active element configuration: Common Emitter

Feedback transformer configuration: Resistive Divider

Details of Design Calculations

The parameters of the 2N336 at $I_e = 1 \text{ MA}$ as given in the manufacturer's data sheets are:

$$I_e = 1 \text{ MA}, V_{cb} = 5 \text{ V}$$

$$h_{ib} = 55 \text{ ohms}$$

$$h_{fb} = -0.99$$

Similarly, for $I_e = 0.4 \text{ MA}$, $V_{ce} = 5 \text{ V}$

$$h_{ie} = 9.7 \text{ K}$$

$$h_{re} = 1.9 \times 10^{-3}$$

$$h_{fe} = 57$$

$$h_{oe} = 12 \times 10^{-6} \text{ mhos}$$

The total load on Q_2 is the load resistor (3 K), the load of the feedback network (set at 50 K), and the coil loss resistance (35 K) all in parallel, constituting a load of 2.6 K. Using the parameters for $I_e = 3 \text{ MA}$ and $R_T = 2.6 \text{ K}$ gives the second stage gain:

$$G_{p2} = 15,000$$

and

$$R_{in} \text{ (transistor alone)} = 1.9 \text{ K}$$

The actual input resistance of the second stage consists of R_{in} in parallel with 7.5 K and 33 K (6.1 K) giving: $R_{in} \text{ (actual)} = 1.3 \text{ K}$

This additional input load reduces the total gain of the second stage by a

factor of $\frac{R}{R + R_{in} \text{ (transistor)}}$, where R is the total resistance in parallel with R_{in} (transistor). Therefore, $G'_{p2} = 0.76 \times 15,000 = 11,000$

Using $R_{in} \text{ (actual)}$ as the load of Q_1 and the parameters for $I_e = 0.4 \text{ MA}$ gives a first stage gain:

$$G_{p1} = 430$$

and

$$R_{in} \text{ (transistor)} = 9.7 \text{ K}$$

Combining this with the biasing network (11.6 K) gives:

$$R_{in} \text{ (actual)} = 5.3 \text{ K}$$

and

$$G'_{p1} = 230$$

The total power gain is:

$$G_p = 11,000 \times 230 = 2.5 \times 10^6$$

which corresponds to a loop voltage gain:

$$G_V = \sqrt{G_P} = 1600$$

For a loop voltage gain of 1.4 (corresponding to a loop power gain of 2), the voltage attenuation of the feedback network is:

$$A_V = \frac{1600}{1.4} = 1150$$

The attenuation ratio of the crystal-transistor input portion of the network is fixed ($R_{in} = 5.3 \text{ K}$, $R_{r \text{ max}} = 200 \text{ K}$); that is:

$$A_C = \frac{205}{5.3} = 39$$

The attenuation required of the feedback resistive divider is therefore:

$$A_R = \frac{1150}{39} = 30$$

The value of A_R used was nominally 26 (51 K and 2 K).

The coil tuning capacitance required was 0.23 UF.

DESIGN EVALUATION DATA, 1-KC TWO-STAGE TRANSISTOR OSCILLATOR

Nominal $V_o = 7.2V$, Oscillator Frequency = 999.94 CPS

EFFECT OF	CHANGE	TEST CONDITIONS
$\pm 10\%$ Change of B+ on Oscillator Frequency	≤ 3 PPM	$R_L = 3K, T_A \approx 25^\circ C$
$\pm 10\%$ Change of B+ on Output Voltage	$\Delta V_o = \pm 8\%$	$R_L = 3K, T_A \approx 25^\circ C$
$\pm 10\%$ Change in R_L on Oscillator Frequency	≤ 3 PPM	$E_{cc} = 28V, T_A \approx 25^\circ C$
$\pm 10\%$ Change in R_L on Output Voltage	$\Delta V_o = \pm 5\%$	$E_{cc} = 28V, T_A \approx 25^\circ C$
$-50^\circ C$ to $+80^\circ C$ Change in T_A on Oscillator Frequency	± 50 PPM	$E_{cc} = 28V, R_L = 3K$
$-50^\circ C$ to $+80^\circ C$ Change in T_A on Output Voltage	$\Delta V_o = \pm 3\%$	$E_{cc} = 28V, R_L = 3K$

APPENDIX N

3-KC TWO-STAGE TRANSISTOR OSCILLATOR (TUNED OUTPUT)

This circuit is similar to the oscillator evaluated in Appendix M. The sole difference is in the tuned circuit elements.

At this frequency the inductor had a Q of 150 which resulted in less loading than in the 1 KC design. However, since the loading was already negligible in the latter design, this had no effect on the calculations. The value of tuning capacitor required was 0.026 UF.

The comments made concerning the 1 KC oscillator of this type are equally applicable to this oscillator.

3-KC TWO-STAGE TRANSISTOR OSCILLATOR (TUNED OUTPUT)

Oscillator Design and Evaluation Sheet

Active Element: Transistor

Manufacturer's Type No.: 2N336

Crystal Used

Resonant Frequency

Resonance Resistance

T-9XY

2999.6 CPS

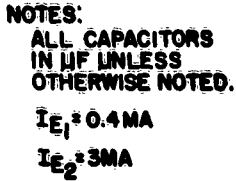
50 Kilohms

Description of Oscillator Type

Crystal: Series

Active element configuration: Common Emitter

Feedback transformer configuration: Resistive Divider



N-2

DESIGN EVALUATION DATA, 3-KC TWO-STAGE TRANSISTOR OSCILLATOR

Nominal $V_o = 7.4V$; Oscillator Frequency = 2999.63 CPS

EFFECT OF	CHANGE	TEST CONDITIONS
$\pm 10\%$ Change of B+ on Oscillator Frequency	≤ 3 PPM	$R_L = 3K, T_A \approx 25^\circ C$
$\pm 10\%$ Change of B+ on Output Voltage	$\Delta V_o = \pm 1\%$	$R_L = 3K, T_A \approx 25^\circ C$
$\pm 10\%$ Change in R_L on Oscillator Frequency	≤ 3 PPM	$E_{cc} = 28V, T_A \approx 25^\circ C$
$\pm 10\%$ Change in R_L on Output Voltage	$\Delta V_o = \pm 6\%$	$E_{cc} = 28V, T_A \approx 25^\circ C$
$-50^\circ C$ to $+80^\circ C$ Change in T_A on Oscillator Frequency	± 115 PPM	$E_{cc} = 28V, R_L = 3K$
$-50^\circ C$ to $+80^\circ C$ Change in T_A on Output Voltage	$\Delta V_o < \pm 2\%$	$E_{cc} = 28V, R_L = 3K$

APPENDIX O

3-KC TUNED OUTPUT TRANSISTOR OSCILLATOR

Object:

The circuits of the two-stage oscillators are rather complex, and the object of this design was to simplify the oscillator circuit.

Design Details:

Calculation showed that the major design problem would be in obtaining sufficient output voltage limiting to prevent crystal overdrive. The major cause of this problem was the lower power gain of the single-stage amplifier compared to that of the two-stage amplifier. The first method used to limit the output voltage swing was to bias the transistor for a $V_{ce} = 2V$, thereby limiting the operating voltage range. This alone was inadequate for a value of $R_T = 20 K$ (the assumed minimum value), due to the relatively large energy storage capability of the π network inductor, and it was necessary to limit the positive collector voltage swing with a zener diode connected between emitter and collector.

To prevent undue loading of the oscillator by the B+ feed resistor, this resistor was connected to the low impedance side of the π network. The effective load of this resistor appearing in parallel with the oscillator load at the collector of the transistor was approximately 220 K, due to the impedance transforming action of the π network. The output power lost in this resistor is therefore less than 10 percent.

Conclusions:

This oscillator has good operating characteristics as shown in the evaluation data, the major disadvantage being its low power output capability of 0.2 MW.

3-KC TUNED OUTPUT TRANSISTOR OSCILLATOR

Oscillator Design and Evaluation Sheet

Active Element:	<u>Transistor</u>	Manufacturer's Type No.:	<u>2N336</u>
Crystal Used	Resonant Frequency	Resonance Resistance	
<u>T-9XY</u>	<u>2999.6 CPS</u>	<u>50 Kilohms</u>	
Description of Oscillator Type			
Crystal: <u>Series</u>			
Active element configuration: <u>Common Emitter</u>			
Feedback transformer configuration: <u>PI Network</u>			

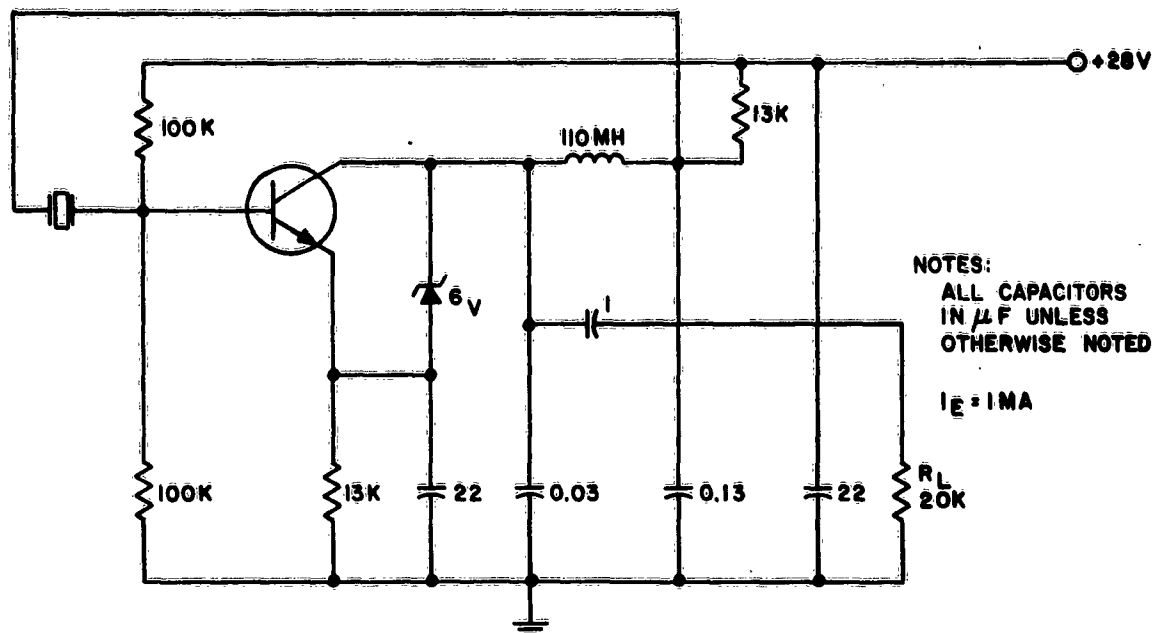


Figure O-1. 3-KC Single-Stage Transistor Oscillator

Details of Design Calculations

Using the notation and equations of the Final Report, the calculations are as follows:

For $I_E = 1\text{MA}$, $V_{CE} = 5\text{V}$, the parameters of the 2N336 are:

$$h_{ie} = 5.5 \times 10^3 \text{ ohms}$$

$$h_{re} = 1400 \times 10^{-6}$$

$$h_{fe} = 100$$

$$h_{oe} = 24 \times 10^{-6} \text{ mhos}$$

which, for $R_T = 17\text{K}$ gives:

$$G_p = 22,000$$

$$R_{in} = 3.8\text{K}$$

The total input resistance consists of 3.8 K and the two 100 K biasing resistors in parallel; that is, 3.6 K. The biasing network resistance R_b reduces the gain to:

$$G_p \times \frac{R_b}{R_b + R_{in}} = 20,000$$

$$R_{T \max} = 200 \text{ K and } R_s = 204 \text{ K}$$

and therefore:

$$G'_p = G_p \cdot \frac{R_{in}}{R_s} = 350$$

or

$$\frac{G'_p}{2} = 175$$

$$R_{FB} = \frac{G'_p}{2} \times R_T = 3 \text{ MEGOHM}$$

Therefore, the transformation ratio is:

$$T_r = \frac{R_{FB}}{R_s} = 15$$

The voltage transformation ratio is:

$$T_v = \sqrt{\frac{R_{FB}}{R_s}} = 4$$

The coil to be used had $L = 110 \text{ MH}$, and $r_L = 13 \text{ ohms}$ at 3 KC, giving:

$$X_L = 2100 \text{ ohms}$$

Ignoring loading (justified below):

$$\frac{X_L}{X_C} = T_v + 1 = 5 \tag{1}$$

where X_C is the reactance of the capacitance in the impedance transforming leg of the π network. Therefore:

$$X_C = 420 \text{ ohms}$$

Comparing X_C with R_s in parallel with the 13-K resistor supplying B+ shows that the phase error will be less than 2 degrees and loading can be ignored. Also r'_s , the series equivalent of the load, will be approximately 14 ohms.

$$X_{L_{eff}} = X_L - X_C = 1700 \text{ ohms}$$

$$\phi_I = \tan^{-1} \frac{X_{L_{eff}}}{r_L + r'_s}$$

$$\phi_I < 1 \text{ degree}$$

Since loading effects are negligible, Equation (1) is justified. Therefore:

$$C = \frac{1}{\omega X_C} = 0.13 \text{ UF}$$

The value of the tuning capacitor is given by:

$$C_T = \frac{1}{\omega X_{L_{eff}}} = 0.031 \text{ UF}$$

Feedback Phase Shift for $R_T = R_T \text{ min}$

It is shown previously that for $R_T = 200 \text{ K}$, the feedback phase shift will be less than 3 degrees. If this network is then used with a crystal with $R_T = 20 \text{ K}$ (lowest R_T value likely to occur), this phase shift may increase. R_s and the 13 K resistor in parallel gives a total secondary load of 8.5 K. Using the parallel to series transforms, C and R_s in parallel transform to:

$$r'_s = 8,500 \left(\frac{1}{1 + Q^2} \right)$$

$$= 21 \text{ ohms}$$

$$X_{C'} = X_C \frac{Q^2}{1 + Q^2} \approx X_C = 420 \text{ ohms}$$

$$\text{Therefore } \phi_{V_o} = \tan^{-1} \frac{X_C}{r'_s} \approx 87 \text{ degrees}$$

$$\phi_I = \tan^{-1} \frac{X_{L_{eff}}}{r_L + r'_s} = \tan^{-1} 50 > 89 \text{ degrees}$$

$$\text{Phase error} = 180 - \phi_I = \phi_{V_0} \approx 3 \text{ degrees}$$

Maximum crystal dissipation will occur for $R_T = 20 \text{ K}$ (the assumed minimum value), and the permissible output voltage is determined as follows:

For a maximum crystal dissipation of 10 UW, the permissible feedback power P_{FB} for $R_{in} = 3.6 \text{ K}$ will be 12 UW. Therefore, the output voltage of the π network must not exceed a value of:

$$V = \sqrt{P_{FB} \times R_{s \text{ min}}} = 0.53 \text{ VRMS}$$

$$\text{and } V_0 \text{ max} = V \times T_V$$

$$= 2.2 \text{ VRMS}$$

The load presented to the transistor by the 13 K resistor supplying B+ when transformed through the π network is:

$$T_T \times 13,000 = 220 \text{ K}$$

Therefore, for $R_T = 17 \text{ K}$, R_L is required to be 19 K.

A value of 20 K was used for R_L .

DESIGN EVALUATION DATA, 3-KC TUNED OUTPUT TRANSISTOR OSCILLATOR

Nominal $V_0 = 2.2V$; Oscillator Frequency = 2999.60 CPS

EFFECT OF	CHANGE	TEST CONDITIONS
$\pm 10\%$ Change of B+ on Oscillator Frequency	≤ 3 PPM	$R_L = 20K, T_A \approx 25^\circ C$
$\pm 10\%$ Change of B+ on Output Voltage	$\Delta V_0 = \pm 3\%$	$R_L = 20K, T_A \approx 25^\circ C$
$\pm 10\%$ Change in R_L on Oscillator Frequency	≤ 3 PPM	$E_{cc} = 28V, T_A \approx 25^\circ C$
$\pm 10\%$ Change in R_L on Output Voltage	$\Delta V_0 < 2\%$	$E_{cc} = 28V, T_A \approx 25^\circ C$
-50°C to +80°C Change in T_A on Oscillator Frequency	± 145 PPM	$E_{cc} = 28V, R_L = 20K$
-50°C to +80°C Change in T_A on Output Voltage	$\Delta V_0 = \pm 13\%$	$E_{cc} = 28V, R_L = 20K$

APPENDIX P

20-KC TUNED-OUTPUT TRANSISTOR OSCILLATOR

This oscillator is similar to that of Appendix O, the major difference being in the biasing arrangement. Because of the increased feedback efficiency and power dissipation of this type of crystal ($R_r \text{ max} = 100 \text{ K}$, $P_c = 0.1 \text{ MW}$), the output voltage limiting requirements are less stringent. In this particular design, V_{ce} was 4 volts, and no additional limiting was required.

This oscillator could also have been designed with the collector biasing resistor in the low impedance side of the π network. If the same inductor (34 MH) was used it would then be necessary to increase R_L to give additional gain. The reason for this is that the departure of ϕV_o from 90° for the π network used in the present design would be further increased by the additional loading. This is undesirable, and the only means of reducing this phase error is by decreasing X_c ; that is, increasing T_r . This, in turn, requires increased gain. Alternatively, a lower value of inductance could be used.

20-KC TUNED-OUTPUT TRANSISTOR OSCILLATOR

Oscillator Design and Evaluation Sheet

Active Element: Transistor

Manufacturer's Type No.: 2N336

Crystal Used

Resonant Frequency

Resonance Resistance

CR-50/U

20,403.0 CPS

14,000 ohms

Description of Oscillator Type

Crystal: Series

Active element configuration: Grounded Emitter

Feedback transformer configuration: Pi Network

Details of Design Calculations

Using the notation and equations of the Final Report, the calculations are as follows:

For $I_e = 1 \text{ MA}$, $V_{ce} = 5 \text{ V}$, the parameters of the 2N336 are:

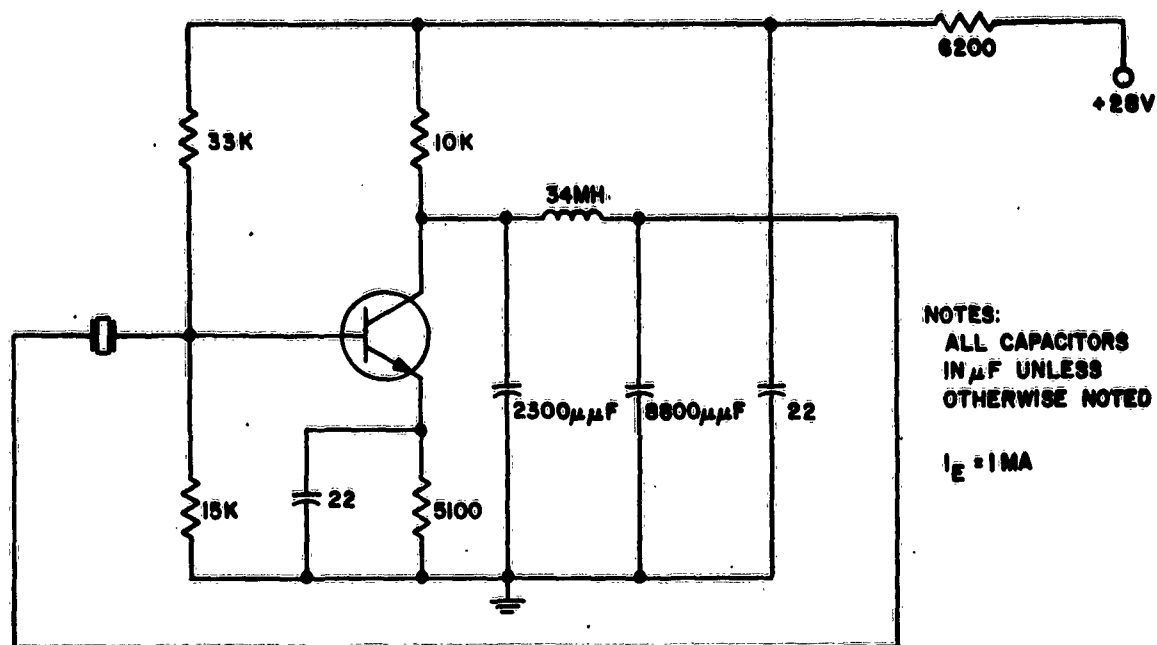


Figure P-1. 20-KC Single-Stage Transistor Oscillator

$$h_{ie} = 5.5 \times 10^3 \text{ ohms}$$

$$h_{re} = 1400 \times 10^{-6}$$

$$h_{fe} = 100$$

$$h_{oe} = 24 \times 10^{-6} \text{ ohms}$$

which, for $R_T = 10 \text{ K}$ gives:

$$G_p = 14,000$$

$$R_{in} = 4.4 \text{ K}$$

The total input resistance consists of 4.4 K and the two biasing resistors in parallel; that is, 3.1 K. The biasing network resistance $R_b = 10 \text{ K}$ reduces the gain to:

$$G_p \times \frac{R_b}{R_b + R_{in}} = 10,700$$

$$R_T \text{ max} = 100 \text{ K and } R_S = 103 \text{ K}$$

Therefore:

$$G'_p = G_p \cdot \frac{R_{in}}{R_S} = 320$$

or $\frac{G'_p}{2} = 160$

$$R_{FB} = \frac{G'_p}{2} \times R_T = 1.6 \text{ MEGO}$$

Therefore, the transformation ratio is:

$$T_r = \frac{R_{FB}}{R_S} = 15$$

The voltage transformation ratio is:

$$T_V = \sqrt{\frac{R_{FB}}{R_S}} = 3.9$$

The coil to be used had $L = 34 \text{ MH}$, $r_L = 4 \text{ ohms}$ at 20.4 KC giving:

$$X_L = 4350 \text{ ohms}$$

Ignoring loading (justified below):

$$\frac{X_L}{X_C} = T_V + 1 = 4.9 \quad (1)$$

where X_C is the reactance of the capacitance in the impedance transforming leg of the π network. Therefore:

$$X_C = 890 \text{ ohms}$$

Comparing X_C with R_S shows that the phase error will be less than 1 degree and loading can be ignored. Also, r'_s will be approximately 8 ohms.

$$X_{Leff} = X_L - X_C = 3460 \text{ ohms}$$

$$\phi_I = \tan^{-1} \frac{X_{Leff}}{r_L + r'_s} = 88 \text{ degrees}$$

Since loading effects are negligible, Equation (1) is justified. Therefore:

$$C = 8800 \text{ UUF}$$

The value of the tuning capacitor is given by:

$$C_T = \frac{1}{\omega \cdot X_{L_{\text{eff}}}} = 2260 \text{ UUF}$$

Feedback Phase Shift for $R_T = R_T \text{ min}$

It is shown previously that for $R_T = 100 \text{ K}$, the feedback phase shift will be less than 3 degrees. If this network is then used with a crystal with $R_T = 10 \text{ K}$ (lowest R_T value likely to occur), this phase shift may increase. ($R_s = 13 \text{ K}$.) Using the parallel-to-series transforms, C and R_s in parallel transform to:

$$r'_s = 61 \text{ ohms}$$

$$X_c' = \approx X_c$$

Therefore $\phi_{V_o} = 86 \text{ degrees}$

$$\phi_I = 89 \text{ degrees}$$

Phase error = 5 degrees

Maximum crystal dissipation will occur for $R_T = 10 \text{ K}$ (the assumed minimum value), and the permissible output voltage is determined as follows:

For a maximum crystal dissipation of 100 UW, the permissible feedback power P_{FB} for $R_{in} = 3.1 \text{ K}$ will be 130 UW. Therefore, the output voltage of the π network must not exceed a value of:

$$V = \sqrt{P_{FB} \times R_{s \text{ min}}} = 1.3 \text{ VRMS}$$

$$\text{and } V_{o \text{ max}} = V \times T_v$$

$$= 5.1 \text{ VRMS}$$

DESIGN EVALUATION DATA, 20-KC TUNED-OUTPUT TRANSISTOR OSCILLATOR

Nominal $V_o = 5.3$ V; Oscillator Frequency = 20,403.0 CPS

EFFECT OF	CHANGE	TEST CONDITIONS
$\pm 10\%$ Change in B+ on Oscillator Frequency	≤ 3 PPM	$R_L = 10K, T_A \approx 25^\circ C$
$\pm 10\%$ Change in B+ on Output Voltage	$\Delta V_o = \pm 3\%$	$R_L = 10K, T_A \approx 25^\circ C$
$\pm 10\%$ Change in R_L on Oscillator Frequency	≤ 3 PPM	$E_{cc} = 28V, T_A \approx 25^\circ C$
$\pm 10\%$ Change in R_L on Output Voltage	$\Delta V_o = < 2\%$	$E_{cc} = 28V, T_A \approx 25^\circ C$
-50°C to +80°C Change in T_A on Oscillator Frequency	± 85 PPM	$E_{cc} = 28V, R_L = 10K$
-50°C to +80°C Change in T_A on Output Voltage	$\Delta V_o = \pm 10\%$	$E_{cc} = 28V, R_L = 10K$

AD _____ DIV. _____	UNCLASSIFIED
<p>The Magnavox Company, Fort Wayne, Indiana QUARTZ CRYSTAL OSCILLATOR CIRCUITS - H. R. Meadows and D. Firth Final Engineering Report, 1 July 1961 to 30 June 1962:204P. incl illus., tables, 9 refs. (Contract DA36-039 SC-88892) DA Project No. 3G-26-05-001</p> <p>Unclassified report</p> <p>This Final Engineering Report presents extensive data supporting the design and operation of quartz crystal oscillators. Design procedures are developed for high and low frequency oscillator circuits in the 1-KC to 200-MC range. Vacuum tubes and transistors were studied in both the low and high frequency ranges (1-KC to 800-KC and 30-MC to 200-MC).</p> <p>The report includes a general discussion of the properties of quartz crystals, the characteristics of tubes and transistors, and impedance transforming networks. The general analysis of an oscillator is presented, a general design specification is developed, and a basic design procedure is established.</p> <p>Separate sections are devoted to design procedures for high-frequency and low-frequency crystal oscillators. The report concludes with a design data section containing the results of oscillator evaluations during the program period.</p>	<p>1. Quartz Crystals 2. Electron Tubes 3. Transistors</p> <p>I. U.S. Army Electronics Research and Development Laboratory Contract No. DA-36-039 SC-88892</p> <p>II. Armed Services Technical Information Agency</p>

AD _____ DIV. _____	UNCLASSIFIED
<p>The Magnavox Company, Fort Wayne, Indiana QUARTZ CRYSTAL OSCILLATOR CIRCUITS - H. R. Meadows and D. Firth Final Engineering Report, 1 July 1961 to 30 June 1962:204P. incl illus., tables, 9 refs. (Contract DA36-039 SC-88892) DA Project No. 3G-26-05-001</p> <p>Unclassified report</p> <p>This Final Engineering Report presents extensive data supporting the design and operation of quartz crystal oscillators. Design procedures are developed for high and low frequency oscillator circuits in the 1-KC to 200-MC range. Vacuum tubes and transistors were studied in both the low and high frequency ranges (1-KC to 800-KC and 30-MC to 200-MC).</p> <p>The report includes a general discussion of the properties of quartz crystals, the characteristics of tubes and transistors, and impedance transforming networks. The general analysis of an oscillator is presented, a general design specification is developed, and a basic design procedure is established.</p> <p>Separate sections are devoted to design procedures for high-frequency and low-frequency crystal oscillators. The report concludes with a design data section containing the results of oscillator evaluations during the program period.</p>	<p>1. Quartz Crystals 2. Electron Tubes 3. Transistors</p> <p>I. U.S. Army Electronics Research and Development Laboratory Contract No. DA-36-039 SC-88892</p> <p>II. Armed Services Technical Information Agency</p>

AD _____ DIV. _____	UNCLASSIFIED
<p>The Magnavox Company, Fort Wayne, Indiana QUARTZ CRYSTAL OSCILLATOR CIRCUITS - H. R. Meadows and D. Firth Final Engineering Report, 1 July 1961 to 30 June 1962:204P. incl illus., tables, 9 refs. (Contract DA36-039 SC-88892) DA Project No. 3G-26-05-001</p> <p>Unclassified report</p> <p>This Final Engineering Report presents extensive data supporting the design and operation of quartz crystal oscillators. Design procedures are developed for high and low frequency oscillator circuits in the 1-KC to 200-MC range. Vacuum tubes and transistors were studied in both the low and high frequency ranges (1-KC to 800-KC and 30-MC to 200-MC).</p> <p>The report includes a general discussion of the properties of quartz crystals, the characteristics of tubes and transistors, and impedance transforming networks. The general analysis of an oscillator is presented, a general design specification is developed, and a basic design procedure is established.</p> <p>Separate sections are devoted to design procedures for high-frequency and low-frequency crystal oscillators. The report concludes with a design data section containing the results of oscillator evaluations during the program period.</p>	<p>1. Quartz Crystals 2. Electron Tubes 3. Transistors</p> <p>I. U.S. Army Electronics Research and Development Laboratory Contract No. DA-36-039 SC-88892</p> <p>II. Armed Services Technical Information Agency</p>

AD _____ DIV. _____	UNCLASSIFIED
<p>The Magnavox Company, Fort Wayne, Indiana QUARTZ CRYSTAL OSCILLATOR CIRCUITS - H. R. Meadows and D. Firth Final Engineering Report, 1 July 1961 to 30 June 1962:204P. incl illus., tables, 9 refs. (Contract DA36-039 SC-88892) DA Project No. 3G-26-05-001</p> <p>Unclassified report</p> <p>This Final Engineering Report presents extensive data supporting the design and operation of quartz crystal oscillators. Design procedures are developed for high and low frequency oscillator circuits in the 1-KC to 200-MC range. Vacuum tubes and transistors were studied in both the low and high frequency ranges (1-KC to 800-KC and 30-MC to 200-MC).</p> <p>The report includes a general discussion of the properties of quartz crystals, the characteristics of tubes and transistors, and impedance transforming networks. The general analysis of an oscillator is presented, a general design specification is developed, and a basic design procedure is established.</p> <p>Separate sections are devoted to design procedures for high-frequency and low-frequency crystal oscillators. The report concludes with a design data section containing the results of oscillator evaluations during the program period.</p>	<p>1. Quartz Crystals 2. Electron Tubes 3. Transistors</p> <p>I. U.S. Army Electronics Research and Development Laboratory Contract No. DA-36-039 SC-88892</p> <p>II. Armed Services Technical Information Agency</p>

AD _____ DNV _____	UNCLASSIFIED
<p>The Magnavox Company, Fort Wayne, Indiana QUARTZ CRYSTAL OSCILLATOR CIRCUITS - H. R. Meadows and D. Firth Final Engineering Report, 1 July 1961 to 30 June 1962:204P. Incl illus., tables, 9 refs. (Contract DA36-039 SC-88892) DA Project No. 3G-26-05-001</p> <p style="text-align: center;">Unclassified report</p> <p>This Final Engineering Report presents extensive data supporting the design and operation of quartz crystal oscillators. Design procedures are developed for high and low frequency oscillator circuits in the 1-KC to 200-MC range. Vacuum tubes and transistors were studied in both the low and high frequency ranges (1-KC to 800-KC and 30-MC to 200-MC).</p> <p>The report includes a general discussion of the properties of quartz crystals, the characteristics of tubes and transistors, and impedance transforming networks. The general analysis of an oscillator is presented, a general design specification is developed, and a basic design procedure is established.</p> <p>Separate sections are devoted to design procedures for high-frequency and low-frequency crystal oscillators. The report concludes with a design data section containing the results of oscillator evaluations during the program period.</p>	1. Quartz Crystals 2. Electron Tubes 3. Transistors I. U.S. Army Electronics Research and Development Laboratory Contract No. DA-36-039 SC-88892 Armed Services Technical Information Agency

AD _____ DNV _____	UNCLASSIFIED
<p>The Magnavox Company, Fort Wayne, Indiana QUARTZ CRYSTAL OSCILLATOR CIRCUITS - H. R. Meadows and D. Firth Final Engineering Report, 1 July 1961 to 30 June 1962:204P. Incl illus., tables, 9 refs. (Contract DA36-039 SC-88892) DA Project No. 3G-26-05-001</p> <p style="text-align: center;">Unclassified report</p> <p>This Final Engineering Report presents extensive data supporting the design and operation of quartz crystal oscillators. Design procedures are developed for high and low frequency oscillator circuits in the 1-KC to 200-MC range. Vacuum tubes and transistors were studied in both the low and high frequency ranges (1-KC to 800-KC and 30-MC to 200-MC).</p> <p>The report includes a general discussion of the properties of quartz crystals, the characteristics of tubes and transistors, and impedance transforming networks. The general analysis of an oscillator is presented, a general design specification is developed, and a basic design procedure is established.</p> <p>Separate sections are devoted to design procedures for high-frequency and low-frequency crystal oscillators. The report concludes with a design data section containing the results of oscillator evaluations during the program period.</p>	1. Quartz Crystals 2. Electron Tubes 3. Transistors I. U.S. Army Electronics Research and Development Laboratory Contract No. DA-36-039 SC-88892 Armed Services Technical Information Agency

AD _____ DNV _____	UNCLASSIFIED
<p>The Magnavox Company, Fort Wayne, Indiana QUARTZ CRYSTAL OSCILLATOR CIRCUITS - H. R. Meadows and D. Firth Final Engineering Report, 1 July 1961 to 30 June 1962:204P. Incl illus., tables, 9 refs. (Contract DA36-039 SC-88892) DA Project No. 3G-26-05-001</p> <p style="text-align: center;">Unclassified report</p> <p>This Final Engineering Report presents extensive data supporting the design and operation of quartz crystal oscillators. Design procedures are developed for high and low frequency oscillator circuits in the 1-KC to 200-MC range. Vacuum tubes and transistors were studied in both the low and high frequency ranges (1-KC to 800-KC and 30-MC to 200-MC).</p> <p>The report includes a general discussion of the properties of quartz crystals, the characteristics of tubes and transistors, and impedance transforming networks. The general analysis of an oscillator is presented, a general design specification is developed, and a basic design procedure is established.</p> <p>Separate sections are devoted to design procedures for high-frequency and low-frequency crystal oscillators. The report concludes with a design data section containing the results of oscillator evaluations during the program period.</p>	1. Quartz Crystals 2. Electron Tubes 3. Transistors I. U.S. Army Electronics Research and Development Laboratory Contract No. DA-36-039 SC-88892 Armed Services Technical Information Agency

AD _____ DNV _____	UNCLASSIFIED
<p>The Magnavox Company, Fort Wayne, Indiana QUARTZ CRYSTAL OSCILLATOR CIRCUITS - H. R. Meadows and D. Firth Final Engineering Report, 1 July 1961 to 30 June 1962:204P. Incl illus., tables, 9 refs. (Contract DA36-039 SC-88892) DA Project No. 3G-26-05-001</p> <p style="text-align: center;">Unclassified report</p> <p>This Final Engineering Report presents extensive data supporting the design and operation of quartz crystal oscillators. Design procedures are developed for high and low frequency oscillator circuits in the 1-KC to 200-MC range. Vacuum tubes and transistors were studied in both the low and high frequency ranges (1-KC to 800-KC and 30-MC to 200-MC).</p> <p>The report includes a general discussion of the properties of quartz crystals, the characteristics of tubes and transistors, and impedance transforming networks. The general analysis of an oscillator is presented, a general design specification is developed, and a basic design procedure is established.</p> <p>Separate sections are devoted to design procedures for high-frequency and low-frequency crystal oscillators. The report concludes with a design data section containing the results of oscillator evaluations during the program period.</p>	1. Quartz Crystals 2. Electron Tubes 3. Transistors I. U.S. Army Electronics Research and Development Laboratory Contract No. DA-36-039 SC-88892 Armed Services Technical Information Agency

DISTRIBUTION LIST FOR FINAL REPORT AND DESIGN DATA SHEETS

CONTRACT DA36-039 SC-88892

CONTRACTOR The Magnavox Company

DATE 26 November 1962

<u>TO</u>	<u>CYS</u>	<u>TO</u>	<u>CYS</u>
OASD (R&E), Room 3E1065 ATTN: Technical Library The Pentagon Washington 25, D. C.	1	Commander Aeronautical Systems Division ATTN: ASNPVE-2, Mr. E. Borgelt Wright-Patterson AFB, Ohio	1
Commanding General U. S. Army Electronics Command ATTN: AMSEL-RD Fort Monmouth, New Jersey	1	Commander Aeronautical Systems Division ATTN: ASAPRL Wright-Patterson AFB, Ohio	1
Commanding General U. S. Army Electronics Command ATTN: AMSEL-RD-4 Fort Monmouth, New Jersey	1	Commander Rome Air Development Center ATTN: RAALD Griffiss AFB, New York	1
Director U. S. Naval Research Laboratory ATTN: Code 2027 Washington 25, D. C.	1	Chief U. S. Army Security Agency Arlington Hall Station Arlington 12, Virginia	2
Commanding Officer & Director U. S. Navy Electronics Laboratory San Diego 52, California	1	Deputy President U. S. Army Security Agency Board Arlington Hall Station Arlington 12, Virginia	1
Chief, Bureau of Ships ATTN: Code 690B, Mr. R. B. McDowell Department of the Navy Washington 25, D. C.	1	Commander Armed Services Technical Information Agency ATTN: TIPCR Arlington Hall Station Arlington 12, Virginia	10
Commander Wright Air Development Division ATTN: WCLNE, Mr. C. Friend Wright-Patterson AFB, Ohio	1		

DISTRIBUTION LIST (Cont)

SC-88892

<u>TO</u>	<u>CYS</u>	<u>TO</u>	<u>CYS</u>
National Bureau of Standards		ATTN: SELRA/DE	1
Boulder Laboratories			
ATTN: Mr. W.D. George		ATTN: SELRA/ADT	1
Boulder, Colorado	1	ATTN: SELRA/PF, Technical Staff	
		(Record Copy)	1
Commander		ATTN: SELRA/TN	3
Air Force Cambridge Research		ATTN: SELRA/PF, Dr. E.A.	
Laboratories		Gerber	1
ATTN: CRXL-R			
L. G. Hanscom Field		ATTN: SELRA/PFP, Miss M.	
Bedford, Massachusetts	1	Herberg	3
		ATTN: SELRA/NRC, Mr. E.	
Commander		Jakubowics	1
Air Force Command & Control Develop-		ATTN: SELRA/SRI, Mr. R. J. Lukas	
ment Division		(Evans Area)	1
ATTN: CRZC		ATTN: SELRA/PFP, Mr. S.	
L. G. Hanscom Field		Schodowski	63
Bedford, Massachusetts	1		
		Commanding Officer	
Commander		U.S. Army Electronics Material	
Air Force Command & Control Develop-		Support Agency	
ment Division		ATTN: SELMA/ADJ	
ATTN: CCRR and CCSD		Fort Monmouth, New Jersey	1
L. G. Hanscom Field			
Bedford, Massachusetts	2	National Aeronautics & Space	
		Administration	
AFSC Liaison Officer		Goddard Space Flight Center	
Naval Air R&D Activities Command		ATTN: Dr. R. Stampfl	
Johnsville, Pennsylvania	1	Greenbelt, Maryland	1
Commanding Officer			
U.S. Army Electronics R&D			
Laboratory			
ATTN: SELRA/LNF			
Fort Monmouth, New Jersey	1		
ATTN: SELRA/LNE	1		
ATTN: SELRA/LNR	1		

DISTRIBUTION LIST (Cont)

SC-88892

<u>TO</u>	<u>CYS</u>	<u>TO</u>	<u>CYS</u>
ARF Products, Inc. 7627 Lake Street River Forest, Illinois ATTN: Mr. A. Przedpelski	1	Delco Radio Division General Motors Corporation 700 East Firmin Street Kokomo, Indiana	1
Bell Telephone Laboratories, Inc. Allentown, Pennsylvania ATTN: Mr. Roger A. Sykes	1	Electromagnetic Technology Corp. 1375 California Avenue Palo Alto, California ATTN: Mr. William Edson	1
Bendix Systems Division Communications Department 3300 Plymouth Road Ann Arbor, Michigan ATTN: Mr. V. Hutton	1	Frequency Electronics Inc. 22-60 46th Street Astoria, New York ATTN: Mr. Martin Bloch	1
Bliley Electric Company Union Station Building Erie, Pennsylvania ATTN: Mr. John Wolfskill	1	Frontier Electronics Co. 4600 Memphis Avenue Cleveland 9, Ohio ATTN: Mr. Patrick Lannan	1
Dr. Virgil E. Bottom McMurry College Abilene, Texas	1	General Dynamics/Pomona Guidance Design Group 252 Mail Zone 6-65, Box 1011 Pomona, California ATTN: Mr. George E. Stanley	1
Bulova Watch Company Electronics Division 61-10 Woodside Avenue Woodside 77, New York ATTN: Mr. John L. Denman	1	General Electric Co. Defense Electronics Div. Syracuse, New York	1
Collins Radio Company Cedar Rapids, Iowa	1	General Electric Co. Communications Prods. Dept. Mountainview Road Lynchburg, Virginia ATTN: Mr. John Sherman	1
Crosley Division AVCO Corporation 1329 Arlington Street Cincinnati 25, Ohio	1	Hoffman Electronics Corp. 3761 S. Hill Street Los Angeles 7, California	1

DISTRIBUTION LIST (Cont)

SC-88892

<u>TO</u>	<u>CYS</u>	<u>TO</u>	<u>CYS</u>
ITT Laboratories 500 Washington Avenue Nutley, New Jersey	1	Midland Manufacturing Co. 3155 Fiberglas Road Kansas City, Kansas	1
ITT Laboratories 492 River Road Nutley, New Jersey ATTN: Mr. E. Neugroschel, Dept. 722-12	1	Motorola, Inc. Communications Division 1450 No. Cicero Avenue Chicago 51, Illinois ATTN: Mr. P. Richardson	1
Jansky & Bailey, Inc. 1339 Wisconsin Avenue Washington 7, D. C.	1	National Company 61 Sherman Street Malden 48, Massachusetts	1
Keystone Electronics Co. 65 Seventh Avenue Newark, New Jersey ATTN: Mr. James Ronan	1	New Mexico State University Engineering Experiment Station Las Cruces, New Mexico ATTN: Mr. William McSpadden	1
The James Knights Co. 131 South Wells Street Sandwich, Illinois ATTN: Mr. M. J. Silver	1	New York University University Heights New York, New York ATTN: Mr. Frank Bloom	1
Manson Laboratories, Inc. 375 Fairfield Avenue Stamford, Connecticut ATTN: Mr. J. Guttman	1	Philco Corporation Government & Industrial Group 4700 Wissahickon Avenue Philadelphia, Pennsylvania	1
McCoy Electronics Co. Mount Holly Springs Pennsylvania ATTN: Mr. L. McCoy	1	Pioneer-Central Division of Bendix Corporation Davenport, Iowa ATTN: Dr. D. E. Newell	1
Melpar, Inc. 3000 Arlington Blvd. Falls Church, Virginia	1		

DISTRIBUTION LIST (Cont)

SC-88892

<u>TO</u>	<u>CYS</u>	<u>TO</u>	<u>CYS</u>
Polartron, Inc. 422 Morris Avenue Long Branch, New Jersey ATTN: Mr. H. D. Tanzman	1	Raytheon Company 1089 Washington Street New Newton, Massachusetts	1
Radio Corporation of America Front & Cooper Streets Camden, New Jersey ATTN: Mr. M. Lysobey	1	Reeves-Hoffman Division Cherry & North Streets Carlisle, Pennsylvania ATTN: Mr. George Spease	1
Strand Engineering Co. Box 76 Ann Arbor, Michigan ATTN: Mr. W. Casto	1	Scientific Radio Products, Inc. 2303 West 8th Street Loveland, Colorado	1
Systems Incorporated 2400 Diversified Way Orlando, Florida ATTN: Dr. W. H. Horton	1	Sylvania Electric Corporation 1100 Wehrle Drive Buffalo, New York ATTN: Mr. E. R. Moss, Dept. 14	1
Valpey Crystal Company 1244 Highland Street Holliston, Massachusetts ATTN: Mr. T. Valpey	1	Westinghouse Corporation Air-Arm Division P. O. Box 746 Baltimore 3, Maryland	1
Institute of Science and Technology The University of Michigan Box 618 Anna Arbor, Michigan ATTN: Technical Documents Service	1		

This contract is supervised by the Solid State and Frequency Control Division, Electronics Components Department, USAELRDL, Fort Monmouth, New Jersey. For further technical information, contact the Project Engineer, Mr. Stanley S. Schodowski, Telephone 535-2602 (New Jersey Area Code 201).



THE **Magnavox** COMPANY • GOVERNMENT AND INDUSTRIAL DIVISION